Strontium-90 Fueled Thermoelectric

Generator Power Source for Five-Watt

U. S. Coast Guard Light Buoy

Final Report

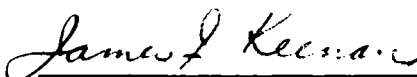# NUCLEAR MARTIN DIVISION

BALTIMORE 3, MARYLAND

Strontium-90 Fueled Thermoelectric

Generator Power Source for Five-Watt

U. S. Coast Guard Light Buoy

Final Report

Nuclear Division,

Martin Marietta Corporation, Baltimore, Md.

February 2, 1962

Approved by

James J. Keenan

James J. Keenan
Ass't Project Engineer

LEGAL NOTICE

This report was prepared as an account of Government sponsored work. Neither the United States, nor the Commission, nor any person acting on behalf of the Commission:

A. Makes any warranty or representation, expressed or implied, with respect to the accuracy, completeness, or usefulness of the information contained in this report, or that the use of any information, apparatus, method, or process disclosed in this report may not infringe privately owned rights; or

B. Assumes any liabilities with respect to the use of, or for damages resulting from the use of any information, apparatus, method, or process disclosed in this report.

As used in the above, "person acting on behalf of the Commission" includes any employee or contractor of the Commission, or employee of such contractor, to the extent that such employee or contractor of the Commission, or employee of such contractor prepares, disseminates, or provides access to, any information pursuant to his employment or contract with the Commission, or his employment with such contractor.
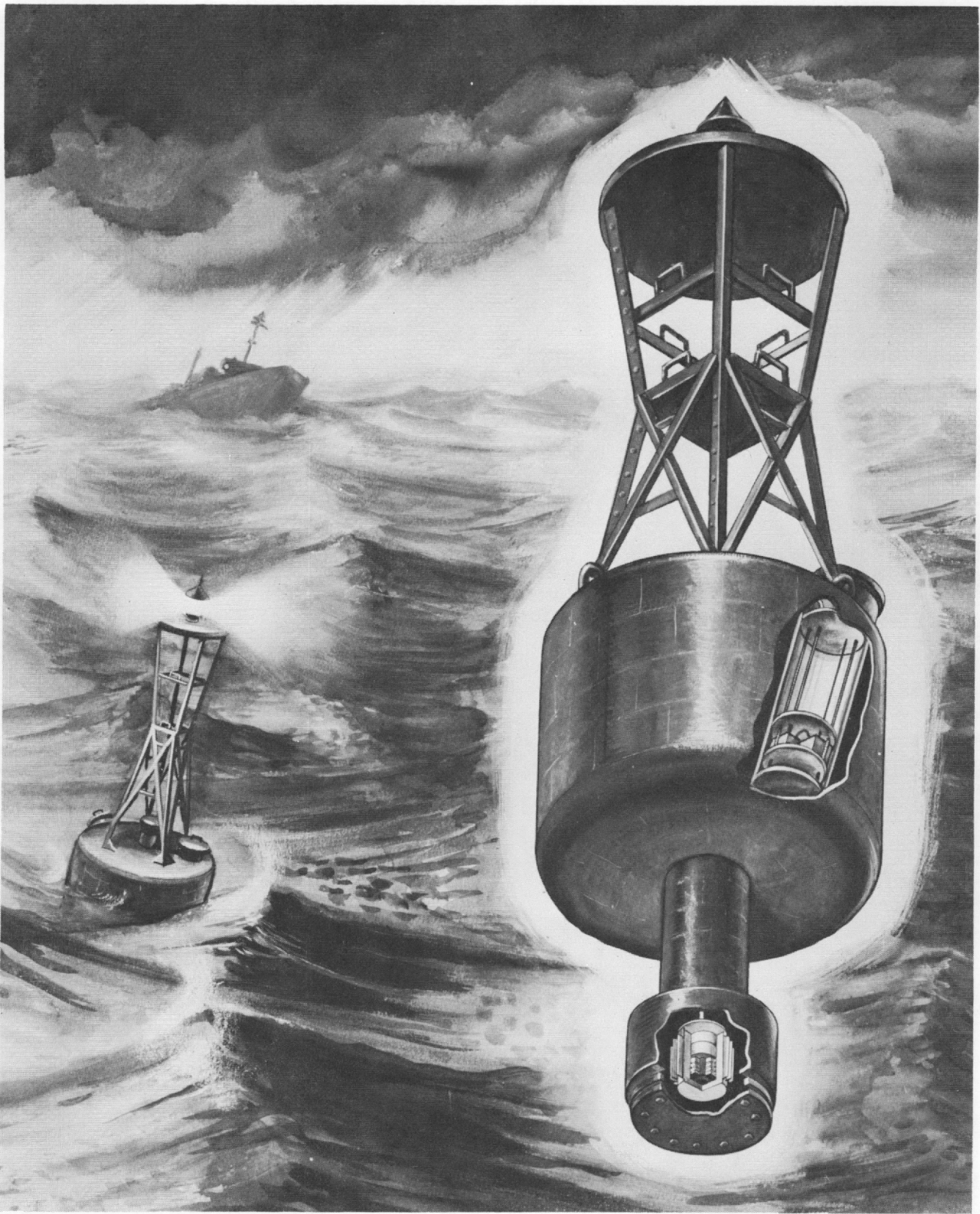
Light Buoy--SNAP 7A Radioisotope-Fueled Thermoelectric Generator System

DISTRIBUTION

This report is to be distributed according to the Division of
Technical Information Extension Category No. UC-33.

FOREWORD

This is the final report on the radioisotope-fueled five-watt electric generation system for a U.S. Coast Guard light buoy. The report has been prepared for the U.S. Atomic Energy Commission in compliance with Contract AT(30-3)-217. The work reported herein was completed by the Martin Marietta Corporation.

CONTENTS

CONTENTS (continued)

SUMMARY

The objectives of the SNAP 7A program were to design, manufacture, test and deliver a five-watt electric generation system for a U.S. Coast Guard 8 x 26E light buoy. This report describes the 10-watt Sr-90 thermoelectric generator, the dc-to-dc converter, batteries and the method of installation in the light buoy.

The SNAP 7A generator was fueled with four capsules containing a total of 40,800 curies of Strontium-90 titanate. The generator was fueled at the Martin Marietta hot cell facility located in Quehanna, Pennsylvania. After fueling and testing, the SNAP 7A electric generating system was installed in the Coast Guard light buoy at Baltimore, Maryland, on December 15, 1961. Operation of the buoy lamp has been continuous since that time.

x

NOMENCLATURE

Chapter II

A_n cross-sectional area of N element (cm^2)

A_p cross-sectional area of P element (cm^2)

C contact resistivity (μ ohm-cm^2)

D_n N element diameter (cm)

D_p P element diameter (cm)

e open circuit voltage (volts)

K thermal conductivity of element pair (watts/°C)

k_n thermal conductivity of N element (watts/cm-C)

k_p thermal conductivity of P element (watts/cm-C)

l thermoelement length

N number of thermoelements

R_c hot junction contact resistance (ohms)

R_i thermoelement internal resistance (ohms)

R_l load resistance (ohms)

α_n N element Seebeck coefficient (μvolts/°C)

α_p P element Seebeck coefficient (μvolts/°C)

T_I hot junction temperature (°K)

ΔT_t thermoelement temperature difference (°K)

v voltage

Z Figure of Merit (°C^{-1})

α total Seebeck coefficient for element pair (μvolts/°C)

η thermoelectric conversion efficiency

ρ electrical resistivity of thermoelement (ohm-cm)

μ Prefix meaning 10^{-6}

Chapter III

A_c area available for heat transfer by convection (ft^2)

A_r area available for heat transfer by radiation (ft^2)

A profile area of fin (ft^2)

e_s fin efficiency

h_c heat transfer coefficient for convection ($Btu/hr\text{-}ft^2\text{-}°F$)

h_r heat transfer coefficient for radiation ($Btu/hr\text{-}ft^2\text{-}°F$)

k thermal conductivity ($Btu/hr\text{-}ft\text{-}°F$)

N number of fins on generator shield surface

r_1 inner radius of insulation (ft)

r_2 outer radius of insulation (ft)

q rate of heat flow (Btu/hr, watts)

q_{conv} rate of heat flow by convection (Btu/hr, watts)

q_{rad} rate of heat flow by radiation (Btu/hr, watts)

ΔT_i temperature difference between inner and outer insulation surfaces

W fin length (ft)

W_c fin length plus one-half fin thickness (ft)

δ one-half fin thickness (ft)

ϵ variable used in calculation of fin efficiency (dimensionless)

ϵ_s surface emissivity (dimensionless)

Chapter VIII

a   amperes

cps   cycles per second

DA   double amplitude displacement

MS   millisecond

Tc   thermocouple

v   volts

W   watts

I. INTRODUCTION AND PHYSICAL DESCRIPTION

The development and manufacture of a radioisotope-fueled thermo-electric generator that supplies power to an automatic flashing light buoy have been successfully completed by the Nuclear Division, Martin Marietta Corporation. The system, designated the SNAP 7A electric generation system, is designed to generate five watts of d-c power with a nominal output of 12 volts for 10 years when operated in accordance with Contractor instructions. The system is required to operate without maintenance or attendance for two-year periods.

A. SYSTEM DESCRIPTION

The power generation system consists of a thermoelectric generator utilizing lead telluride thermoelements, a transistorized dc-dc converter-regulator, and a nickel-cadmium battery pack.

The generator converts the radioisotope decay heat of Strontium-90 into electrical energy. The dc-dc converter-regulator raises the low voltage output of the generator to 12 volts for the purpose of providing the system with a voltage capable of operating the flashing buoy light. The nickel-cadmium battery pack stores the converted electrical energy in order to adequately supply the intermittent power demands of the flashing light.

The system is mounted in a standard light buoy as illustrated in Fig. 1. The generator is mounted in the buoy counterbalance tube and is located at the bottom of the tube in order to assist buoy stability and to utilize the cooling effect of the sea water to its best advantage. The converter and battery pack are mounted within the body of the buoy slightly below the water line.

The buoy will be anchored in Arundel Cove at the U.S. Coast Guard Depot, Curtis Bay, Maryland (see Fig. 2) during its first year of operation. It will then be placed in service as part of the system of navigational aids maintained by the U.S. Coast Guard.

B. THERMOELECTRIC GENERATOR

The SNAP 7A thermoelectric generator consists of a Strontium-90 heat source, a thermoelectric conversion circuit, a heat rejection system and a biological shield (see Figs. 3 and 4).
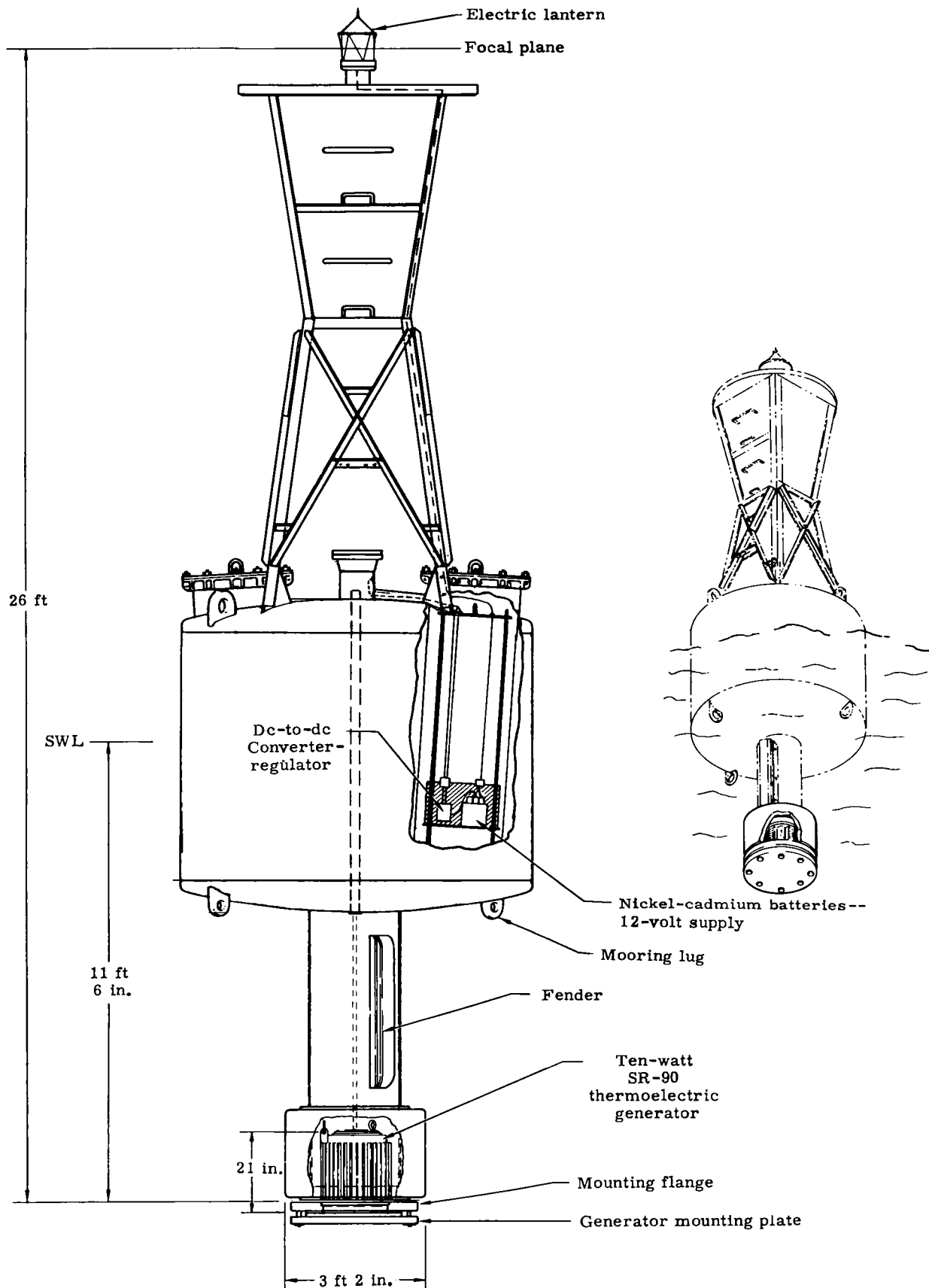
Fig. 1. Sr-90 Fueled Thermoelectric Generator System Mounted in Standard U. S. Coast Guard Flashing Light Buoy
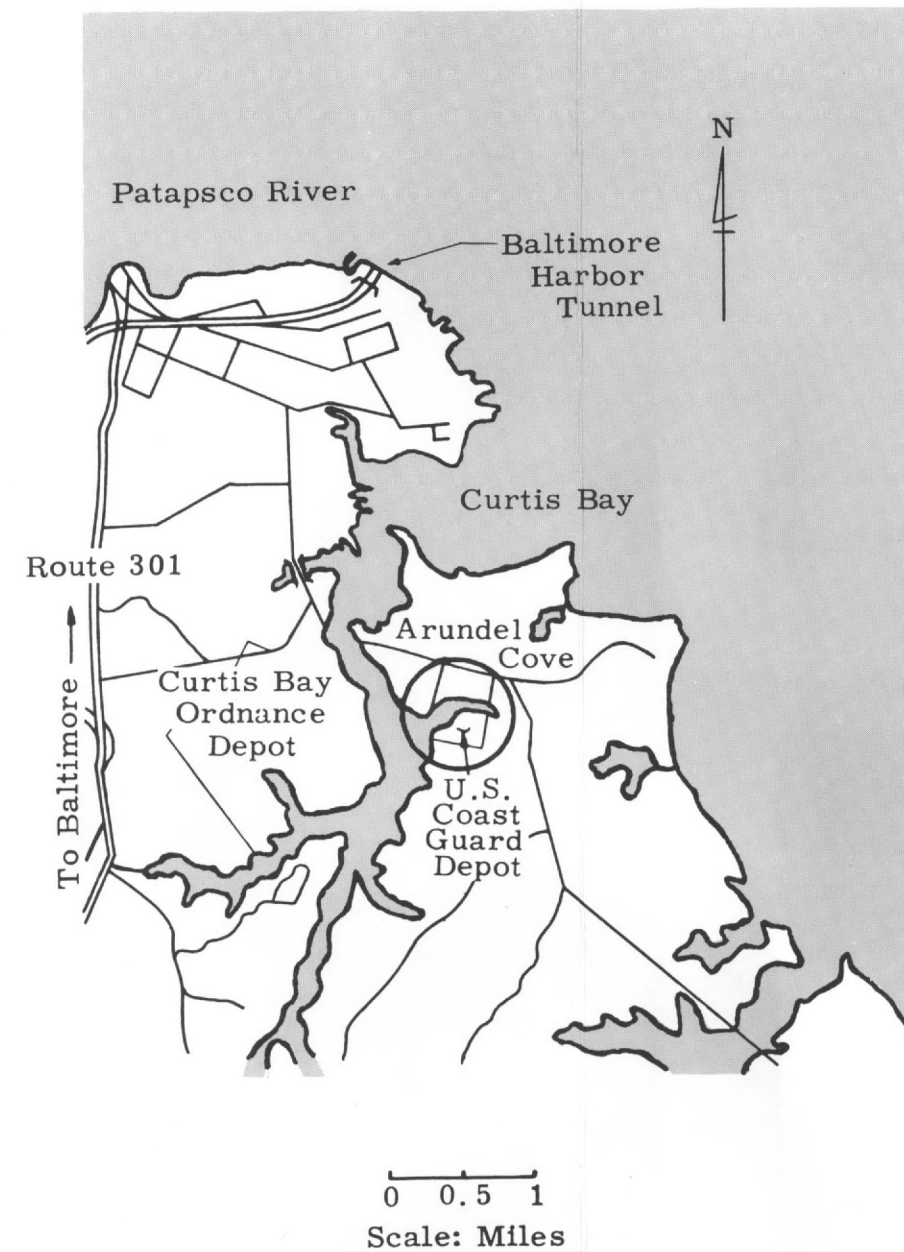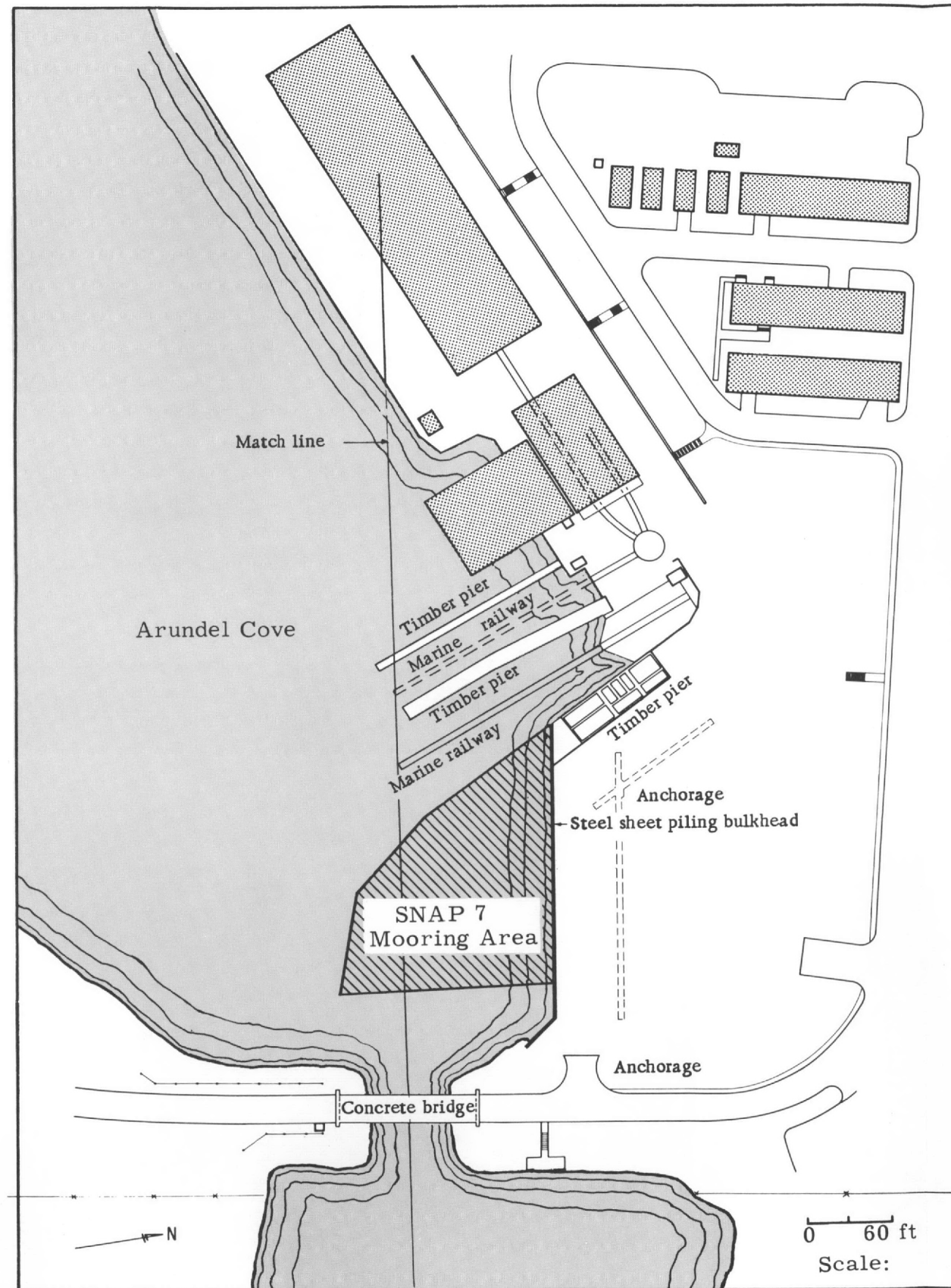
Fig. 2. Location of SNAP 7A Within Coast Guard Yard and Location of Yard in Curtis Bay Area
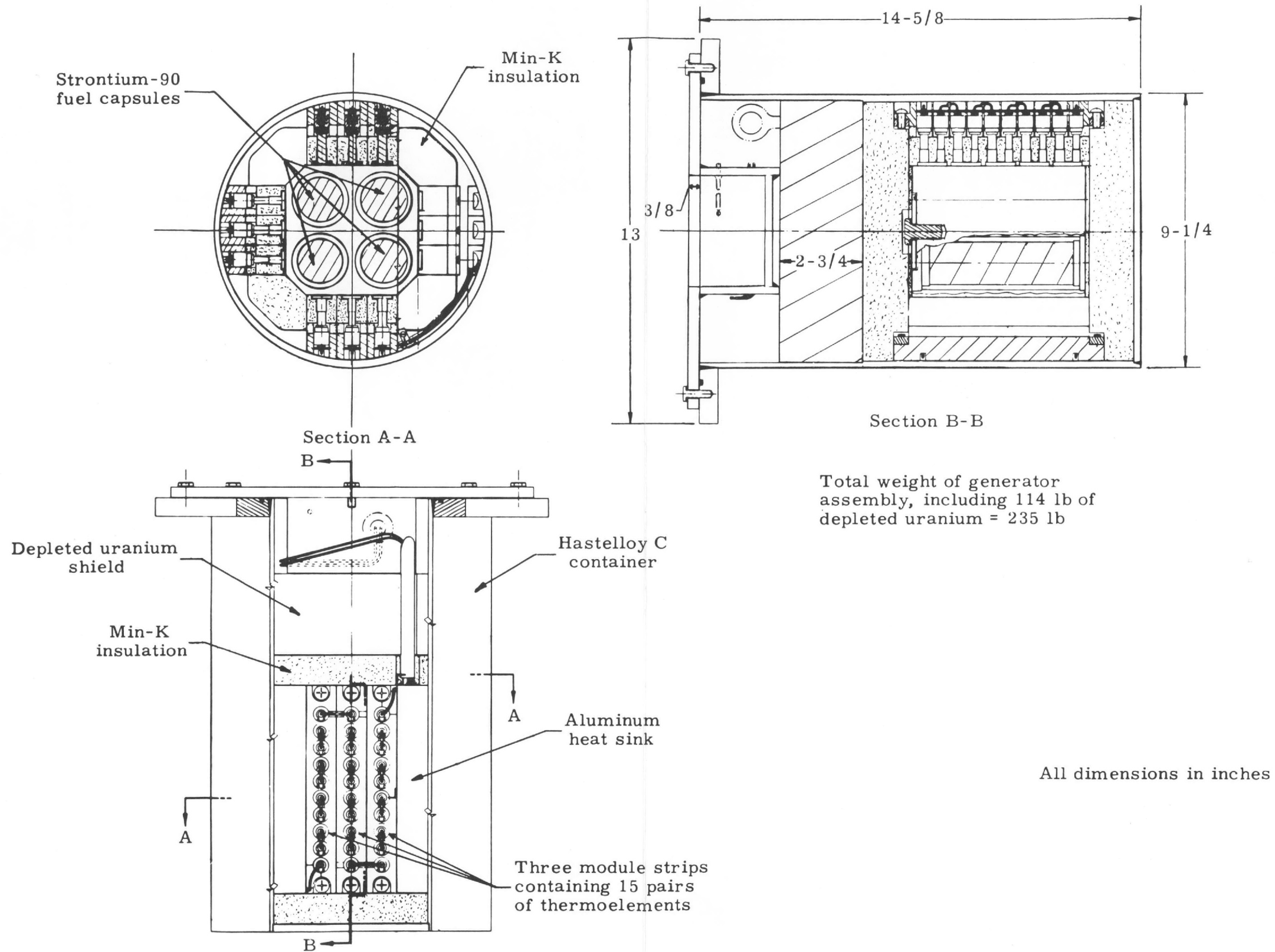
Fig. 3. Ten-Watt Generator Assembly

Strontium-90 fuel capsules

Min-K insulation

Section A-A

Depleted uranium shield

Min-K insulation

Hastelloy C container

Aluminum heat sink

Three module strips containing 15 pairs of thermoelements

Section B-B

Total weight of generator assembly, including 114 lb of depleted uranium = 235 lb

All dimensions in inches

1-1/2

19-3/4

20-7/8

2-5/8

2-5/8

Depleted
uranium

Section A-A

16-1/4

19-1/4

All dimensions in inches

A

A

Removable
lifting hooks

Total weight of generator and shield = 1840 lb

Fig. 4. Ten-Watt Generator--Biological Shield Assembly

The heat source contains 40,800 curies of the Strontium-90 isotope chemically compounded as the titanate. The fuel is compacted to form discs. The discs are sintered and then encapsulated in Hastelloy-C containers. Four containers of encapsulated Strontium-90 titanate are inserted into a Hastelloy-C fuel block. The flat surfaces of the fuel block are coated with aluminum oxide. The aluminum oxide electrically insulates the thermoelements from the fuel block without retarding heat flow.

Sixty pairs of lead telluride thermoelements are used to convert the heat produced by isotope decay into 10 watts of electrical power. Five pairs of thermoelements are assembled into one module strip. Three module strips are assembled on each of the four sides of the fuel block. The remaining space surrounding the fuel block is filled with Johns-Manville Min-K insulation.

The thermoelectric elements are assembled as shown in Figs. 5 and 6. Iron shoes serve as the hot junction electrical connection. Copper caps are soldered to the cold end of the elements to conduct heat from the element and to serve as an electrical connector.

The fuel, fuel block, thermoelectric elements, and associated hardware are contained within a Hastelloy-C housing. The housing is flushed and backfilled with one atmosphere of an inert gas. The flushing and backfilling remove the oxygen which would ordinarily poison the thermoelectric elements if allowed to remain in the high temperature environment of the generator. The inert gas is replaced at the end of each two-year period of operation with another inert gas or a mixture of inert gases with a lower thermal conductivity. In this manner a step-wise power flattening method is achieved which alleviates the detrimental effect of the reduction in thermal output by retarding heat flow and maintaining hot junction temperatures as the isotope decays. It is thus possible for the generator to meet design power requirements for the 10-year period of operation with relatively simple maintenance demands.

The generator is installed in a biological shield container. The gap between the generator housing and shield container is filled with mercury to provide a heat conducting path. The heat rejected at the cold junction is conducted through the generator housing, mercury gap, and biological shield to 36 fins mounted on the outside of the shield container.

Depleted uranium metal is used for radiation shielding. The top portion of the radiation shield is located in the same housing as the generator. The shielding for the bottom and sides consists of a separate assembly contained within a Hastelloy-C shell (Fig. 7). The shielding thickness is sufficient to safely meet ICC shipping and handling requirements.
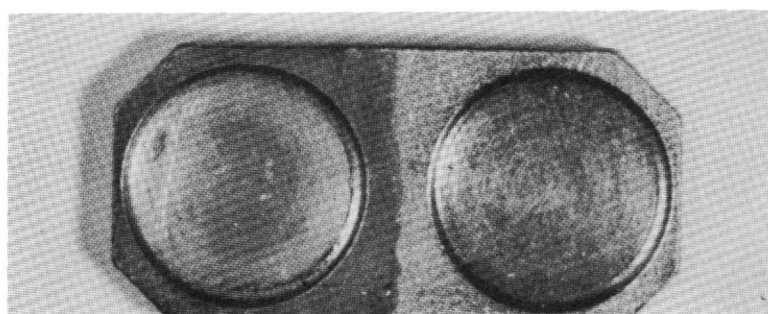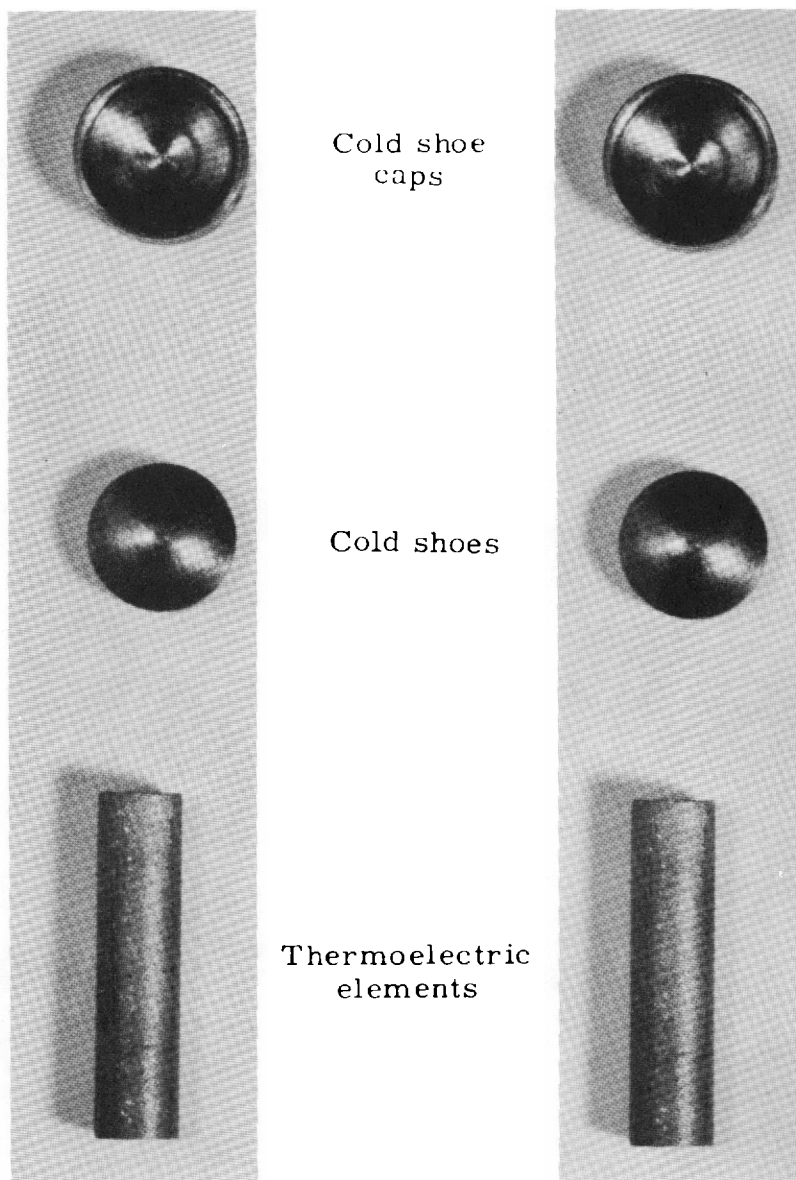
Cold shoe caps

Cold shoes

Thermoelectric elements

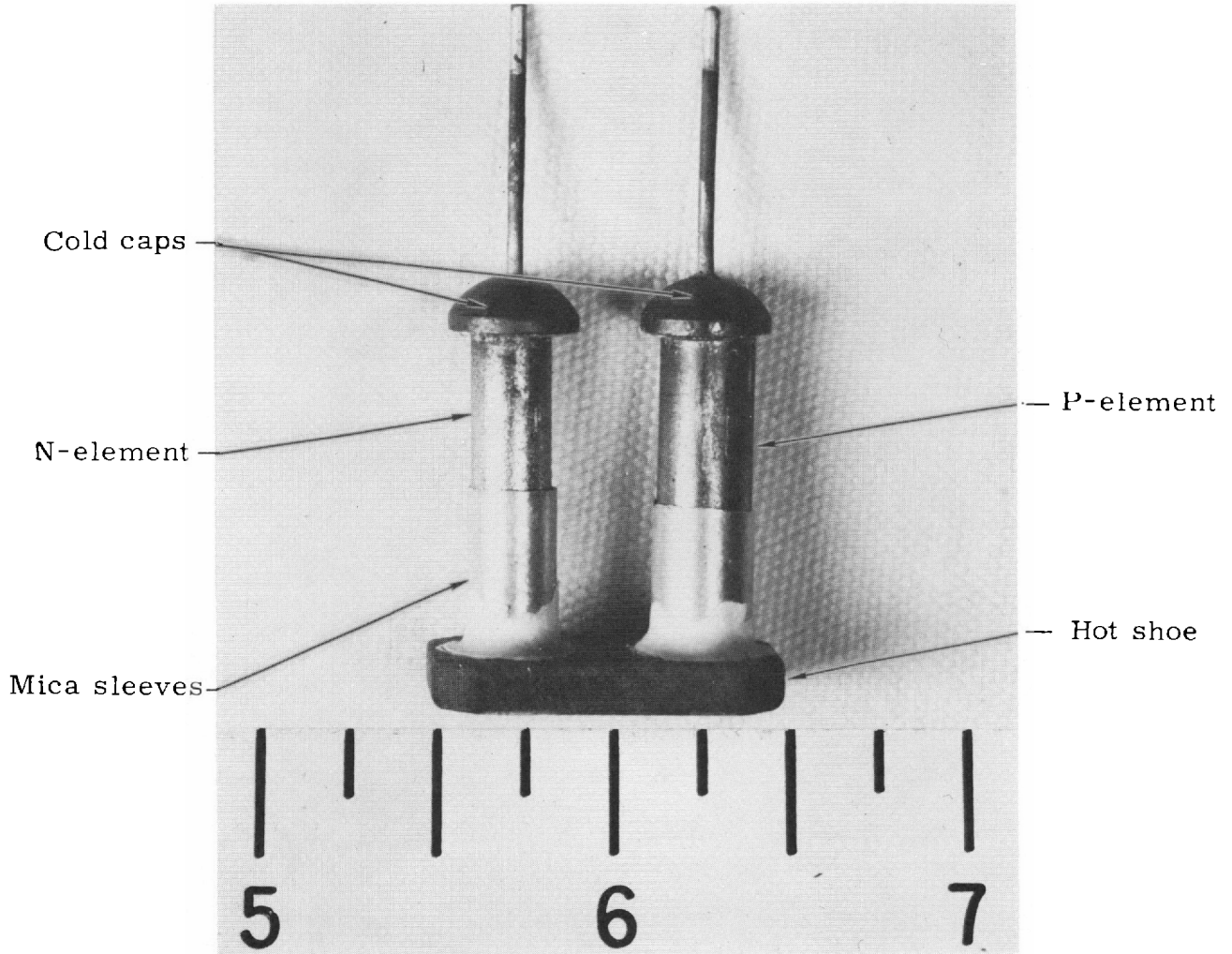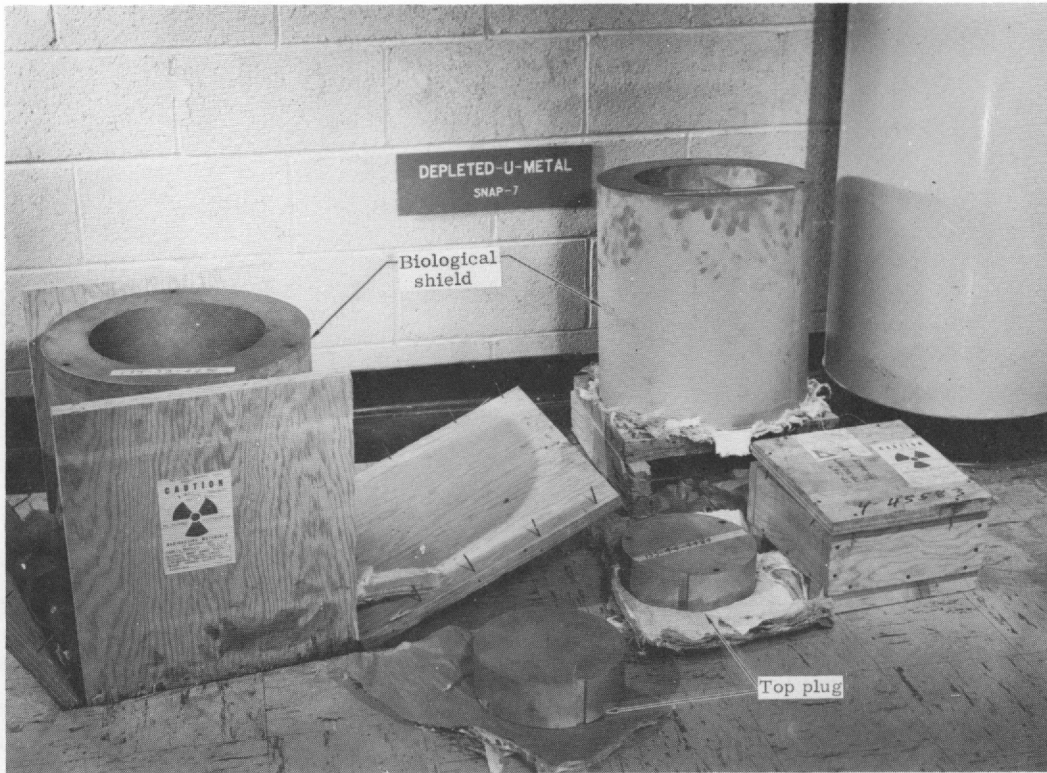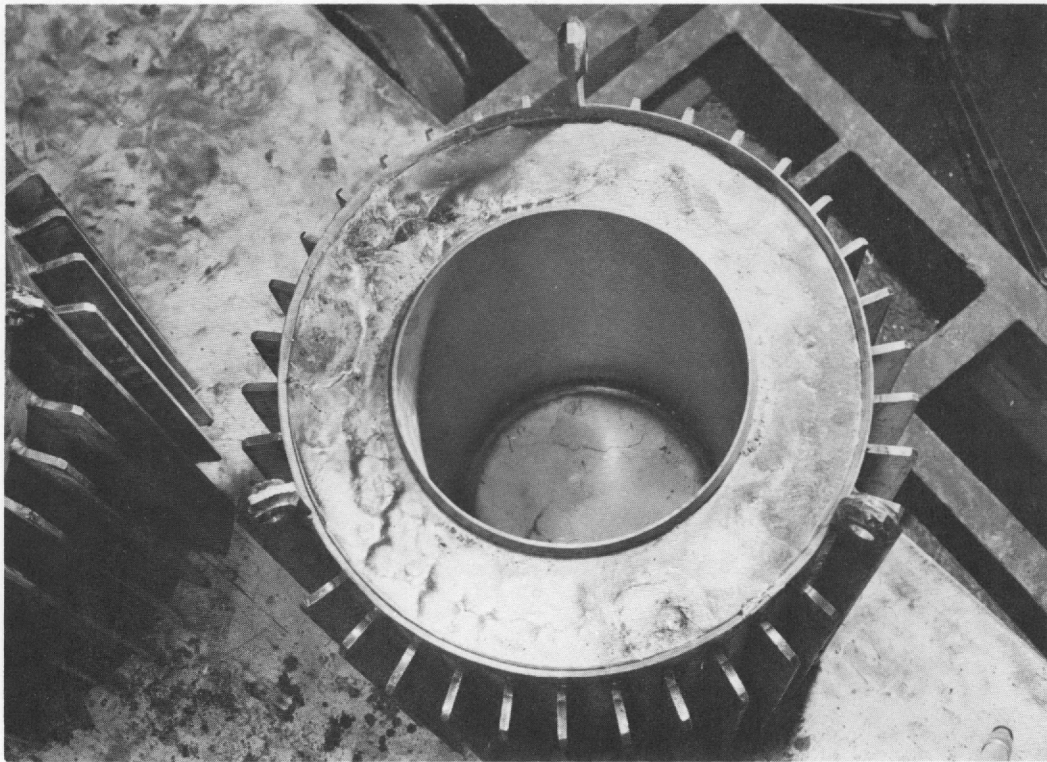Hot shoe

Fig. 5. Components of Thermoelectric Couple

Fig. 6. SNAP 7A Thermoelectric Couple

(A) Depleted-Uranium Metal Received From Y-12 ORNL

(B) Uranium Metal Installed with Hastelloy-C Cladding Both Inside and Outside

Fig. 7. Biological Shield--Assembly and Fabrication

The hazards associated with the use of radioisotopes result in stringent requirements for containment. Hastelloy-C, the material from which the generator housing and fuel containers are fabricated, has been subjected to extensive corrosion testing by the International Nickel Company at its Harbor Island Test Station, Wrightsville Beach, North Carolina. On the basis of the behavior of specimens exposed to sea water for a 10-year period, the corrosion rate was estimated to be less than 0.0001 inch per year.

The Hastelloy-C fuel containers, generator housing, and system container actually provide for triple containment of the radioisotope.

C. BATTERY AND CONVERTER

The battery and converter are housed within a steel container in the body of the buoy (Fig. 8). Also housed with the battery and converter are the input and output electrical connectors, interconnecting wiring, and test circuits. A pressure relief valve on the battery prevents pressure buildup that may occur due to possible gassing.

1. Battery

The electrical storage system required to meet the intermittent high power demands of the flashing light is a nickel-cadmium, rechargeable battery. The battery consists of nine cells divided into three sections. Each section of three cells is individually charged to a nominal voltage of four volts. This division of the battery into sections minimizes voltage deviations in individual cells and groups of cells.

2. DC-to-DC Converter

The SNAP 7A dc-to-dc converter-regulator is a transistorized component that converts the delivered generator voltage into useful operating voltage. The generator supplies a nominal 10 watts of electrical power at the end of design life (10 years) with an operating voltage of approximately five volts. The converter-regulator transforms and directs this power into three voltage-regulated output sections of 4.02 ± 0.06 volts for battery charging.
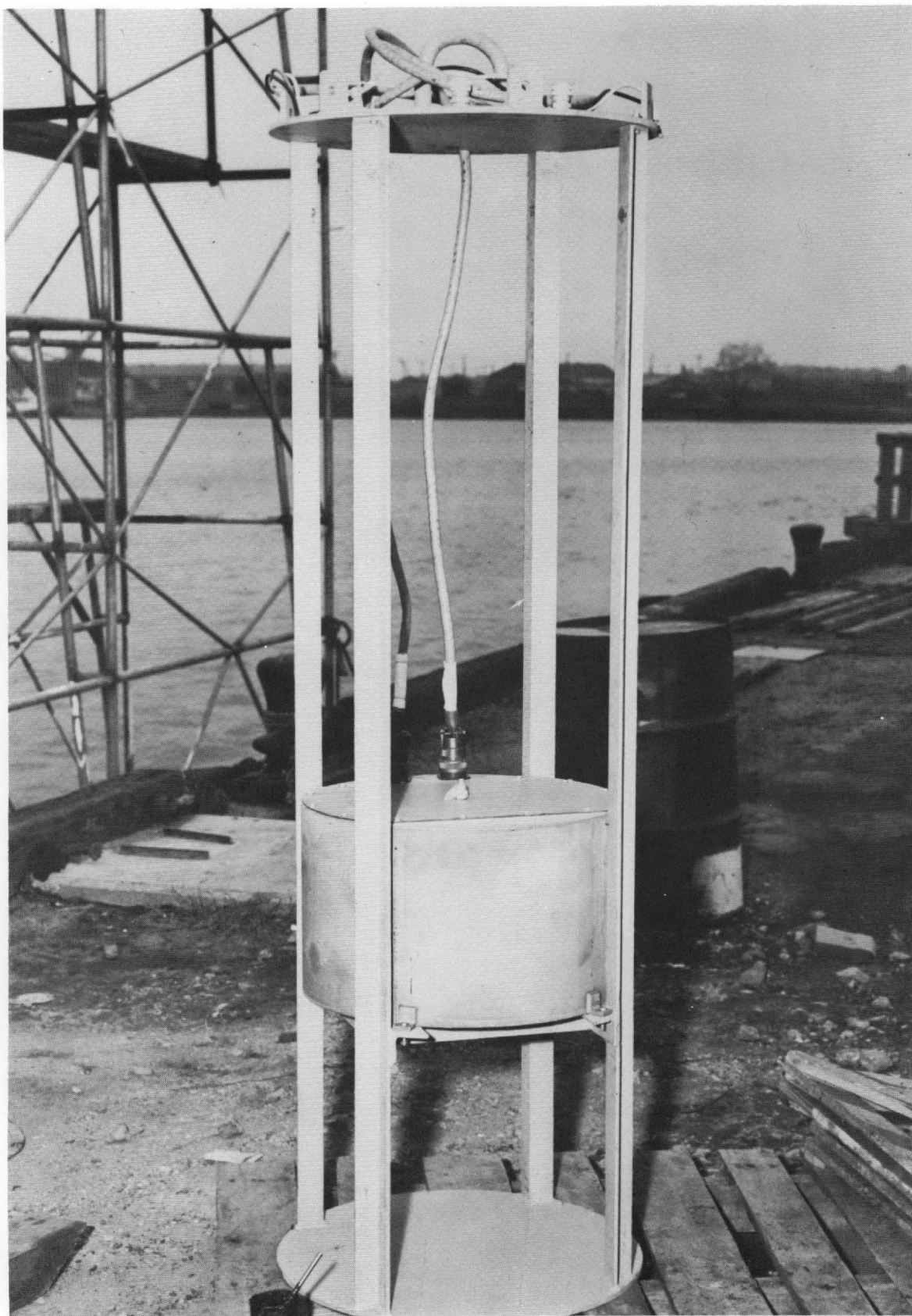
Fig. 8. Battery-Converter Container Before Installation in Buoy

II. THERMOELECTRIC ANALYSIS

A. MATERIAL SELECTION

The basic parameter involved in the choice of a thermoelectric material to operate over a given temperature range is the figure of merit, Z. Materials exhibiting high figures of merit will give higher heat to electrical conversion efficiencies than those with low values. This is especially important in radioisotope-fueled thermoelectric generators because of the high cost of the isotope. The figure of merit is defined by:

$$Z = \frac{\alpha^2}{k_\rho}$$

where

α = Seebeck coefficient

k = thermal conductivity

ρ = electrical resistivity.

The figure of merit, however, is not the sole basis for thermoelectric material selection. Other factors which must be taken into consideration are the structural stability and bonding characteristics of the material. If a thermoelement is brittle and should happen to crack while within the generator, an open circuit will result. Or, if low electrical resistance bonds cannot be made between the thermoelement and its hot and cold shoes, large electrical losses will occur at these junctions, thus resulting in lowered heat to electricity conversion efficiencies.

Lead telluride is the thermoelectric material which has the highest figure of merit over the temperature range considered for this generator. Even though lead telluride is a brittle material, it still possesses enough structural stability to be usable in a properly designed generator; also, with lead telluride relatively low junction resistances can be obtained. Further, this material is readily available from several manufacturers.

Lead telluride, the thermoelectric material selected for the generator, is a semiconductor which is doped with carefully controlled, minute concentrations of impurities in much the same manner as a transistor. Also, like a transistor, the properties of lead telluride thermoelectric material vary radially with the type and concentration of doping and the method of manufacture. Therefore, a further choice

of the type of lead telluride material to be used must also be made. This choice is based on the same considerations that were given previously in the basic selection of a material.

Samples of lead telluride materials were obtained from another manufacturer for comparison with the Martin Marietta-produced material. These samples were bonded to simulate the hot and cold shoe installation in the generator (Figs. 5 and 6) and operated over the anticipated temperatu re differential expected at the end-of-life condition (700° to 320° K). Measurements made during these tests were used to calculate the Seebeck coefficient, electrical resistivity and electrical contact resistivity. The properties of the test samples were statistically averaged, and are shown with independently measured values of thermal conductivity in Table 1.

The N and P designations given in Table 1 simply represent the two legs of materials used in a thermoelectric couple. The N material develops a plus-to-minus potential in going from the hot to cold end while P material develops a minus-to-plus potential. In this manner N and P materials may be connected in series to form a couple, and an additive rather than a bucking voltage output is obtained.

Based on the figures of merit determined from the measured properties, the best combination of thermoelements would be the Martin Marietta N and P types. Operation over long periods of time showed these materials to be durable and to experience only slight degradation in performance.

B. THERMOELECTRIC EFFICIENCY AND ELEMENT SIZING

Once a thermoelectric material has been selected, based on a specified temperature range, the number and size of the thermoelements and their conversion efficiency must be determined. These values may be obtained from the desired voltage and power output of the generator to be produced. The thermoelement properties listed in Table 1 were used in these determinations.

The maximum heat to electricity conversion efficiency of a thermoelement operating over a specified temperature range is given by:

$$\eta = \frac{\Delta T_t}{T_I} \cdot \frac{\left(\dfrac{R_1}{R_i + R_c}\right)}{\left(\dfrac{R_1}{R_i + R_c}\right) + \dfrac{K(R_c + R_i)\left(\dfrac{R_1}{R_i + R_c} + 1\right)^2}{\alpha^2 T_I} - \dfrac{\Delta T_t\left(\dfrac{R_i}{2} + R_c\right)}{T_I(R_i + R_c)}}$$

TABLE 1

Summary of Module Test Thermoelectric Properties*

	Martin N	Average Properties Outside Vendor	Martin P	Outside Vendor
Seebeck voltage (μ v/°C)	204	257	177	213
Resistivity (μ ohm-cm)	1310	2870	2675	4300
Contact resistivity (μ ohm-cm^2)	386	575	830	760
Thermal conductivity (watts/cm-°C)	0.0199	0.0180	0.0208	0.0196
Figure of Merit (°C^{-1})	1.585×10^{-3}	1.325×10^{-3}	0.564×10^{-3}	0.538×10^{-3}

*Based on a hot-end temperature of 700° K and a cold-end temperature of 320° K.

where

$\alpha = \alpha_n + \alpha_p$ = combined Seebeck coefficient (μ volts/°C)

α_n = Seebeck coefficient of N element (μ volts/°C)

α_p = Seebeck coefficient of P element (μ volts/°C)

R_1 = load resistance (ohms)

$R_i = \dfrac{\rho_1}{A}$ = thermoelement resistance (ohms)

ρ = thermoelement resistivity (ohm-cm)

1 = thermoelement length (cm)

A = thermoelement cross-sectional area (cm^2)

$R_c = \dfrac{C}{A}$ = contact resistance (ohms)

C = contact resistivity (ohm-cm^2)

ΔT_t = thermoelement temperature difference (°K)

T_I = thermoelement hot junction temperature (°K)

$K = \dfrac{kA}{1}$ = thermal conductance (watts/°C)

k = thermoelement thermal conductivity (watts/cm-°C)

The impedances of the generator and the load are not matched in the design of isotope thermoelectric generators as they are in classical electrical problems. Since a discussion of justification and derivation of the equation would be lengthy, the reader is referred to "Semiconductor Thermoelements and Thermoelectric Cooling," by Ioffe, and to report MND-SR-2428, page D20, for clarification.

Other expressions required for this optimum sizing of the thermoelements are:

$$e = N \alpha \Delta T_t$$

and

$$\frac{R_l}{R_l + R_c} = \left[1 + \frac{\alpha^2 T_I}{K(R_c + R_l)} - \frac{\alpha^2 \Delta T_t \left(\frac{R_l}{2} + R_c\right)}{K(R_c + R_l)^2} \right]^{1/2}$$

where

e = open circuit voltage of the generator, volts

N = number (quantity) of thermoelement pairs.

An iterative balance may now be performed between the previous three equations and the insulation losses which are given in Chapter III, and all of the thermal and electrical characteristics of the generator may be determined. In this procedure the generator system is treated as though it is a simple d-c electrical circuit. Either the thermoelement length or diameter must be arbitrarily specified. The thermoelement length was chosen to be 2.54 centimeters for the design of this particular generator and the material properties used were those listed in Table 1 for the Martin N and P thermoelements. Based on these inputs, the generator characteristics listed in Table 2 were determined.

It may be noted that the end-of-life power output is given as 9.3 watts(e) which is slightly lower than the design goal of 10 watts(e). The design goal will be achieved by altering the thermal losses through the generator insulation. This will be accomplished by changing the insulation gas fill at each maintenance period with successively poorer conducting gases. The range of gases to be used will vary from highly conductive helium at the beginning of life, when excess thermal power is available, to a poorer conductor such as krypton or xenon at the end of life. A discussion of this method of varying the thermal conductivity of Johns-Manville Min-K insulation may be found in Chapter III.

TABLE 2

Generator Physical and Operational Characteristics

Thermoelement length, N-type (cm)	2.54
Thermoelement length, P-type (cm)	2.54
Thermoelement diameter, N-type (cm)	0.585
Thermoelement diameter, P-type (cm)	0.705
End-of-life thermal power (watts)	200 (based on initial fuel loading)
Insulation losses (watts)	50.75
Thermoelement efficiency (%)	6.23 (end of life)
Generator efficiency (%)	4.65 (end of life)
Power output (watts)	9.3 (end of life)
Number of element pairs	60
Open circuit voltage (volts)	8.70 (end of life)
Load voltage (volts)	4.71 (end of life)

III. THERMAL ANALYSIS

The analysis of heat flow and temperatures within the SNAP 7A system was divided into two general areas: thermal analysis of the outer shell of the generator and thermal analysis of the SNAP 7A system with the generator as a heat source. The outer shell analysis was necessary to determine the temperature difference between the thermoelement hot and cold junctions and the heat losses through the Min-K 1301 thermal insulation. The thermal analysis of the system with the generator as a heat source was required to determine the actual operating temperature of the generator and other temperature-sensitive system components.

The most critical temperature in the thermal analysis is the hot junction temperature. Lead telluride thermoelectric elements deteriorate rapidly by sublimation at temperatures greater than 1000° F. For an extended period of life such as is desired in the SNAP 7A generator, the maximum tolerable hot junction temperature was chosen as 980° F. This fixes the maximum beginning-of-life temperature and, assuming no change in the thermal properties of the generator, enables calculation of the end-of-life hot junction temperature as 800° F.

The initial step in the thermal analysis of the generator was to determine the ambient conditions in which the generator will operate. Given a rough configuration of the generator, the outer heat rejecting surface can be designed to maintain the inner temperatures at desired levels. The outer shell of the generator acts as the heat rejection surface. The design of fuel block, thermoelements, inner container shield, and outer container fixes the minimum dimensions of the outer generator silhouette. Additional surface in the form of thermal fins could be added if required for an additional heat rejection capability.

A thermal study was made to determine the best location for the generator radiation shielding. The choice of location included either completely enclosing the heat source, thus requiring a shield of smaller volume, or completely enclosing the generator. The study indicated that the shield should be located on the outside of the generator. The increase in fuel block surface area, resulting from incorporation of the shield into the fuel block, results in lower hot junction temperatures and higher insulation heat losses, thus reducing generator efficiency.

The generator must be adaptable to operation in two different environments:

   (1) During shipment, when the air temperature may go as high as 125° F in an enclosed space. (However, the generator

terminals may be short-circuited during shipment, producing lower hot junction temperatures due to the Peltier effect.)

(2) During operation, submerged at the base of the floating buoy.

Condition (2) poses no problem to cooling the generator surface. The generator design point is for operation in the temperature range resulting from this condition.

Since there is a possibility of high ambient temperature and lack of circulating air during shipment, the surface of the generator had to be designed so that it operated at temperatures no higher than 175° F to prevent the excessively high temperatures from damaging the thermo-elements. This was accomplished in the following manner.

The maximum heat input to the generator was anticipated to be 256.5 watts. The heat lost from the generator surface is given by:

$$q_{total} = q_{conv} + q_{rad} = 256.5 \text{ watts} \tag{1}$$

where

$$q_{conv} = h_c \, A_c \, \Delta T \quad \text{(heat rejected by convection)} \tag{2}$$

$$q_{rad} = h_r \, A_r \, \Delta T \quad \text{(heat rejected by radiation)} \tag{3}$$

where

h_c is the convective heat transfer coefficient, $\dfrac{\text{Btu}}{\text{hr-ft}^2\text{-}°F}$

h_r is the radiative heat transfer coefficient, $\dfrac{\text{Btu}}{\text{hr-ft}^2\text{-}°R^4}$

The generator surface was considered to consist of a cylinder 16.25 inches in diameter and 17 inches high with a number of 1.5-inch long fins running longitudinally along the cylindrical surface. The 1.5-inch fin length represents an optimum for Hastelloy-C, a poor conductor of heat but which is desirable for its corrosion resistance. The number of fins required was determined as follows.

The surface area available for radiant heat transfer is approximately the area of the cylinder taken over the edge of the fins, including the top of the cylinder but excluding the bottom (Ref. 11),

$$A_r = 8.59 \text{ sq ft}$$

The convective heat transfer area is approximately the area of the cylinder excluding the bottom plus the effective fin area. The effective fin area is the total fin surface area multiplied by the fin efficiency. The fin efficiency accounts for the reduced heat rejection capability of the fin that results from the temperature gradient along its length. The fin efficiency is given by (Ref. 3, p. 72):

$$e_s = \left(\frac{1}{\sqrt{2\epsilon}} \right) \quad (\tanh \sqrt{2\epsilon}) \tag{4}$$

where

$$\epsilon = W_c^{3/2} \sqrt{h_c/kA} \tag{5}$$

$$W = \text{fin length}$$

$$W_c = W + \delta$$

$$\delta = \text{one-half of fin thickness } (0.125 \text{ in.})$$

$$h_c = 0.27 \, (\Delta T)^{0.25} \quad (\text{Ref. 3, p. 474}). \tag{6}$$

The resulting fin efficiency is then:

$$e_s = 0.826$$

Therefore:

$$A_c = 7.46 + 0.291 \, N \text{ sq ft}$$

where

$$N = \text{number of fins required}.$$

The radiant heat transfer coefficient was determined by:

$$h_r = \sigma \epsilon_s \frac{\left[(T_s/100)^4 - (T_r/100)^4 \right]}{T_s - T_r} \tag{7}$$

where

$$\epsilon_s = \text{surface emissivity} = 0.50$$

$$\sigma = \text{Stefan-Boltzmann constant} = 0.173, \text{ Btu}/(\text{sq ft}) \, (\text{hr}) \, (^\circ R^4)$$

T_s = generator surface temperature, °R

T_r = ambient temperature, °R.

The heat rejected by the outer surface is thus given by (Eqs. 1, 2 and 3):

$$q_{total} = (0.718)(7.46 + 0.291N)(50) + (0.692)(8.59)(50)$$

which must equal the total design input of 877 Btu/hr. From this consideration

$$N = 29.9 \text{ fins}.$$

It was thus shown that a minimum of 30 fins was required on the outer surface. In order to supply a margin of safety to the calculation, the number of fins actually used was 36.

A. INSULATION HEAT LOSSES

A limited test program was conducted to determine the thermal conductivity of the Min-K insulation filled with various gases. The gas serves a twofold purpose, preventing sublimation of the thermoelements and changing the thermal conductivity of the insulation to reduce heat losses as the heat input to the generator is reduced by isotopic decay. (A less conductive gas is used to fill the generator at each biennial maintenance.)

The following values of insulation thermal conductivity were obtained for various gas fills at a pressure of one atmosphere.

Gas Fill	Thermal Conductivity, Btu/hr-ft-°F
Air	0.2865
Argon	0.2285
Hydrogen	0.597
Vacuum	0.118

The fuel block is separated from the cold portions of the generator by a layer of Min-K 1301 insulation chosen for its low thermal conductivity, good structural qualities, and machinability. The insulation fits between the fuel block and cold junction heat sink snugly enough to provide support for the block. Powdered Min-K is packed around the thermoelements to further reduce heat losses. The mean insulation thickness is 1.38 inches.

For the generator design calculation, a nominal value of thermal conductivity of 0.0175 Btu/(hr)(ft)(°F) was selected. This corresponds roughly to a mixture of approximately 90% argon, 10% hydrogen in the Min-K insulation.

Heat losses through the insulation were calculated by the following relationship which holds for cylinders with a length-to-diameter ratio of one, surrounded by a constant thickness of insulation.

$$q = \frac{6\pi r_1 r_2 k \Delta T_1}{r_2 - r_1}$$

where

q = insulation heat loss (Btu/hr)

r_1 = inner radius of insulation (ft)

r_2 = outer radius of insulation (ft)

k = thermal conductivity of insulation (Btu/hr-ft-°F)

ΔT_1 = temperature drop across insulation (°F)

The total heat loss at the end of life was calculated as 50.75 watts including an estimated 2.75 watts lost through the mica sleeves surrounding the thermoelements. The mica insulator loss was estimated by treating it and the thermoelement heat flow by analogy with current flow through resistors connected in parallel.

B. EXCESSIVE THERMAL POWER IN FUEL

In the fission product waste obtained by processing spent reactor fuel elements, Strontium-90 is accompanied by the shorter-lived Strontium-89 which may produce as much as 80 times the heat of the heavier isotope when discharged from the reactor. Although the half life of Strontium-89 is only 51 days, production schedules indicate that appreciable quantities could be present at the time the generator was to be loaded, causing temporary overheating and consequent damage to the thermoelectric elements. However, because of its short duration, the heat supplied by the absorption of Strontium-89 beta emissions cannot be considered part of the thermal power requirement.

24

Figure 9 illustrates the combined thermal output of the two strontium isotopes for 47 kilocuries of the heavier isotope as a function of months after discharge from the reactor. Atomic ratios of Strontium-89 to Strontium-90 were estimated to be 0.20 and 0.64. Analysis showed that with the proper conducting gas in the insulation, the excess heat can be accommodated without seriously affecting generator performance over its design lifetime.

This analysis takes into account the SNAP 7A fuel specification permitting a thermal overload of 40 watts due to Strontium-89 content.

C. ANALYSIS OF SUBMERGED GENERATOR

A temperature analysis was conducted to determine the operating temperatures of the generator while it was submerged in water. Using the equation recommended by McAdams (Ref. 11, p 172) the convective heat transfer coefficient (h_c) was calculated as 40.4 Btu/hr-ft^2-°F.

$$\frac{h_c L}{k_f} = 0.59 \left[\frac{L^3 \rho_f{}^2 g \beta_f \Delta T C_p}{\mu_f k_f} \right]^{0.25}$$

where

L = height of heated surface (ft)

k_f = thermal conductivity of fluid (Btu/hr-ft-°F)

ρ_f = density of fluid (lb/cu ft)

g = gravitational constant (4.17×10^8 ft/hr^2)

β_f = thermal expansion coefficient of fluid (°F^{-1})

ΔT = temperature difference between heated surface and fluid (°F)

C_p = heat capacity of the fluid (Btu/hr-ft)

μ_f = viscosity of the fluid (lb/hr-ft)

Using the convection relationship, the temperature difference

$$q = h_c A_c \Delta T$$

between water and generator surface was calculated at 4.5° F at the beginning of generator life. (A_c = convective heat transfer area.)

$$R = \frac{\text{atoms Sr-89}}{\text{atoms Sr-90}} \text{ at reactor discharge}$$

T = 0 at reactor discharge

Half life of Sr-89 = 51 days
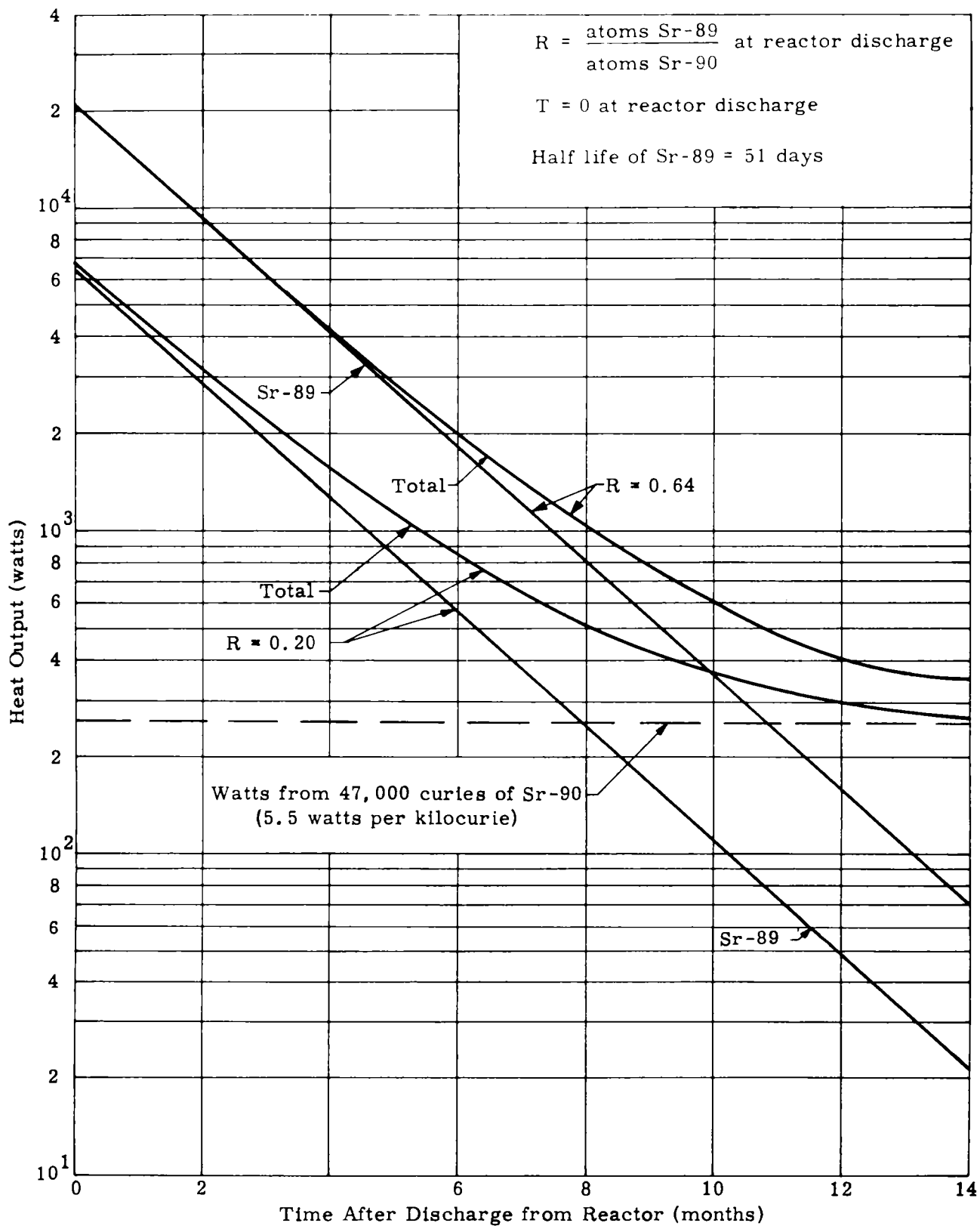
Fig. 9. Effect of Strontium-89 on Heat Output of SNAP 7A 10-Watt Generator

A maximum water temperature of 80° F proved that there was no danger of overheating the thermoelements.

Initial operation resulted in a hot junction temperature of 903° F with a water temperature of 41° F.

The battery and converter, mounted on the buoy, are maintained within temperature limits by the water surrounding the buoy and by their own internal heat. Environmental testing showed acceptable operational limits to be less than 0° F and greater than 90° F.

IV. FUEL FORM AND SHIELDING REQUIREMENTS

A. FUEL FORM

Strontium-90, with its relatively long half life (27.7 years), was selected as the radioisotope to provide the thermal energy for the SNAP 7A system. The form selected was the titanate ($SrTiO_3$), a stable ceramic compound with extremely low solubility in sea water. In the original design of the generator the specific thermal power of the prepared fuel form was estimated at 0.5 watt/cm^3.

Because of the long lead time required for chemical processing of the fuel, it was necessary to fix the fuel volume prior to the detailed design of the generator. Assuming a 5% overall conversion efficiency, producing 10 watts after 10 years, the end-of-life thermal power was 200 watts. From the decay rate of the isotope, an initial requirement of 256.5 watts was calculated. This resulted in a design volume of 513 cm^3.

The fuel is distributed into four capsules (refer to Figs. 3 and 4). The total loading was estimated as 47 kilocuries of Strontium-90 based on a conservative estimate of 0.0055 watt/curie. Considerations in the fuel capsule design were minimum heat loss, i.e., maximum heat flow to thermoelectric elements, ceramic fuel pellet diameter of 2 inches or less, and the use of an existing remote welder at Oak Ridge National Laboratory for capsule sealing.

Each fuel capsule (see Fig. 10) has a button protruding from its top surface to facilitate remote handling in the hot cells and loading into the fuel block. The fuel container is made of Hastelloy-C, chosen for its excellent structural properties and high resistance to corrosion. Results of a 10-year corrosion test in sea water at Wrightsville Beach, N. C., show that Hastelloy-C has an average corrosion rate of 0.1 mil/year with no tendency toward pitting. This ensures safe cladding for over 1000 years, even if the corrosion rate is double that experienced in the test.

The Strontium-90 titanate received from Oak Ridge National Laboratory produced a higher specific power than the 0.5 watt/cm^3 anticipated in the design. The pellets received for loading had specific powers of 0.7 to 0.9 watt/cm^3, so that excess volume was available. The total thermal output of the four capsules was 255 watts from Strontium-90 at installation as compared to the design input of 256.5 watts. The actual amount of isotope fuel was 40,800 curies at about 6.25 watts/kc. The excess capsule volume was filled with inert spacers by Oak Ridge National Laboratory.

SrTiO$_3$

1.48 in.

4.55 in.

64.1-watt thermal output

1.872 $^{+0.000}_{-0.001}$ in.

5.199 $^{+0.000}_{-0.005}$ in.

Hastelloy-C clad
fuel capsule

Chamfer 0.063 x 45°

Seal weld (1/16-in. minimum penetration)
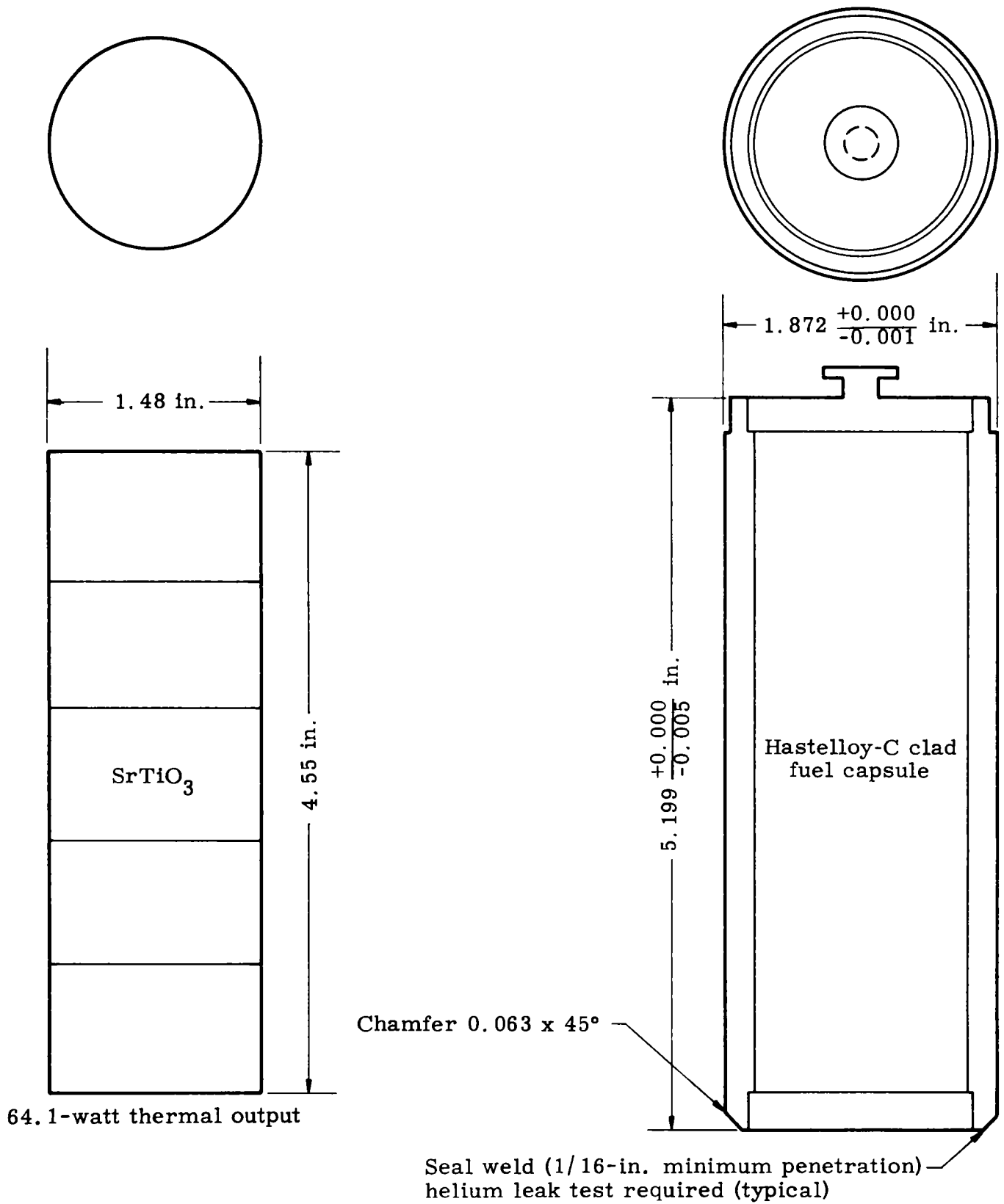helium leak test required (typical)

Fig. 10. Fuel Capsule Assembly of Strontium-90 Generator

B. SHIELDING REQUIREMENTS

Radiation dose rates from the unshielded capsules of the 10-watt thermoelectric generator were calculated by means of an IBM 709 digital computer. Each capsule was assumed to contain one-fourth of the total 47,000 curies of Strontium-90 in the geometrical configuration of the fuel block. On this basis, the dose from one bare capsule was as follows:

	Dose at Side (r/hr)	Dose at Top and Bottom (r/hr)
At surface	89,000	62,000
At one meter from surface	136	59

From the four capsules loaded into the fuel block without shielding, the total dose rate was calculated as follows:

At one meter from surface of fuel block	500 r/hr (at side)	235 r/hr (at top and bottom)

Shielding values were computed for depleted uranium to reduce the dose rate from 47 kilocuries of Strontium-90 to 100 mr/hr at one meter from the center of the generator, in accordance with the specifications established at the inception of the program. Uranium is employed as the shield material because its use results in a generator of smaller size and weight. The minimum thicknesses of uranium required are as follows:

Shield	Thickness (in.)
Top	1.87
Side	1.54
Bottom	1.67

However, the biological shield for the 10-watt generator was designed with a thickness greater than the minimum to permit the use of the shield as a shipping container for transportation by common carriers in interstate commerce. The designed thicknesses and the resulting dose rates are as follows:

Shield	Thickness (in.)	Dose Rate at one meter (mr/hr)
Top	2.75	1.92
Side	2.625	3.61
Bottom	2.625	2.88

A comparison of calculated and measured dose rates was made for the SNAP 7A and SNAP 7C generators, and is shown as follows:

		SNAP 7A 40,800 Curies		SNAP 7C 40,000 Curies	
		Calculated	Measured*	Calculated	Measured**
At one meter	Top	1.89	2.5	1.86	3
	Side	1.87	1.0	1.84	1.5
At surface	Top	29.9	30	29.4	50
	Side	31.3	15	30.8	20

The shielding is adequate to meet ICC regulations for unescorted shipments (10 mr/hr maximum at one meter and 200 mr/hr maximum at surface).

Calculated dose rates were originally based upon 47,000 curies of Strontium-90, and have been adjusted to conform to the estimated curie loading of the generators.

The measured and calculated dose rates agree within a factor of about two, which is considered good in shielding work.

Note that the measured dose rates are higher for the SNAP 7C generator even though this generator contains less curies. Possible explanations for this are differences in instruments used for measuring, uncertainty in the location at which readings were taken, differences between design and actual generator construction, or a combination of several of these items. It is concluded that the shielding for the 10-watt generator is conservative.

---

*Letter dated November 28, 1961 (Ref. No.--p. 1404) to Commander Culwell from J. J. Keenan.

**Letter dated September 19, 1961 (Ref. No.--p. 1313) to Commander Culwell from J. J. Keenan.

A complete safety analysis report concerning the use of strontium-fueled thermoelectric generators has been prepared and is given in Ref. 5.

Subsequent to the original calculation of the shield thickness, it was found that the strontium isotope produced by spent element processing at Hanford would contain 2.5 millicuries of Cerium-144 per curie of Strontium-90. Cerium-144 is a beta emitter which also emits a hard gamma photon at each disintegration. Examination of the results presented below reveals that even with the additional radiation contributed by the cerium, the total dose rate is still well below the 10 mr/hr at one meter that is the ICC shipping requirement.

Power (thermal watts)	250
Strontium-90 (curies)	4.0×10^4
Cerium-144 (curies)	100
Dose rate for Cerium-144 at one meter (mr/hr)	1.7
Dose rate from Strontium-90 at one meter (mr/hr)	2.5
Total dose rate at one meter (mr/hr)	4.2

The calculations and comparison of calculated with experimental results were carried out as described in Appendix A.

V. GENERATOR ASSEMBLY

The SNAP 7A generator was custom assembled, with special precautionary measures taken to assure integrity, reliability and safety.

The thermoelectric elements were assembled by bonding the doped lead telluride elements (one N type and one P type) to a common iron shoe as shown in Fig. 11. Five couples, a block of Min-K 1301 insulation and copper caps (one soldered to each element) were assembled to form a module (see Fig. 12).

The Hastelloy-C fuel block was centrally located within the aluminum heat sink frame and held in place by corner blocks of Min-K insulation. A base plate of Min-K insulation supports the heat sink and positions the fuel block at the desired height in the generator.

Twelve thermoelectric modules (60 pairs), mounted in groups of three against each of the four flat surfaces of the fuel block, were held in position by means of Min-K filler strips and aluminum heat sink bars. Each bar was attached to the aluminum frame with screws (see Figs. 13 and 14).

The thermoelectric module components (see Fig. 15) were inserted through each heat sink bar after individual module installations.

Element pairs and modules were electrically interconnected with copper straps and each group of three modules connected to the next with ceramatemp wire (see Fig. 16). The series connection of element pairs and modules was terminated in a single output lead.

During generator assembly, resistance measurements were recorded for all pairs, modules and module groups. The complete total resistance of the generator was also measured.

The Hastelloy-C shell containing the assembled generator was inserted into the biological shield containing 18 pounds of mercury. The mercury is used as a conductive medium to reduce the temperature difference between generator and shield. After positioning, the generator container was welded into place. The mercury level was above the top of the heat sink.

Generator fueling, which took place in a hot cell at the Quehanna facility, included installation of the four fuel capsules, the fuel block cover plate, the Min-K insulation plate and the uranium shield block (see Fig. 17). Thermocouples were permanently attached, one to the fuel block and one to the hot junction of one of the thermoelectric elements. The attachment of the generator closure completed the assembly of the generator. The output leads and thermocouple leads are terminated at a hermetically sealed electrical connector located in the generator closure.
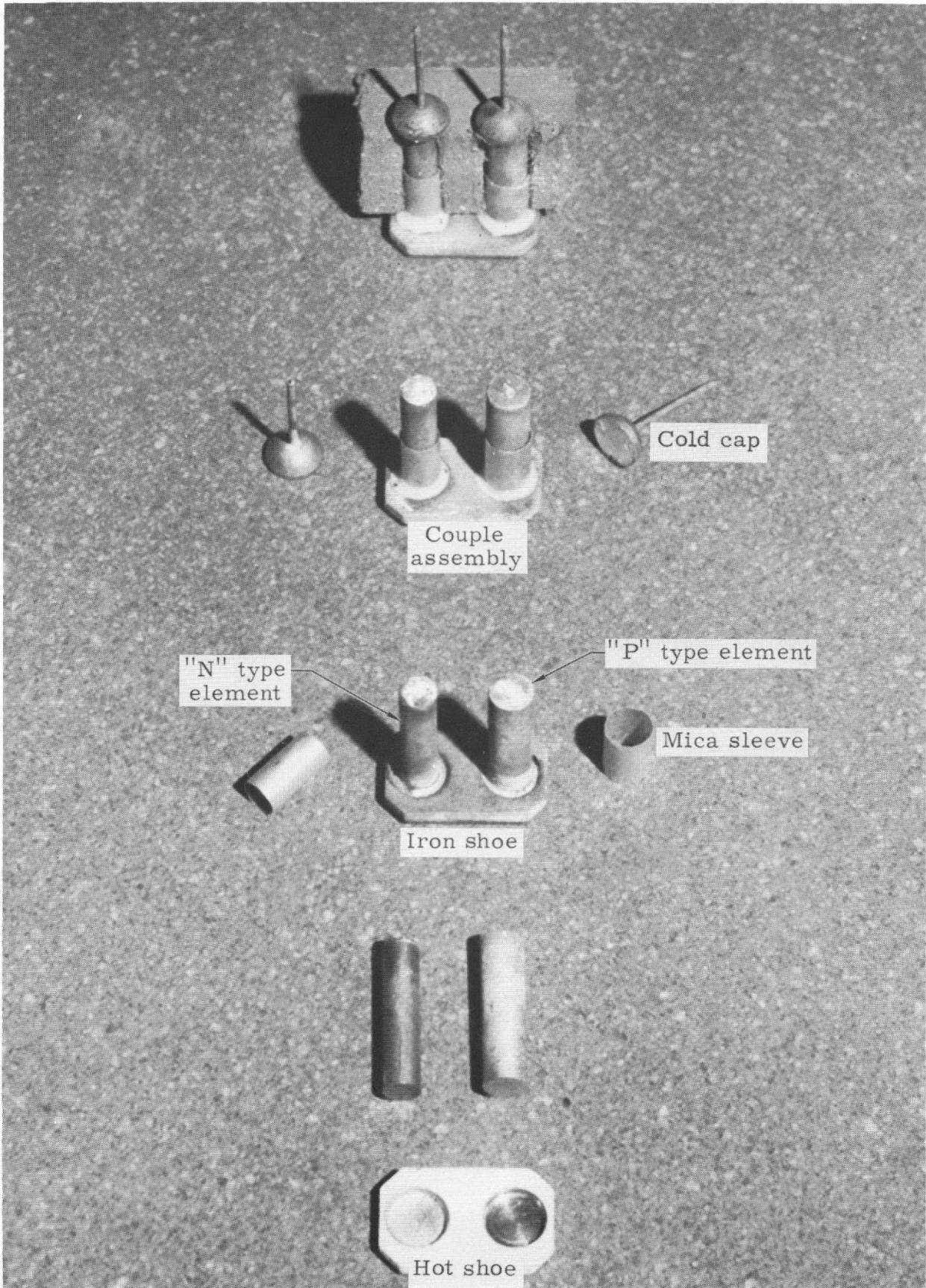
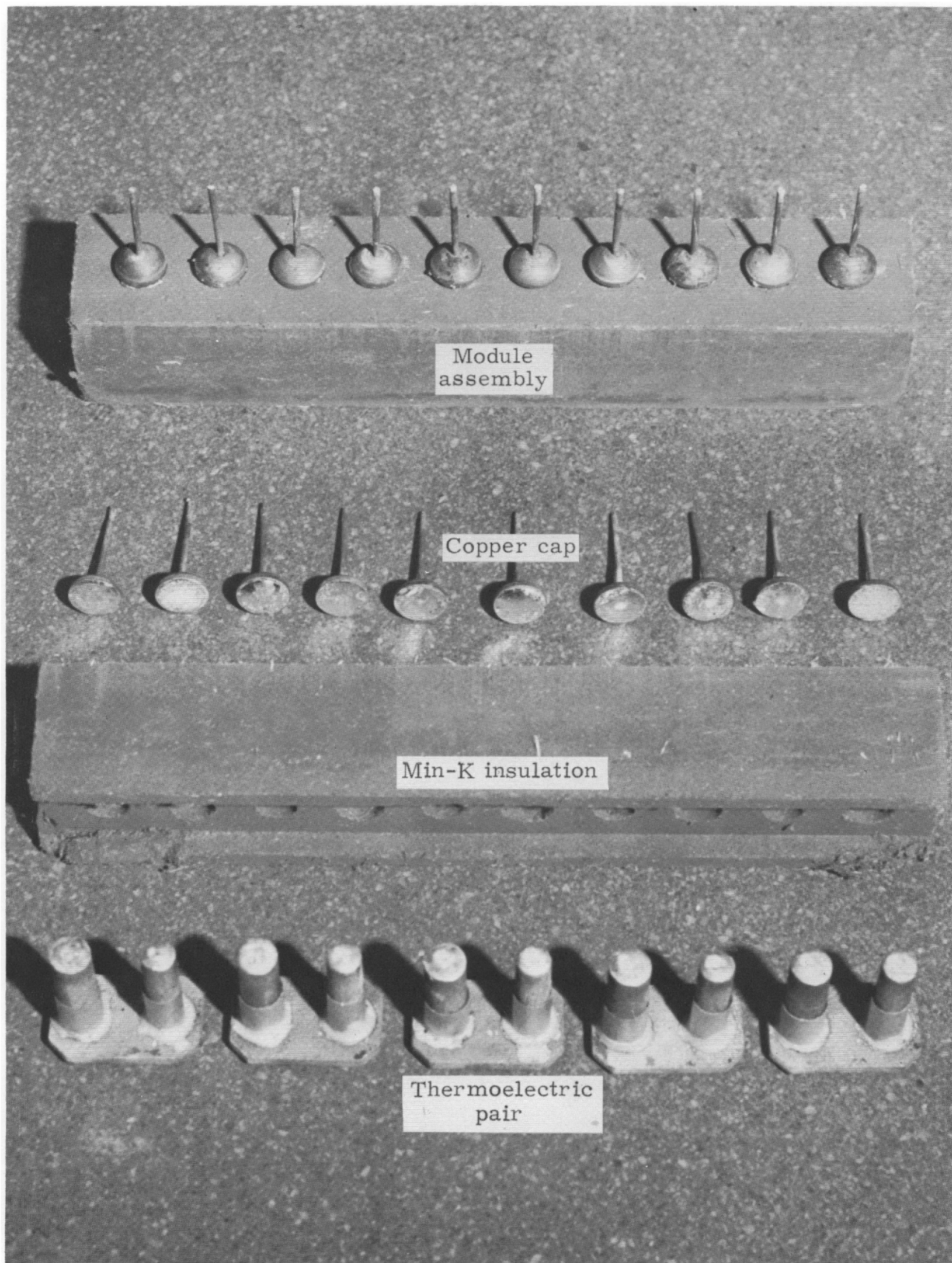Fig. 11. Thermoelectric Element Pair
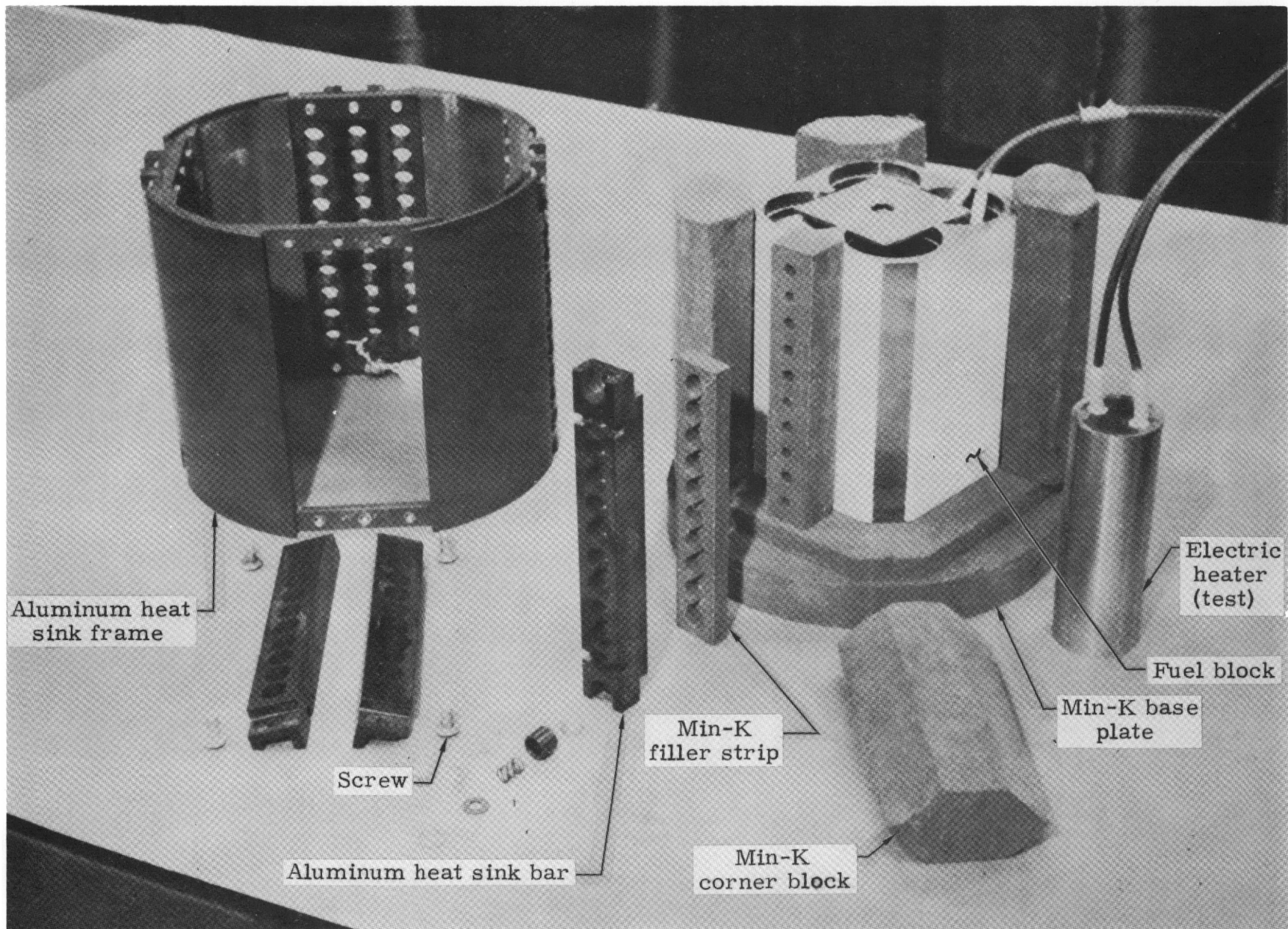
Fig. 12. Thermoelectric Module
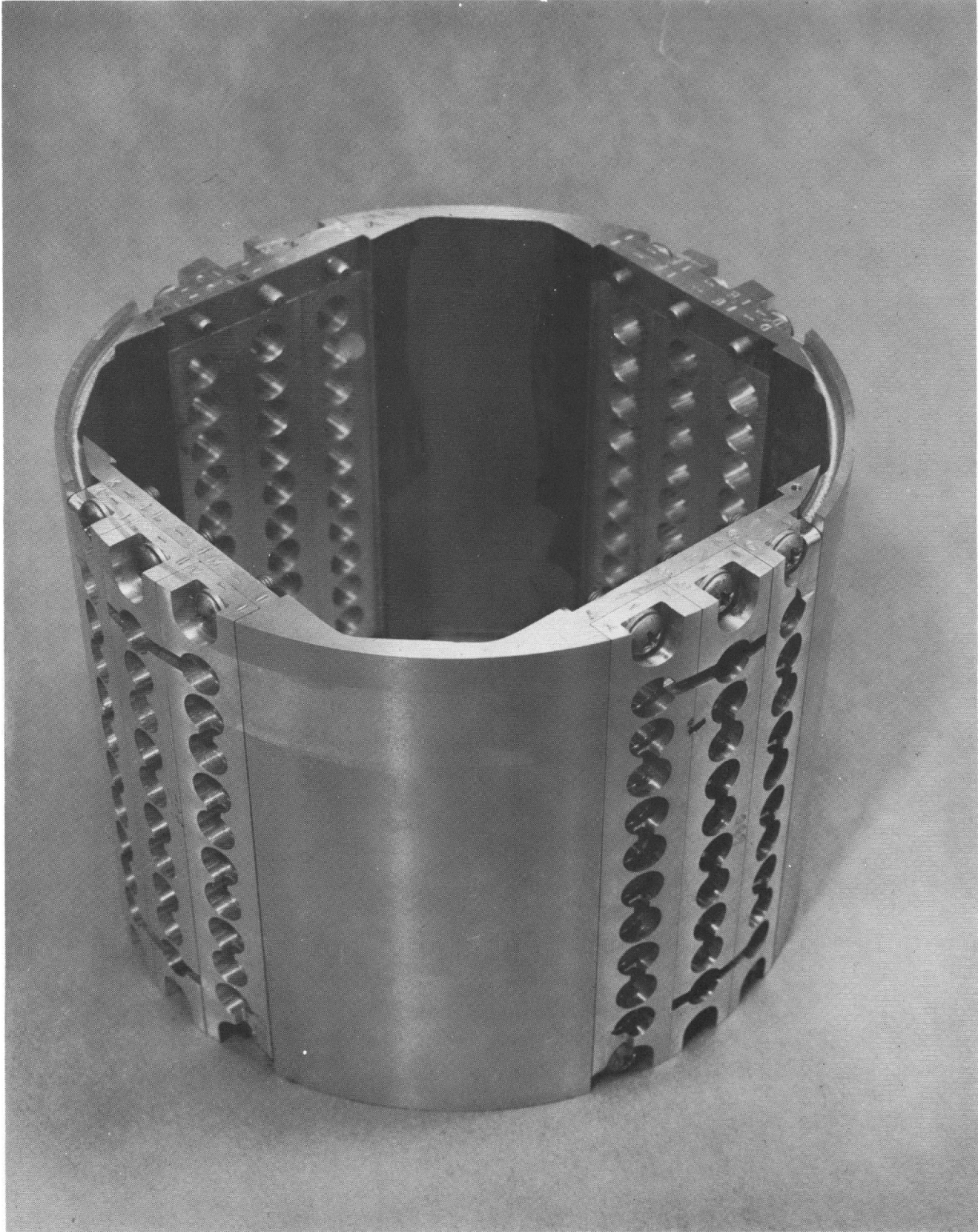
Fig. 13. Generator Assembly

Fig. 14. Heat Sink Showing Heat Sink Bars
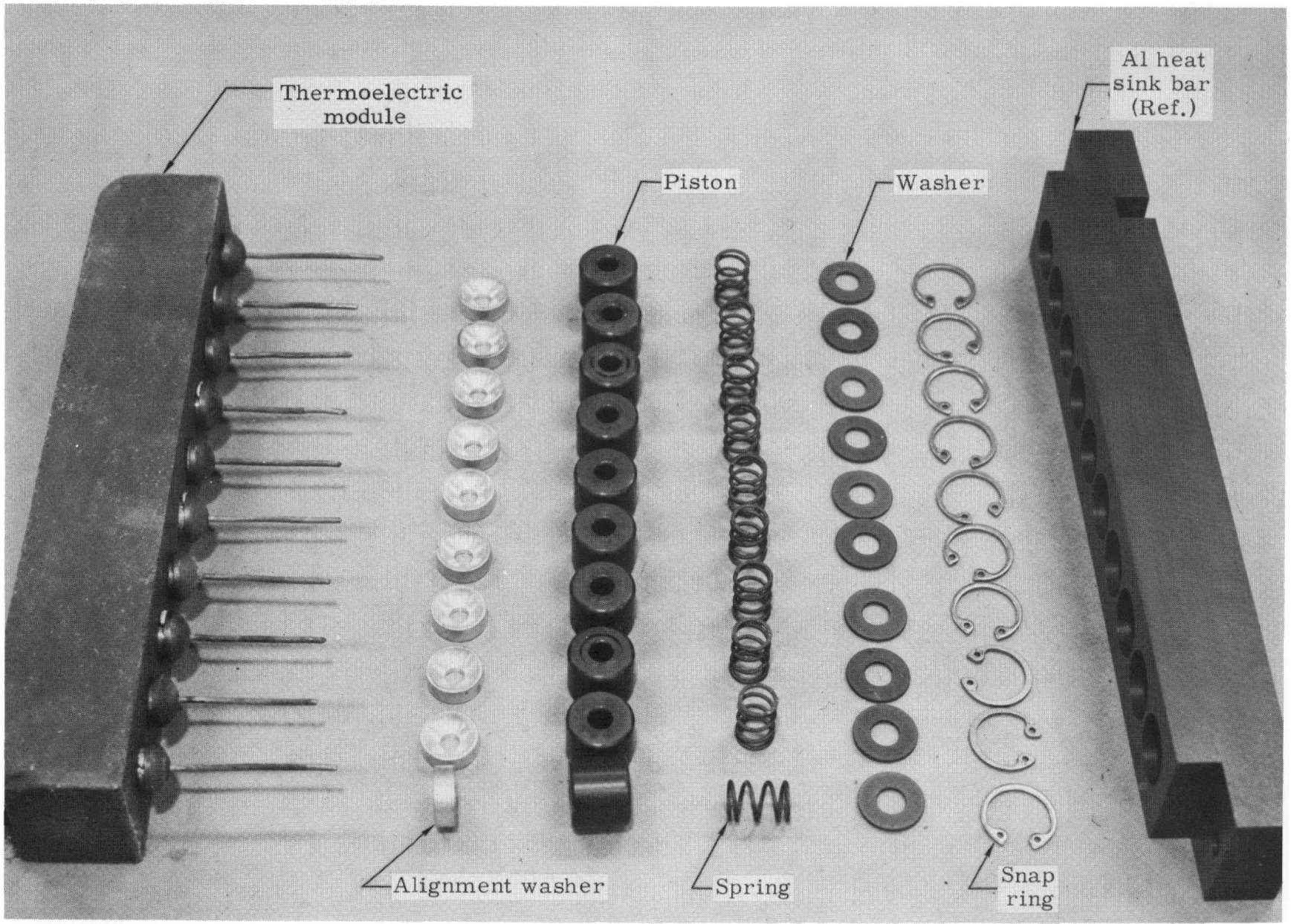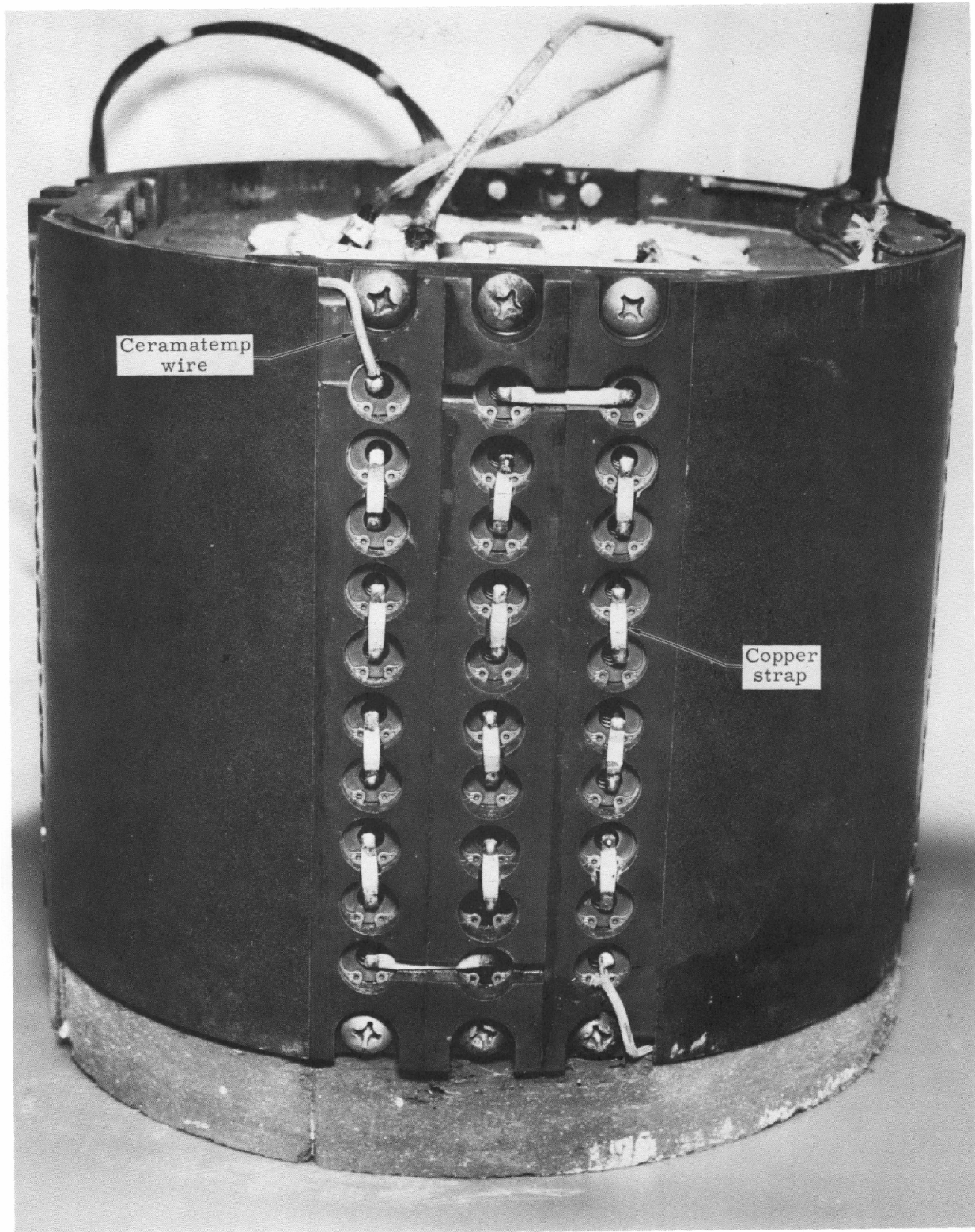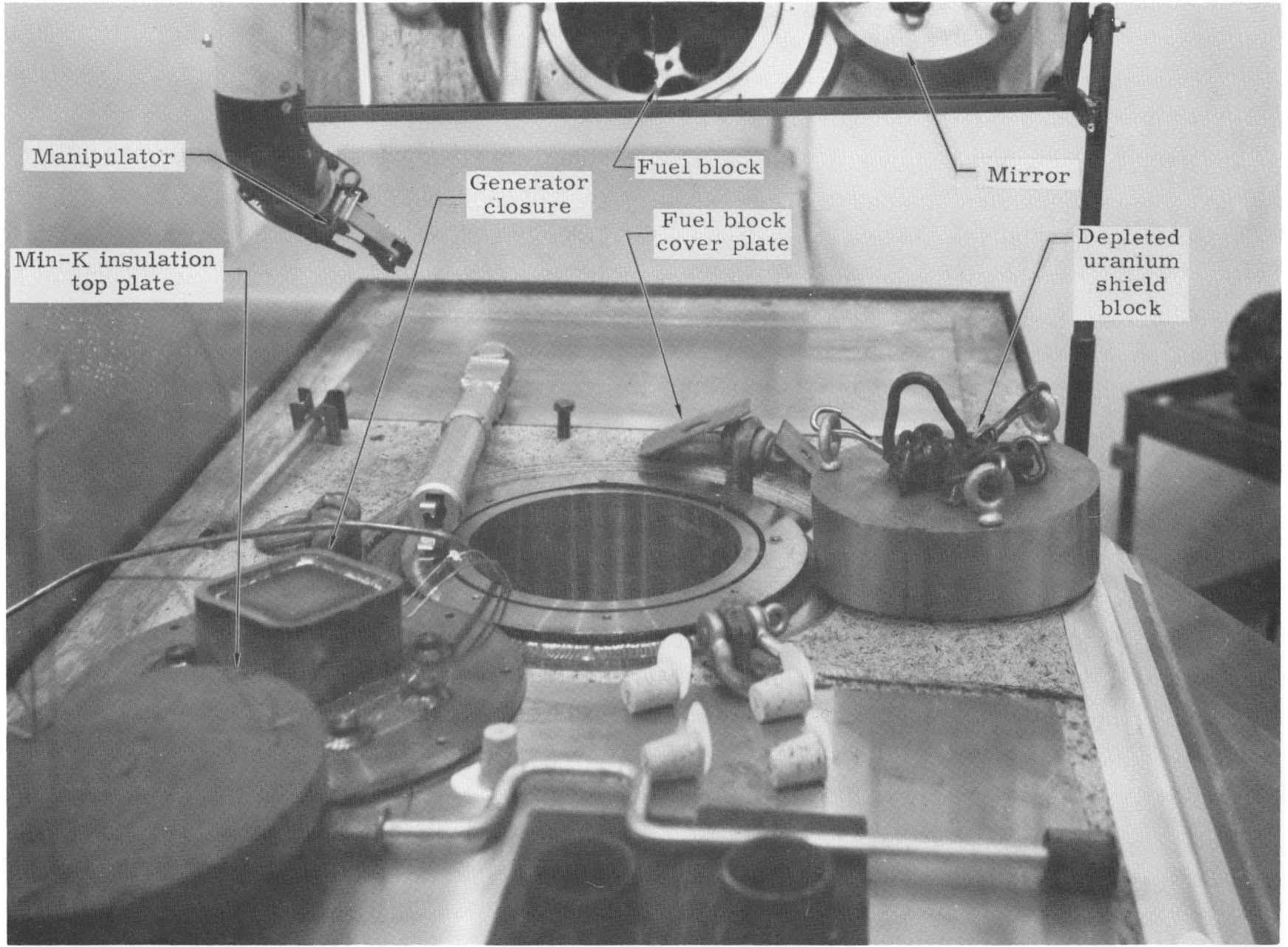
Fig. 15. Thermoelectric Module Components

Fig. 16. Generator Wiring

Fig. 17. Generator Fueling

After completion of electrical testing to verify generator operation, the closure was welded into place and delivered for operational and system testing (Fig. 18).
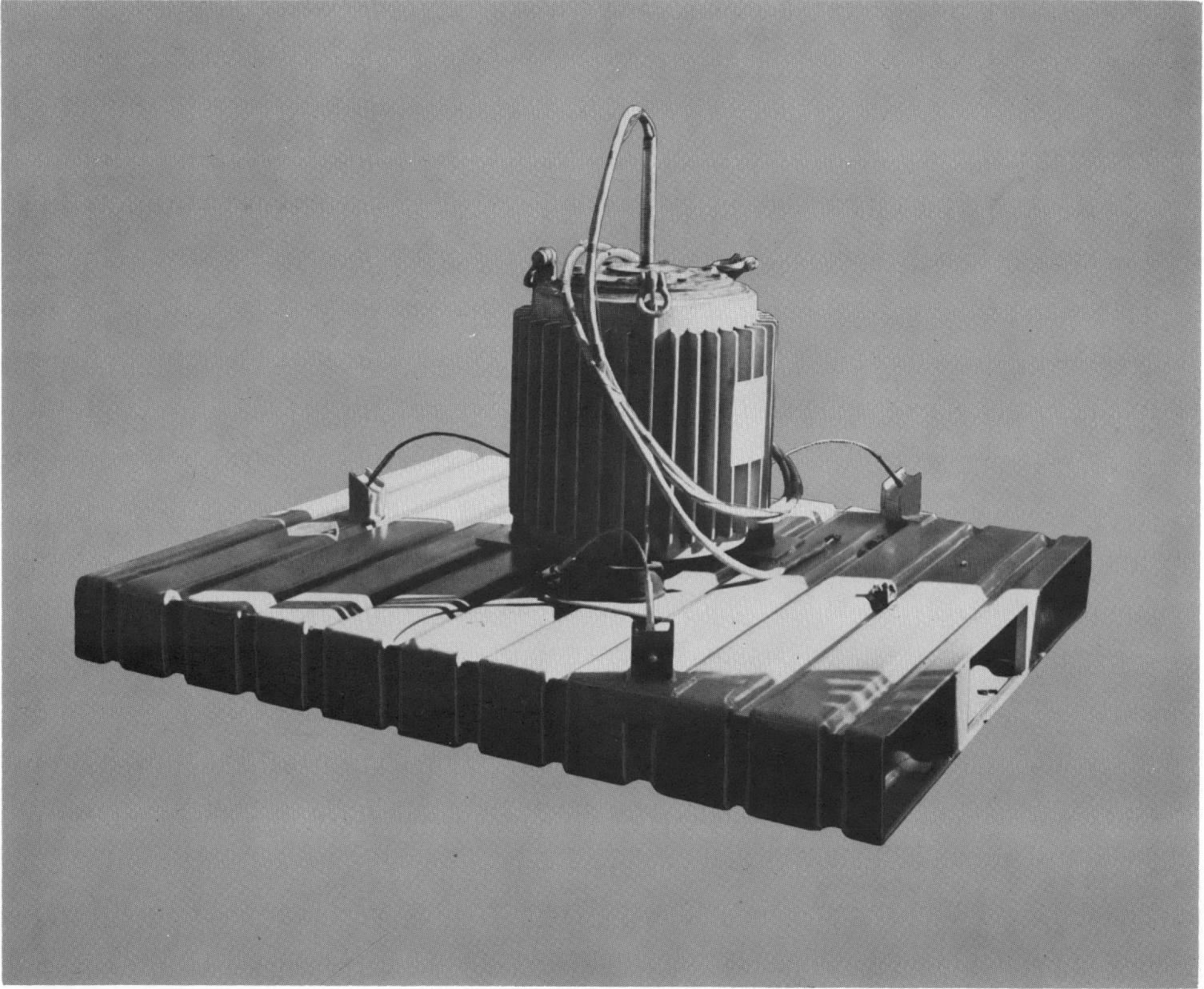
Fig. 18. SNAP 7A Thermoelectric Generator

VI.   ELECTRICAL SYSTEM

The SNAP 7A electrical system is designed to convert the electrical energy supplied by the nuclear-powered thermoelectric generator into a form which can be used by a standard 8 x 26E U. S. Coast Guard flashing light buoy. The thermoelectric generator supplies a nominal 10 watts of electrical power. The output voltage of the generator is converted by a dc-to-dc converter to the proper voltage to charge a storage battery.

The stored energy of the battery in the SNAP 7A electrical system satisfies the intermittent power demand of the buoy light. Since the generator is designed for end-of-life operating conditions, the generator output will always exceed the integrated power demand of the load and will maintain the battery in a fully charged condition.

A.   BATTERY

The electrical storage battery consists of a group of nine nickel-cadmium, rechargeable cells capable of supplying a high discharge current during short periods of time. The cells are divided into three series-connected sections of three cells each. Each section is individually charged to a nominal voltage of 4 volts. The technique of charging the individual section minimizes spreading the cell voltages and consequently eliminates excessive loss of electrolyte.

The system operates at +12 volts with the negative terminal grounded to the buoy through the light casing. A two-wire system is used for high reliability.

B.   DC-TO-DC CONVERTER

The SNAP 7A dc-to-dc converter is a transistorized electronic component that converts the SNAP 7A generator voltage into the charging voltages required by the nickel-cadmium storage cells. Power supplied to the converter by the generator is a function of the isotope life. The SNAP 7A generator supplies a nominal 10 watts of electrical power at end of life with an operating voltage of approximately 5 volts. The converter transforms this power into three voltage-regulated output sections of 4.02 ± 0.06 volts. The regulators are designed to function with a load current variation of 0 to 700 milliamps and an ambient temperature range of 28° to 80° F.

44

The converter schematic is shown in Fig. 19. The input section operates as an overdriven, push-pull, transformer coupled oscillator. It consists of two transistors, Q_1 and Q_2, two resistors, R_1 and R_2, and a toroidal transformer, T_1. The transformer is wound and connected to provide a positive feedback from the collector of each transistor to its emitter. When Q_1 starts to conduct, a voltage is developed across the primary winding of the transformer, inducing a voltage in the feedback winding that drives the emitter of Q_1 positive and causes increased conduction. The current increases rapidly until the collector of Q is driven into the saturation region of its characteristics. When this occurs, the primary voltage can no longer increase and a condition of quasi-stable equilibrium is attained. During this equilibrium period, the voltage drop in the transistor from collector to emitter is very small, and essentially the full generator voltage appears across that half of the transformer primary.

With a constant voltage applied across the transformer primary, the magnetic flux begins to increase with time. Eventually the transformer core reaches saturation and the required exciting current increases rapidly to a value greater than can be supplied. As a result, the primary voltage decreases, reducing the emitter voltage and decreasing the collector current. Thus, transistor Q_1 turns off regeneratively, ending the half cycle. As the flux collapses, voltage is induced in the winding which biases transistor Q_2 to conduction thereby initiating the next half cycle.

The operating of Q_2 during the next half cycle is identical with the operation of Q_1 during the first half cycle with the exception that Q_2 conducts until the core of the transformer is driven into negative saturation. After the core saturates, the flux collapses, and the cycle is complete. The starting circuit of the oscillator consists of two resistors which make up a low impedance bleeder circuit. This circuit will bias the transistors to conduction before oscillations start. A switching frequency of approximately 500 cycles per second was chosen to optimize the core and copper losses in the transformer.

The output section consists of a full wave, center-tapped, capacitor filtered rectifier circuit. It is coupled to the first section by the toroidal wound transformer. The full wave rectifier consists of two diodes, CR_1 and CR_2. When CR_1 is conducting current, CR_2 is biased negative and does not conduct. When this polarity of the transformer secondary changes, CR_2 will conduct current and CR_1 will be biased negative. The center-tap of the secondary winding provides the
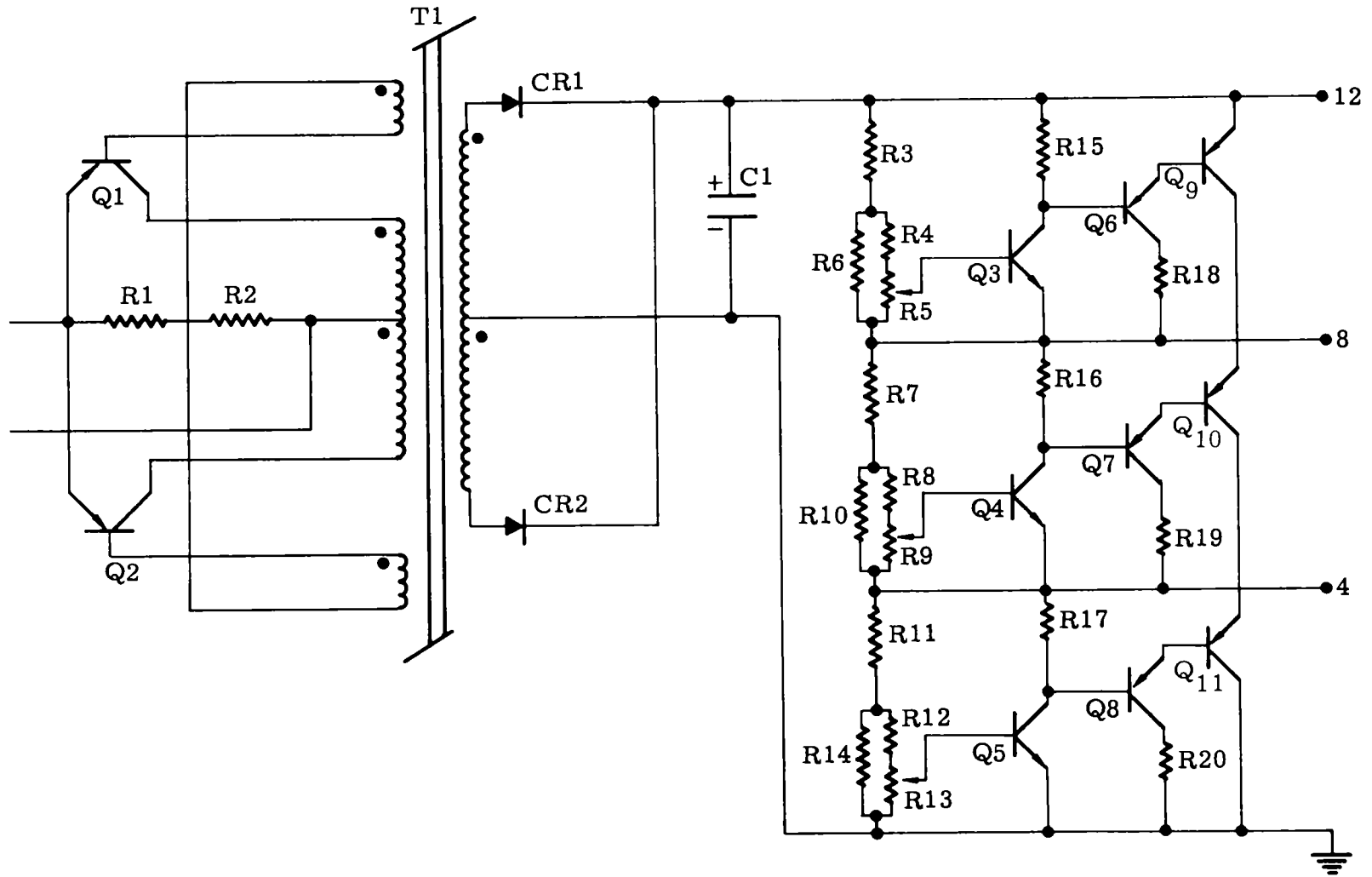
MND-P-2720

Fig. 19. Schematic of SNAP 7A Converter P/N SI611119 DC-to-DC Converter (3 outputs)

ground for this circuit. The capacitor, C_1, acts as a filter to any a-c component that is presented.

The regulator section consists of three series-connected, individually regulated output sections. The voltage across C_1 is equally divided among the three outputs by a temperature-compensated voltage divider network. The operation of the three regulating circuits are identical and only one section will be functionally described. As the voltage across the voltage divider network increases due to a fully charged battery, it causes an increased current to flow through the circuit. This current causes a higher voltage drop across R_5 which biases the switching transistor, Q_3, into higher conduction. This increase in current flow is further amplified by transistor Q_6 which biases the current-dumping transistor, Q_9, into high conduction. The increased current flow through Q_9 loads the converter and slightly reduces its output voltage. This action prevents the batteries from being over-charged, and keeps a constant load on the generator. The output voltage regulation can be adjusted by varying the potentiometer, R_5. This changes the bias voltage swing on the switching transistor, and determines its operational parameters. Temperature effects that would normally change the operating characteristics of this circuit are automatically compensated by resistors R_3 and R_4. These resistors are copper wire wound, and have a positive coefficient of resistance.

Losses in the converter unit were minimized by component selection and design criteria. The 2N1360 switching transistors used in the oscillator were chosen because of their low saturation (typically 0.3 volt at 2 amperes collector current). They have a typical current gain of 40 at 2 amperes collector current. The base drive voltage is typically 0.6 volt at collector current of 2 amperes.

The voltage regulators present the largest single power loss in the circuit. Since the thermoelectric generator supplies more power at the beginning of life than is required by the system, the regulator must detect and dump this excess energy to keep from overcharging the batteries. In addition, the regulator must present a constant load to the generator during fully charged condition of the batteries. This requires complex circuitry which increases the power losses. As a result, the overall efficiency of the converter (including regulators) during normal operation condition is approximately 66%.

Schematic representation of the converter is shown in Fig. 19 and the parts are listed in Table 3. The complete unit was enclosed as a module with the variable resistors mounted for external adjustment. This permits final matching of the converter to the system during installation and subsequent servicing.

TABLE 3

Parts List--SNAP 7A Converter (three outputs)
P/N SI611119

Schematic Part No.	Manufacturer's Part No.	Description	Manufacturer
Q_1 Q_2 Q_9 Q_{10} Q_{11}	2N 1360	Transistor PNP	Motorola
Q_6 Q_7 Q_8	2N 526	Transistor PNP	General Electric
Q_3 Q_4 Q_5	2N 358	Transistor NPN	General Transistor
R_1		68-ohm 1/2-watt resistor 5%	Ohmite
R_2		330-ohm 1/2-watt resistor 5%	Ohmite
R_3 R_4 R_7 R_8 R_{11} R_{12}		50-ohm wire-wound No. 38 wire	
R_5 R_9 R_{13}		0 to 100-ohm 2-watt carbon pot.	Ohmite
R_6 R_{10} R_{14}		39-ohm 1/2-watt resistor 5%	Ohmite
R_{15} R_{16} R_{17}		220-ohm 1/2-watt resistor 5%	Ohmite
Cr_1 Cr_2	IN 538	Rectifier Diode	General Electric
C_1		100-μf capacitor tantalum	Ohmite
T_1	SLT 611125	Transformer	Martin Marietta

VII. OPERATIONAL TESTING OF SNAP 7A
SYSTEM AND COMPONENTS

The operational tests conducted on the SNAP 7A system and components were cyclic and environmental variation tests to determine performance, power requirements, and stability of operation. The tests were conducted with both a simulated system and the actual system. The simulated system differs from the actual system in that an external d-c power supply is employed rather than the power supply of SNAP 7A thermoelectric generator. The wiring diagram and test data for the simulated system are presented in Figs. 20 and 21, respectively. Other system components tested were the dc-dc voltage converter, the nickel-cadmium battery, and the buoy light.

A. SNAP 7A GENERATOR

The SNAP 7A generator was tested with both an electrical heat source and the isotope heat source. Electrical tests were conducted with argon-helium internal gas mixtures and varying power inputs. Typical operational curves are presented in Figs. 22 through 25. After tests with the electric heat source verified satisfactory operating characteristics, the generator was shipped to the Martin hot cell facility at Quehanna, where Strontium-90 (40,800 curies) in the form of the titanate was loaded into the generator.

The testing of the fueled SNAP 7A generator was begun on November 22, 1961. The generator ambient air was maintained at a temperature of 0° F (equivalent to approximately 55° F water temperature). The power out at matched load (3.75 ohms) was 11.59 watts with a hot junction temperature of 934° F. Hot junction temperatures were checked at ambient temperatures of 10°, 20° and 25° F (equivalent to 65°, 75° and 80° F water temperature). The maximum hot junction temperature measured was 946° F, well below the upper limit of operating temperatures (980° F).

B. FLASHER CIRCUIT

Component tests were initiated on September 15, 1961. The initial tests were carried out on the flasher circuit to determine its power requirements over the maximum temperature range conceivable. The first flasher tested required 4.73 watts at 0° F ambient temperature and 4.48 watts at 125° F. This flasher froze when the ambient temperature was decreased to -40° F, and had to be replaced. It was later found that improper lubrication had caused moving parts to freeze.
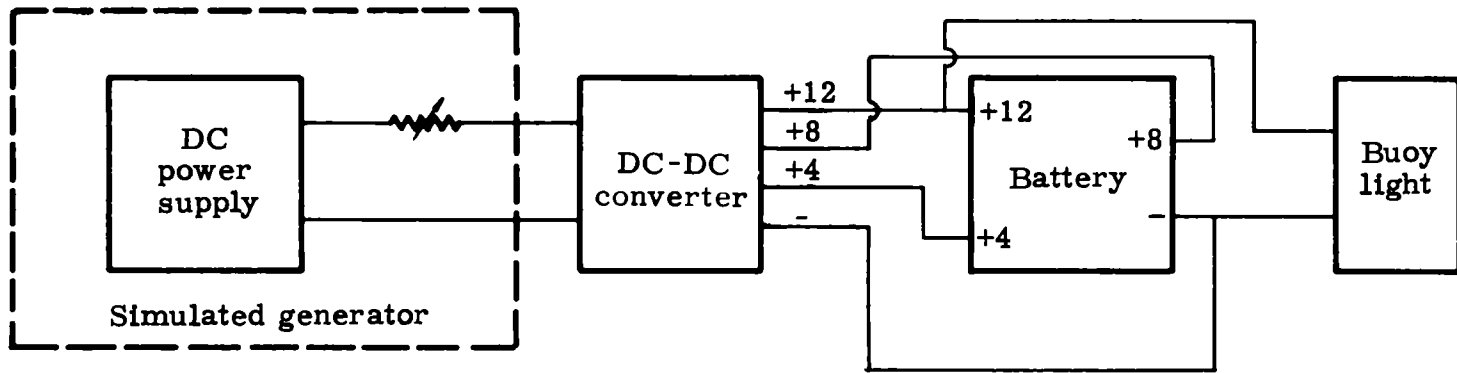
Fig. 20. Wiring Diagram of Simulated SNAP 7A System
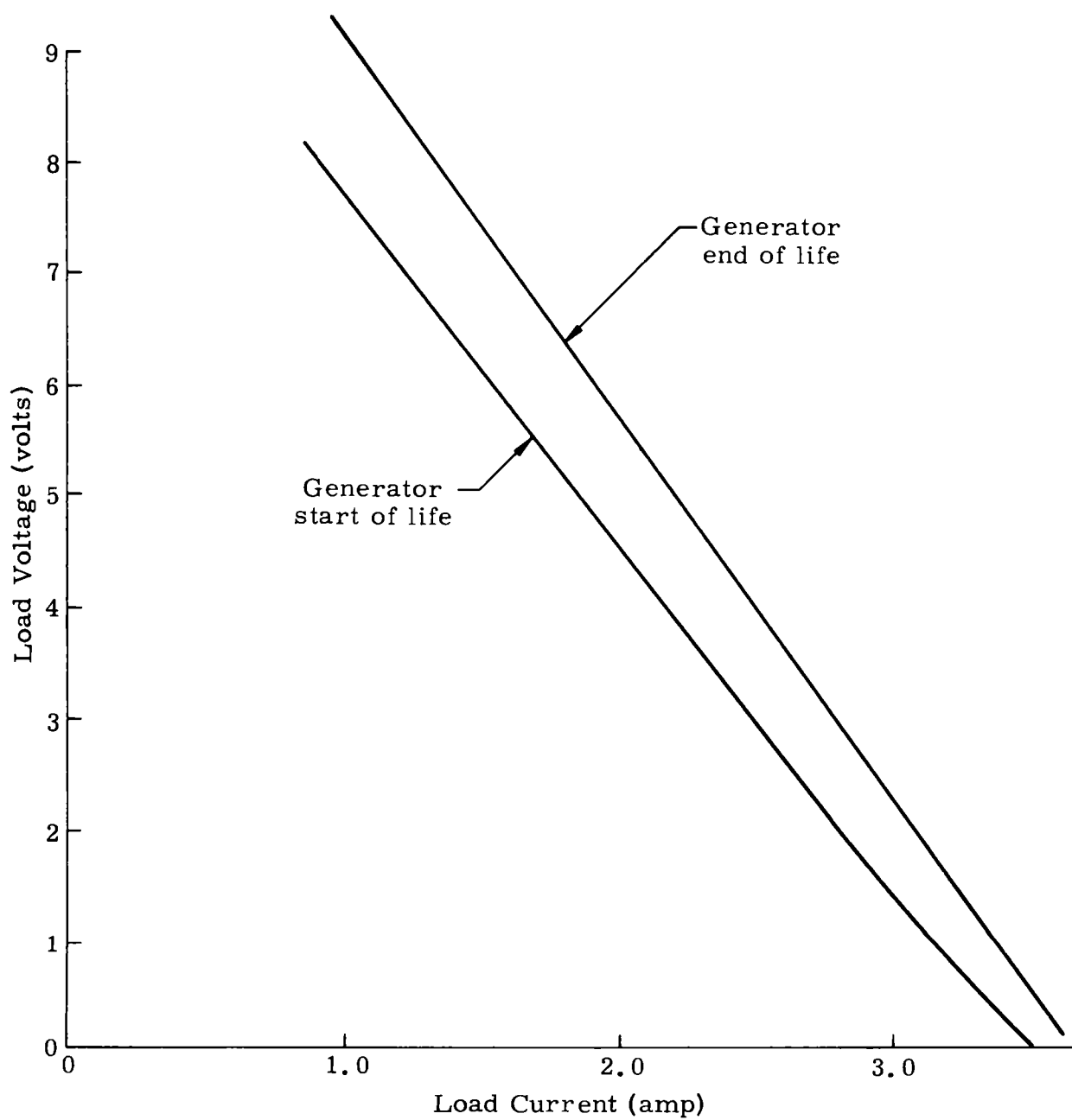
Fig. 21. Load Voltage Versus Current Curves for Simulated SNAP 7A System

Fig. 22. Plot of Parametric Data for SNAP 7 A-C Operating Model, Where Power Input Was 266. Electrical Watts and Internal Gas Composition Was 100% Helium (1.05 atm)

Fig. 23. Plot of Parametric Data for SNAP 7A Generator, Where Power Input Was 248 Electrical Watts and Internal Gas Composition Was 100% Helium (1.05 atm)

MND-P-2720

Fig. 24. Plot of Parametric Data for SNAP 7A Generator, Where
Power Input Was 252 Electrical Watts and Internal Gas
Composition Was 75% Argon and 25% Helium (1.05 atm)

Fig. 25. Plot of Parametric Data for SNAP 7A Generator, Where Power Input
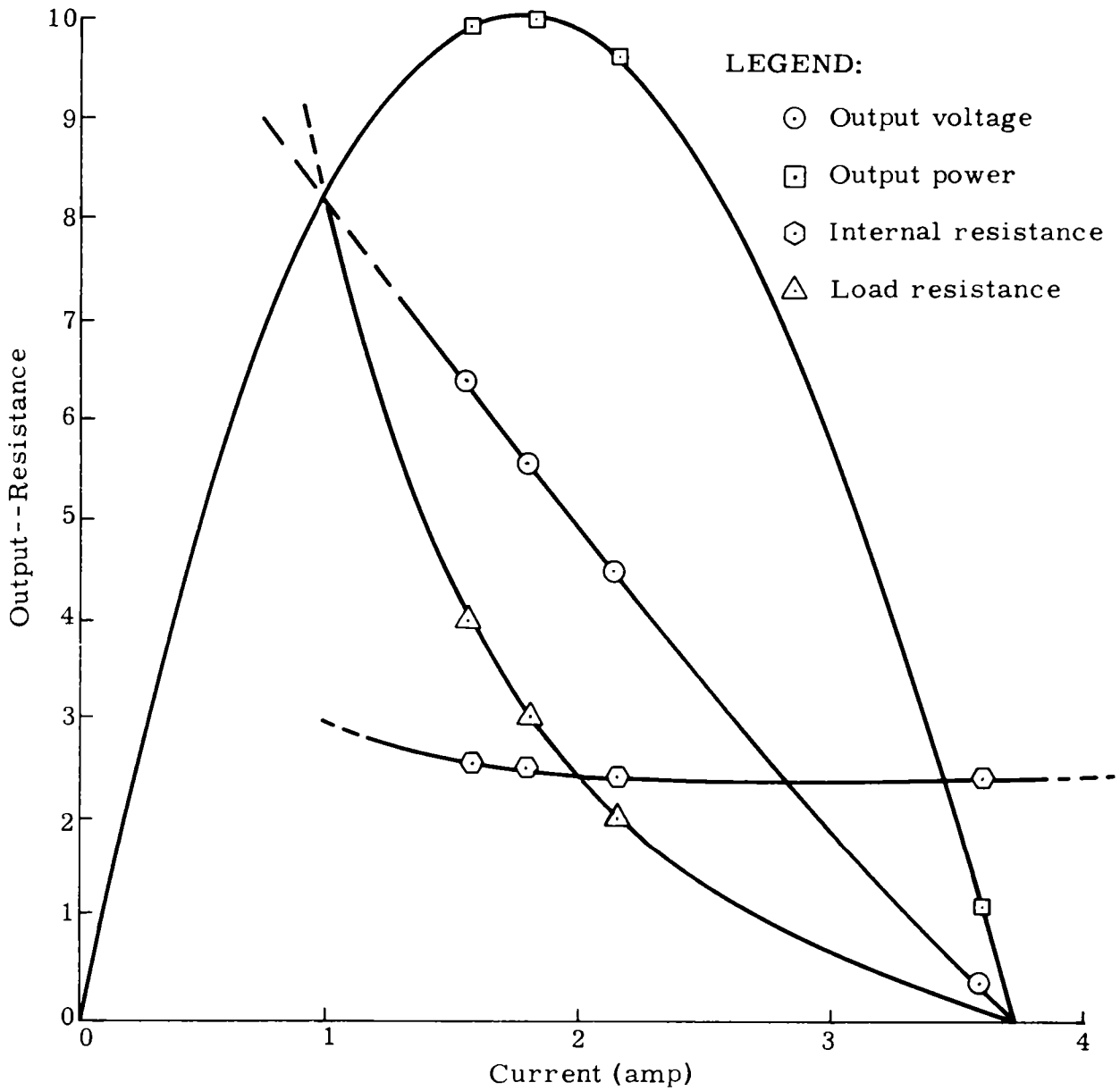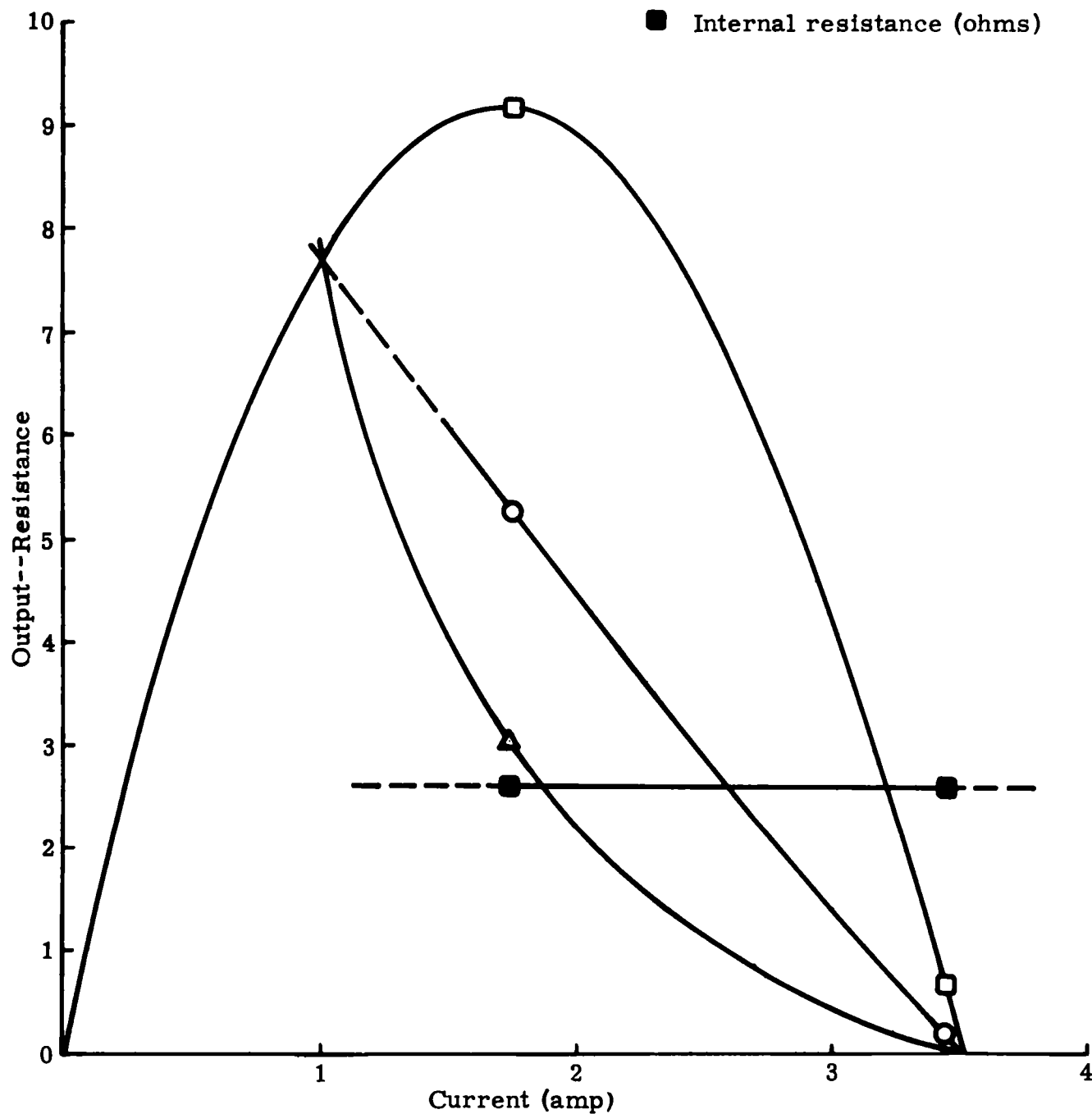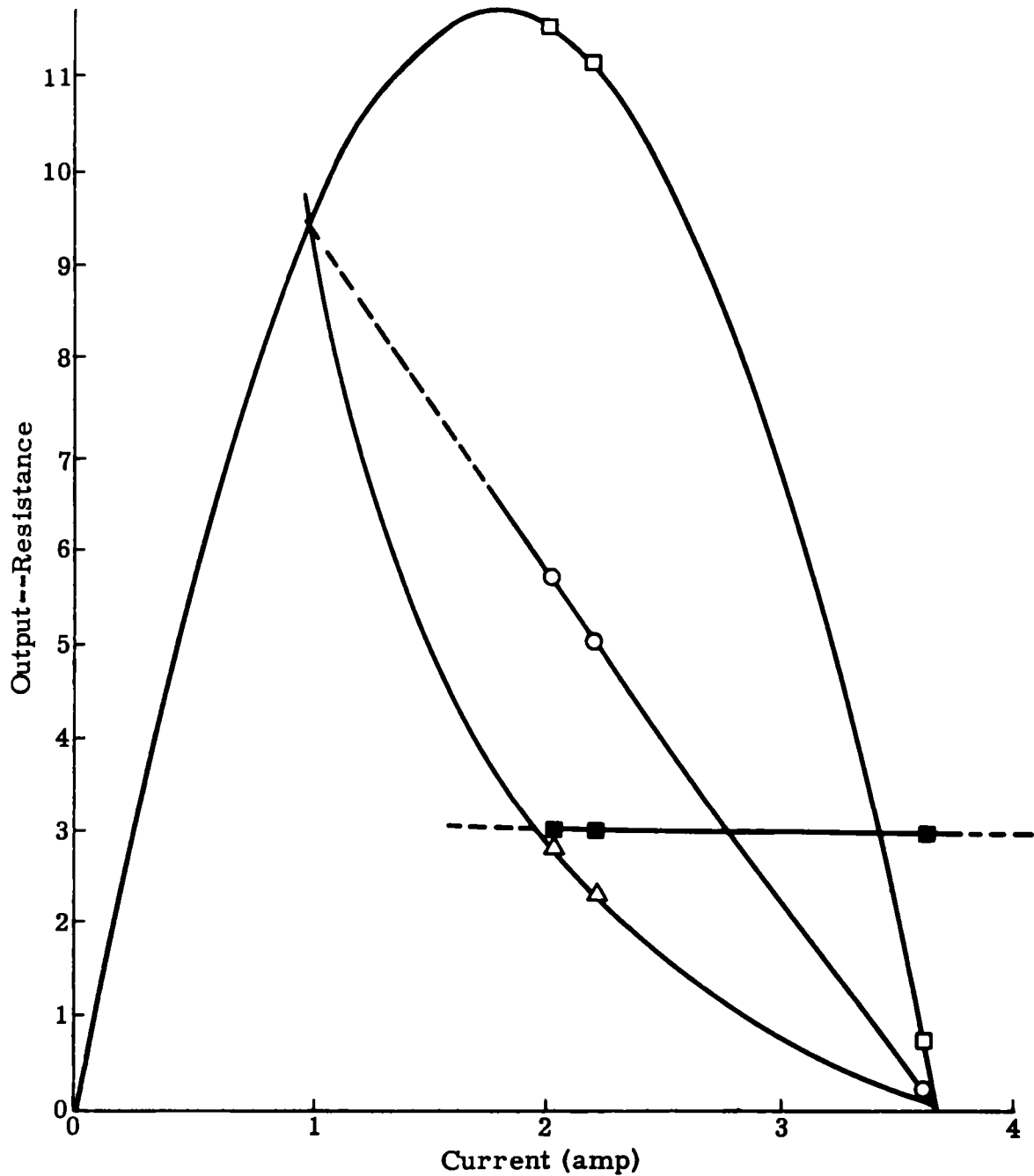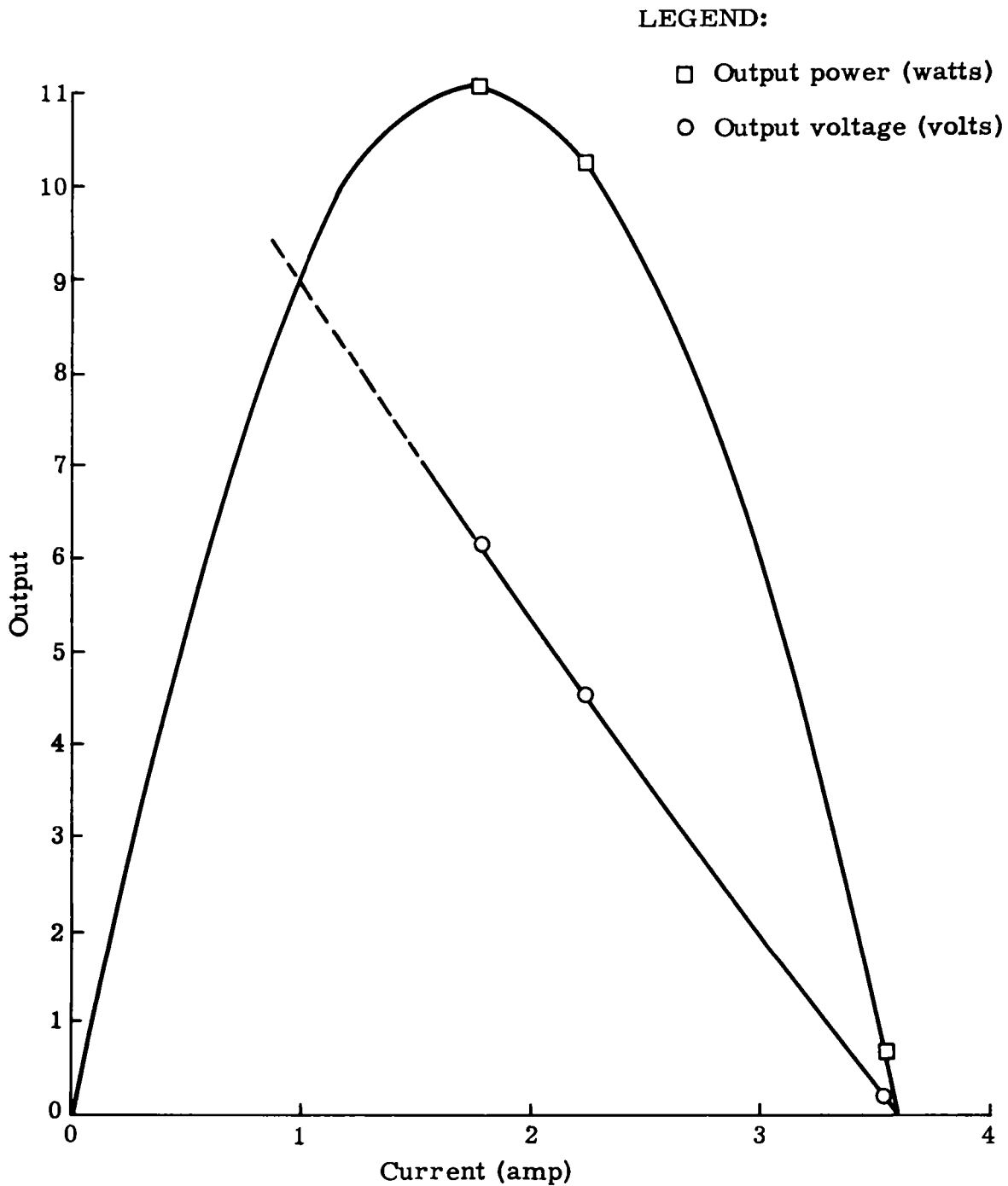Was 240 Electrical Watts and Internal Gas Composition Was 75%
Argon and 25% Helium (1.05 atm)

The average power consumption of the replacement was 4.86 watts at -40° F and 4.81 watts at 125° F. The average duration of the flash was 0.305 second out of an average cycle time of 4.007 seconds. Typical test results are presented in Fig. 26.

C. BATTERY AND CONVERTER

Operational tests of the SNAP 7A battery began on September 15, 1961. The primary object of the test was to ensure that the battery voltage remained within the specified voltage of 1.33 to 1.38 volts per cell. The lower limit was established to utilize the maximum capability of each cell, and the upper limit was fixed to hold cell electrolyte loss to a minimum.

Much difficulty was first encountered in maintaining uniform voltage between the prescribed limits throughout the battery. Attempts were made to remedy this situation by discharging and recharging the battery, and by replacing individual cells with those of an extra battery pack, but the variation in voltage between the individual cells was not appreciably reduced. Because of the voltage variation, the original single output converter was replaced with the triple output converter described in Chapter VI. With each of the three converter outputs controlling the voltage across three of the nine battery cells, the fluctuation in cell voltage was markedly reduced. The final result of the battery voltage room temperature tests showed variations of 32, 26 and 6 millivolt with an average of 1.35 volts per cell. Cell voltage data for the single output (section) and triple output (three-section) converters are presented in Figs. 27 and 28.

The triple output converters were found to be more sensitive to variations in temperature than the original converter. Efforts to correct this fault by changing the variable potentiometer adjustments and changing the Zener diodes were not successful. Another modification, that of using copper-wound resistors and eliminating the Zener diodes, improved the temperature stability, and initiated a change of only 0.20 volt per section between 25° and 75° F as shown in Fig. 29.

D. SNAP 7A SYSTEM ACCEPTANCE AND OPERATION

The SNAP 7A system acceptance test was conducted on December 12, 1961. All acceptance specifications were met. The generator system was delivered to the U. S. Coast Guard on December 15, 1961 and was installed in the buoy the same day. The hot junction temperature was measured by contractor personnel on December 18, 1961. This temperature was found to be 903° F with a water temperature of 41.5° F. Measurements taken on December 22, 1961, resulted in a fuel block temperature of 932° F, a hot junction temperature of 897° F, and a power output of 10.52 watts at 6.1 volts. All phases of operation were satisfactory.
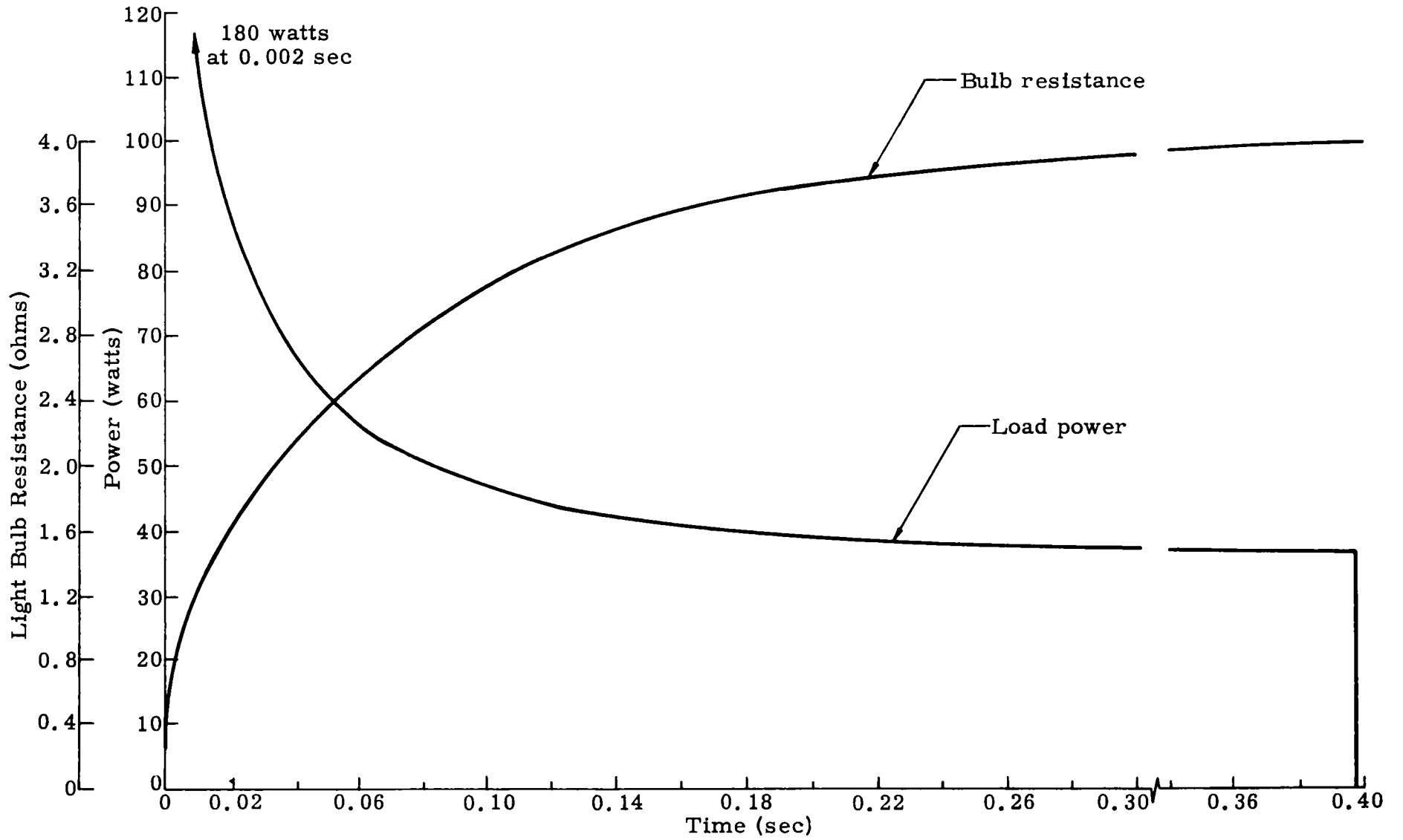
Fig. 26. Power and Resistance of Light Bulb Versus Time During One
Light Flash (ambient bulb temperature = -40° F)

58

0 to 9 days at room temperature
10 to 13 days at 0° F
14 to 21 days at 90° F
29 to 39 days at room temperature

● No. 2 replaced by No. 1'
No. 5 replaced by No. 4'
No. 10 replaced by No. 9'

——— Cell No. 2
- - - Cell No. 5
—·— Cell No. 10

● No. 6 replaced by No. 6'

Prime Nos. are cells
from 2nd battery

——— Cell No. 4
- - - Cell No. 6
—— Cell No. 8

——— Cell No. 3
- - - Cell No. 7
—— Cell No. 9

Fig. 27. Cell Voltages Versus Time (single-section converter)

MND-P-2720
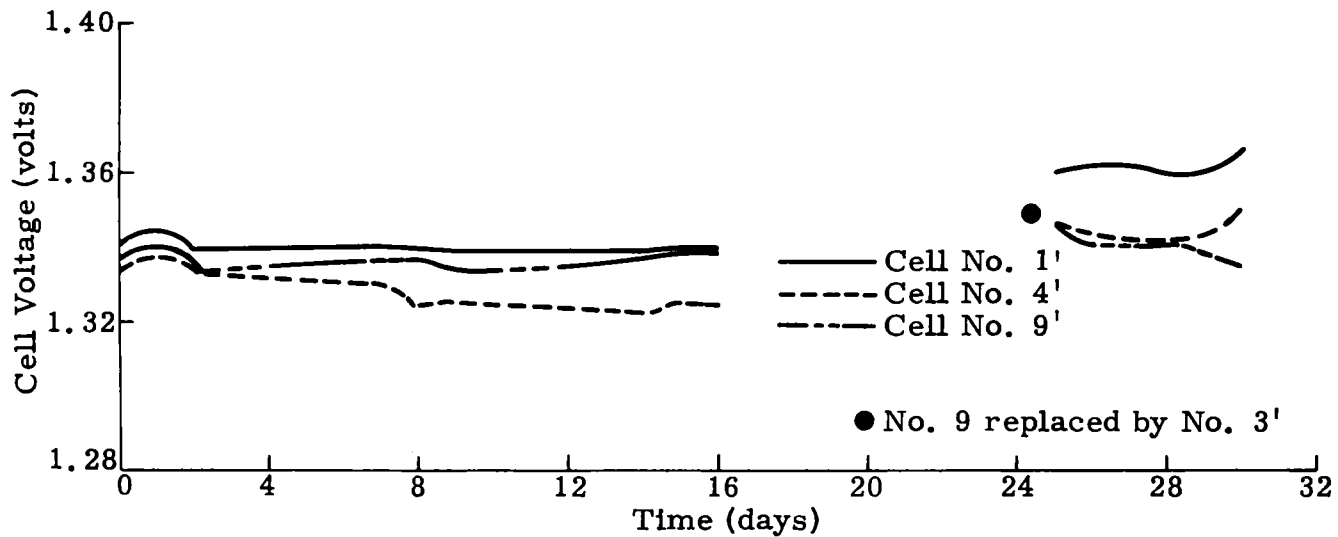
Fig. 28. Cell Voltages Versus Time (three-section converter)--Battery at
Room Temperature

MND-P-2720
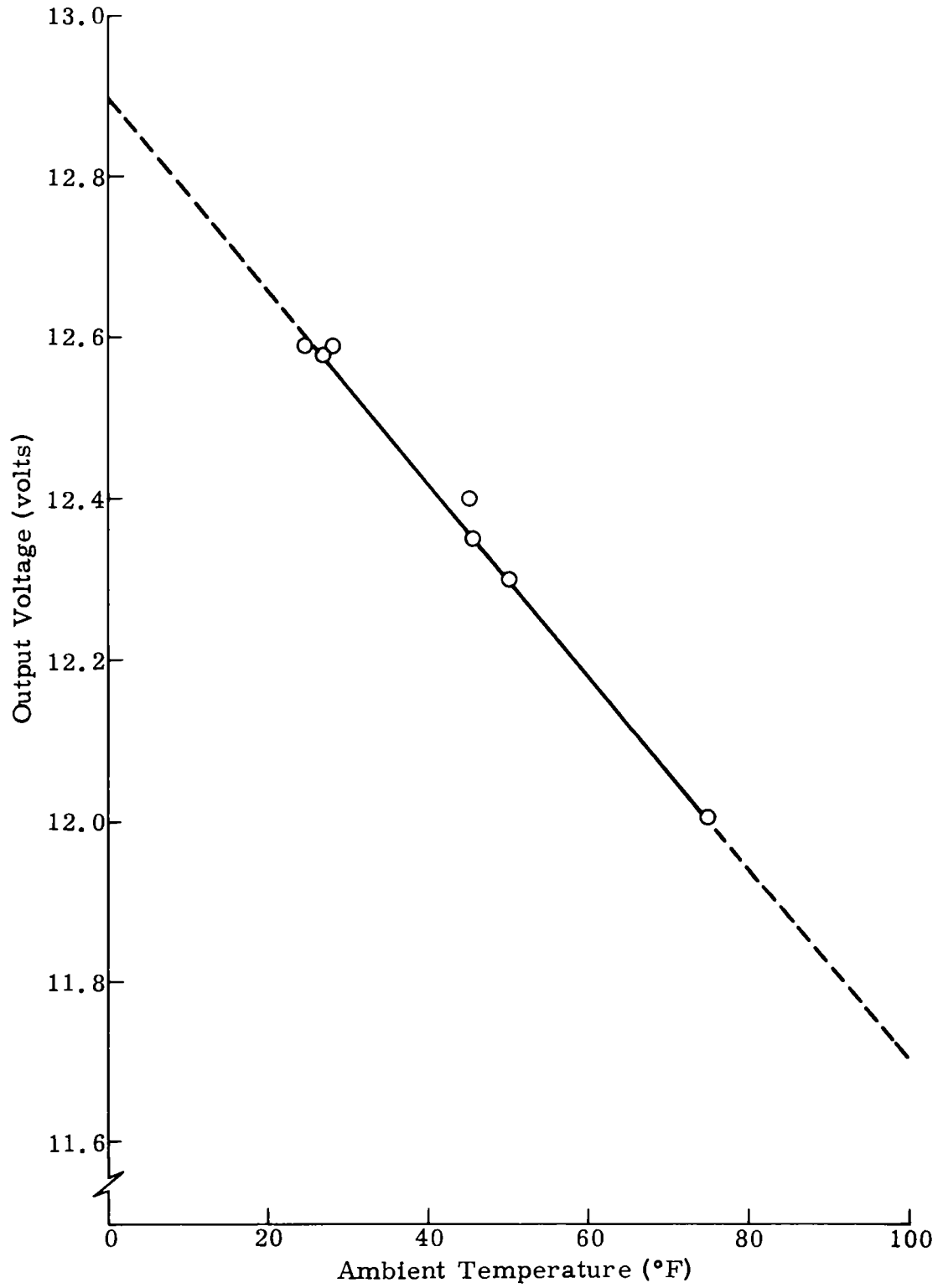
Fig. 29. Output Voltage Versus Ambient Temperature for Three-Section Converter

VIII. ENVIRONMENTAL TESTING OF SNAP 7A ELECTRICAL GENERATION AND STORAGE SYSTEM

Environmental qualification of the major system components is necessary because:

(1) The equipment, after exposure to normal accelerations and vibrations, must be operable and must sustain no major damage from induced shock or vibration loads.

(2) The equipment must be capable of operation under the environmental conditions encountered at the installation site.

The tests were conducted under the conditions set forth in applicable portions of the statement of work (Ref. 4).

A. DESCRIPTION OF TEST SPECIMENS

The SNAP 7A-7C test generator was used for the environmental tests.

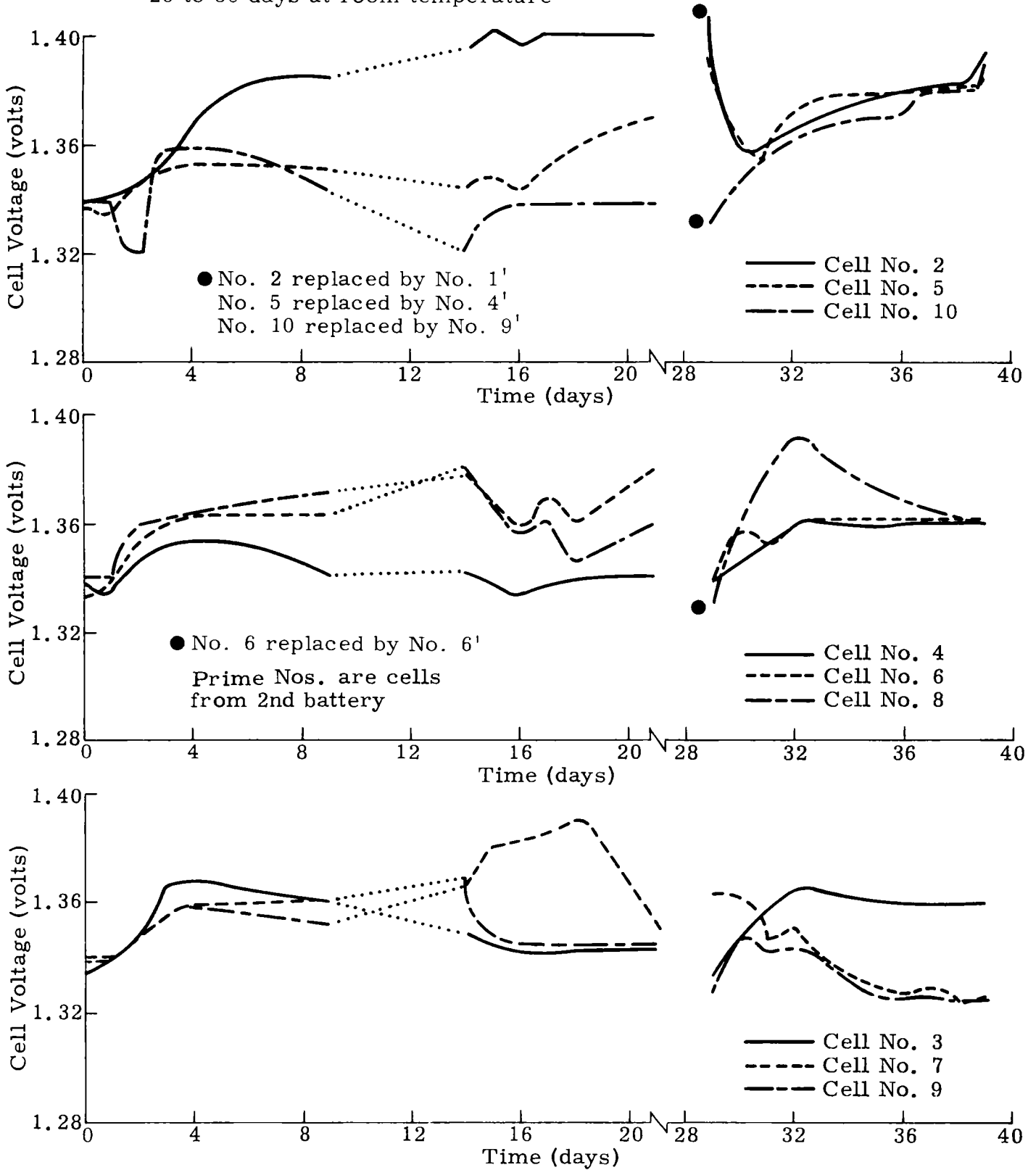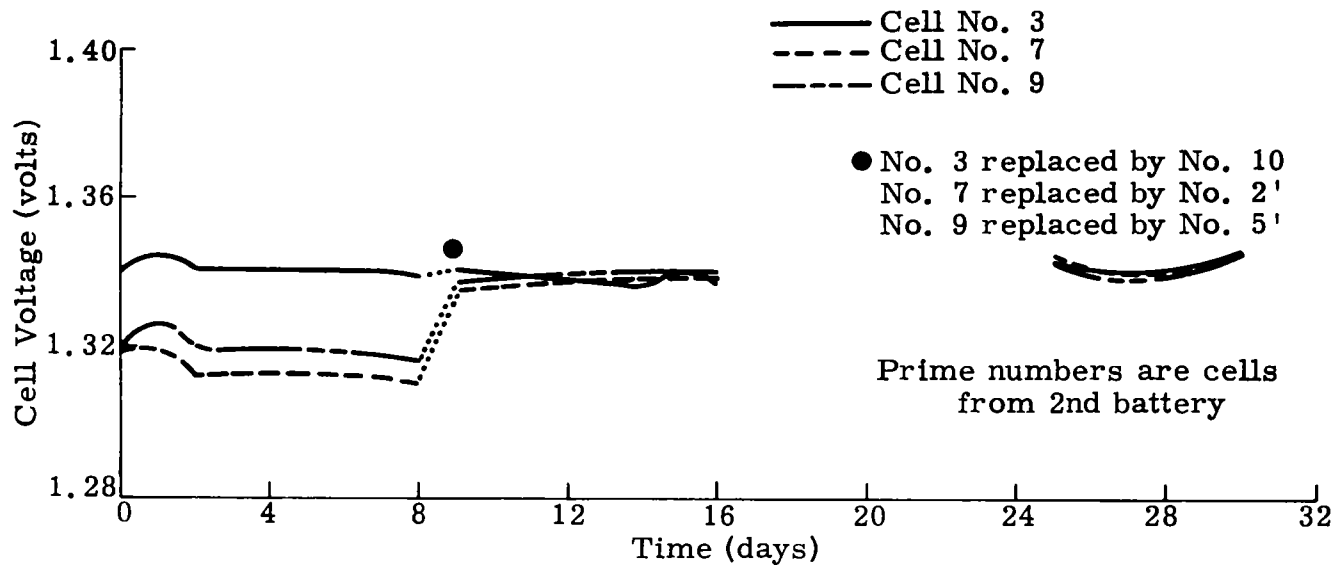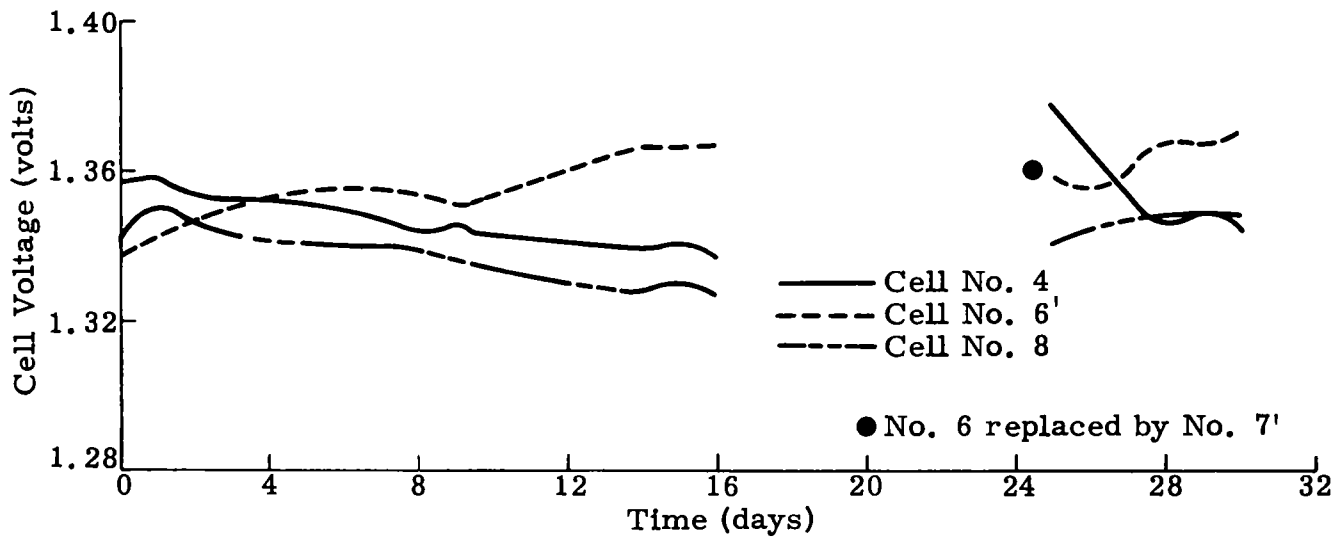The biological shield was not used in the mechanical tests, since it had no effect on the mechanical properties of the generator; to include the shield would considerably complicate the tests. The simulated decay heat was removed by circulating water through an aluminum cooling jacket (see Fig. 30). The temperature tests, on the other hand, were conducted with the unit assembled in the biological shield so that the heat-transfer properties were duplicated as indicated by Fig. 31. The battery and converter were tested at the same time. Typical test configurations are shown in Fig. 32 and 33.

B. TEST CONDITIONS

The thermoelectric generator, converter, and battery were subjected to vibration, shock, and temperature tests as described in this subsection.

1. Vibration Tests

Since the SNAP 7A and 7C generators are identical, one model was subjected to a composite environment consisting of the following:
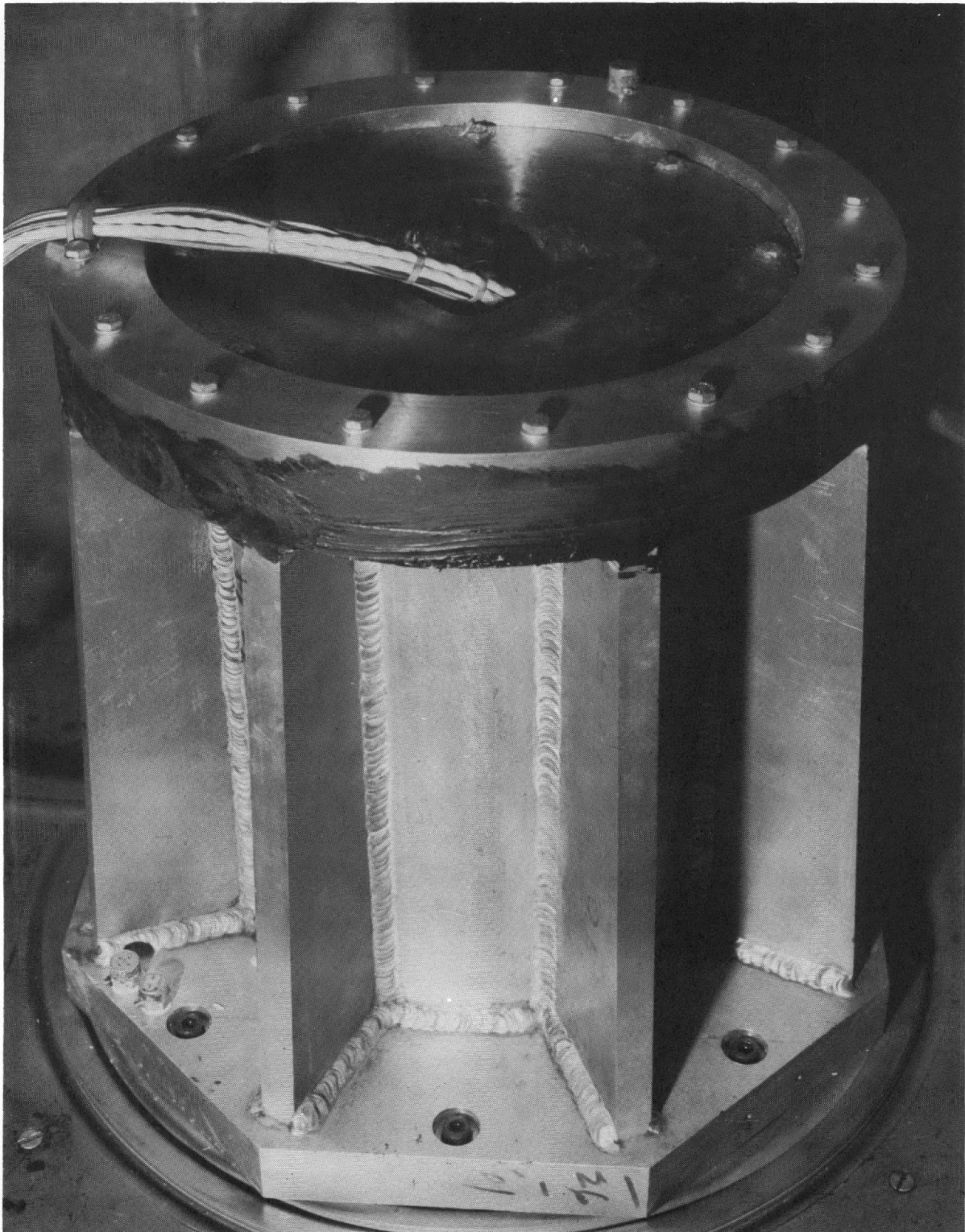
Fig. 30. SNAP 7A-7C Thermoelectric Generator and Test Fixture Positioned on MB-C25 Electrodynamic Shaker for Vertical Excitation

LEGEND:

○   Hot junction, TC No. 27   △   Fin temperature (avg)

□   Cold cap, TC No. 28   ●   Power output
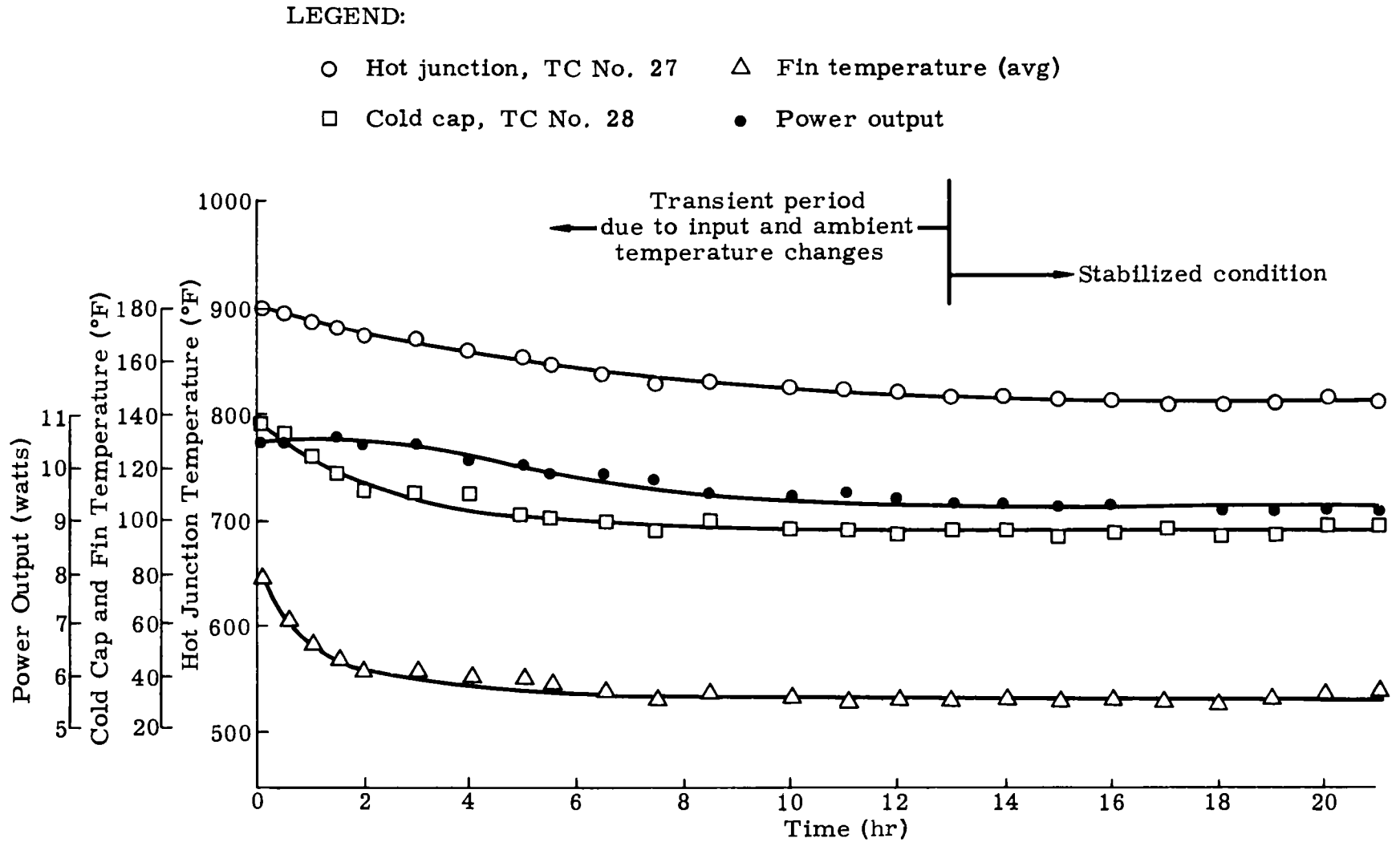
Fig. 31.   Results of SNAP 7A and SNAP 7C Generator Temperature
Chamber Tests, Where Nominal Power Input Was 247.5 Watts,
Ambient Air Temperature Was 28° F, and Generator Atmosphere
Was 50% Argon and 50% Hydrogen
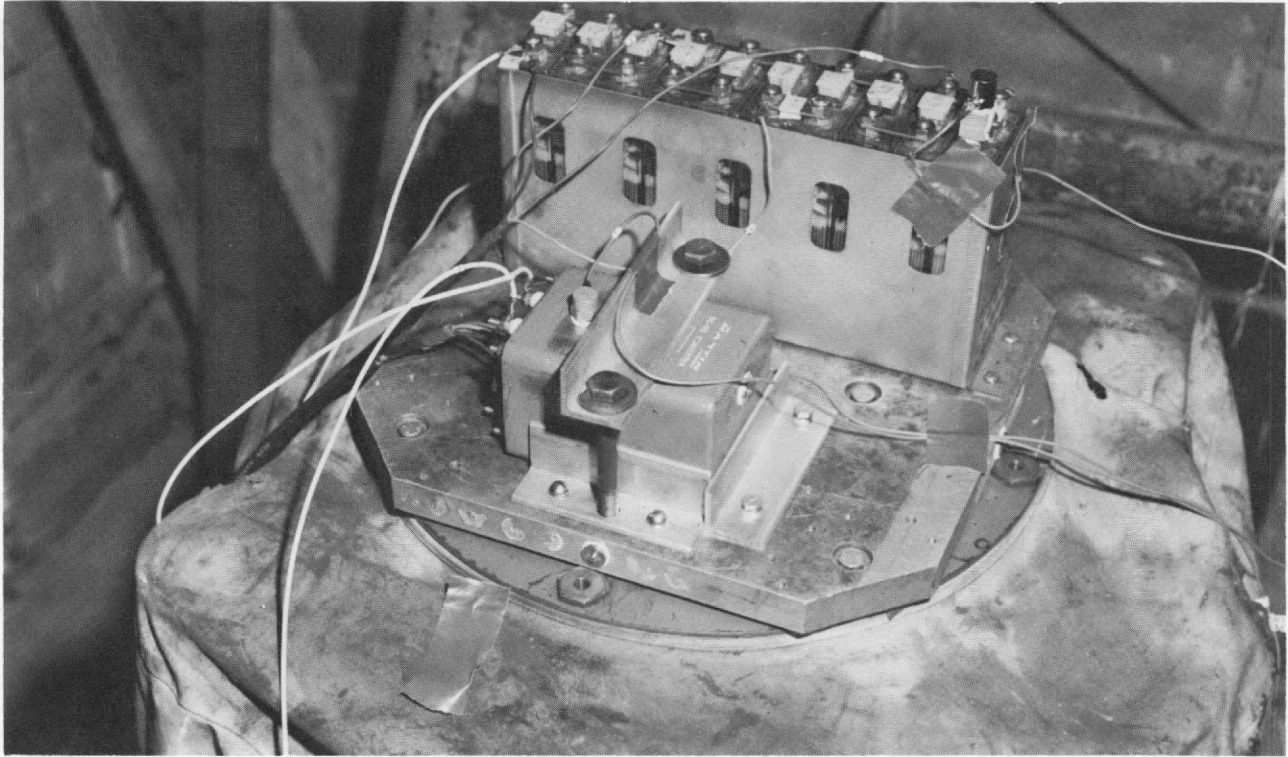
Fig. 32. SNAP 7A Battery and Converter Positioned on MB-C25 Electrodynamic Shaker for Vibration Test in Vertical Plane
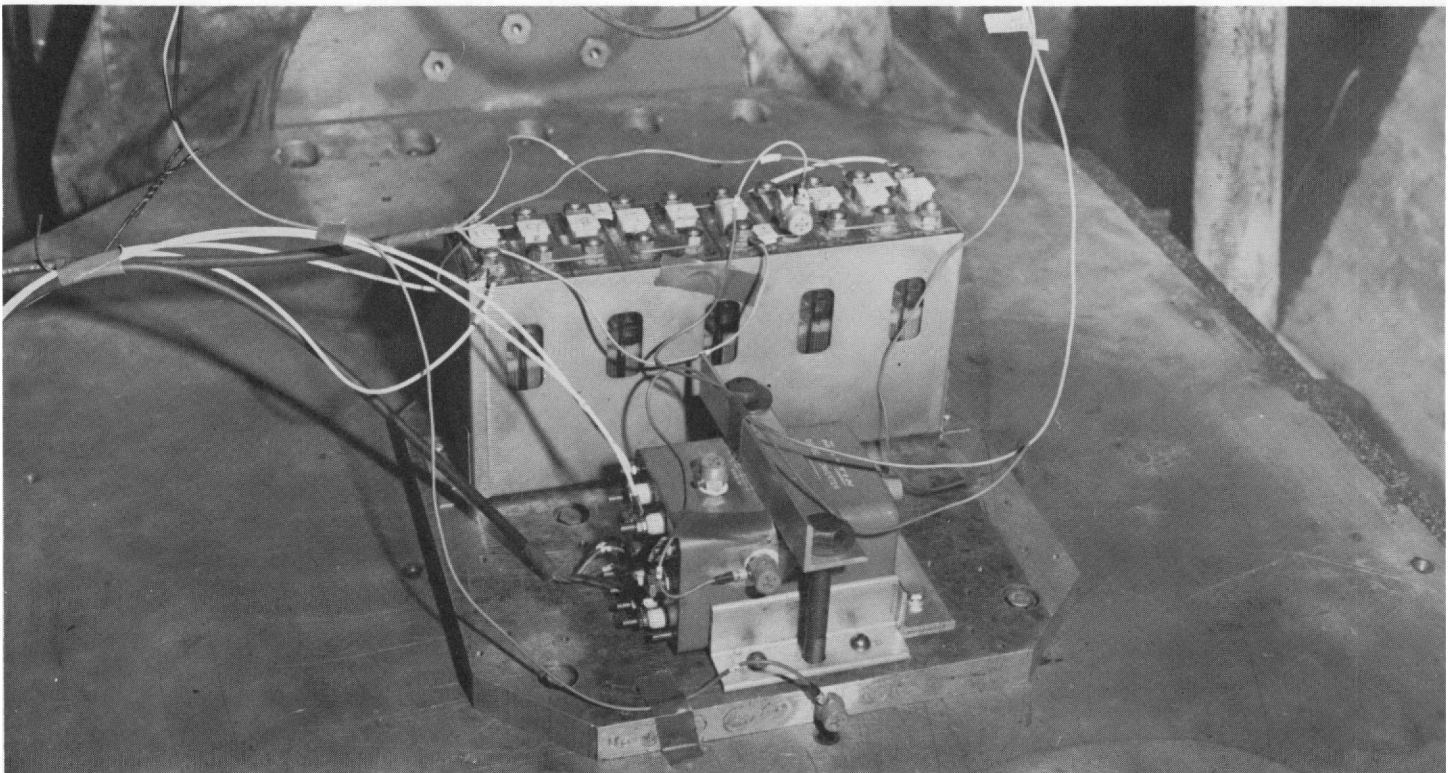
Fig. 33. SNAP 7A Battery and Converter Positioned on Slide Table for Vibration Test in Horizontal Plane

(1) Vertical plane

    (a) 5 to 33 cps in discrete frequency intervals of one cps, dwell for 3 minutes at each frequency, 3-g level or 0.060 ± 0.006-inch displacement, whichever is less.

    (b) 5 to 300 to 5 cps sweep in 15 minutes at a 3-g level or 0.050 ± 0.006-inch displacement, whichever is less.

(2) Repeat (1) for the two remaining principal orthogonal axes.

(3) Dwell at the most severe resonant condition, at the input level consistent with the frequency, for a period of two hours.

The battery and converter were subjected to parts (1) (a), (2), and (3), only, since this is the SNAP 7A requirement.

2. Shock Tests

The following requirement is identical for the SNAP 7A and 7C system:

(1) Subject the specimen to two 6-g shocks that have a 6-millisecond half sine wave pulse, in each of the three principal orthogonal axes.

3. Temperature

(1) Generator--Record performance and specimen temperature after stabilization at the following ambient conditions:

    0° F--sea level pressure*

    +28° F--sea level pressure

    +70° F--sea level pressure*

    +125° F--sea level pressure**

---

*Anticipated extremes of ambient temperature during operation-- composite of SNAP 7A and SNAP 7C.

**Maximum anticipated ambient temperature during shipment with generator output short circuited to take advantage of the Peltier cooling effect.

(2) Battery and converter--Record performance and specimen temperatures after stabilization at the following ambient conditions:

0° F--sea level pressure

+60° F--sea level pressure

90° F--sea level pressure

C. TEST METHOD AND RESULTS

1. Generator Vibration

The thermoelectric generator was attached to a test fixture and positioned on an MB-C25 electrodynamic shaker for excitation in the vertical plane (Figs. 34 and 30).* After testing, the generator and fixture were attached to a slide plate resting on an oil table for excitation in the horizontal planes (Fig. 35).

The generator functioned properly throughout exposure to vibration. During the test in horizontal plane No. 1, discontinuities in generator output occurred at approximately 90 and 250 cycles per second (see Fig. 36 and Figs. 37 through 47).

The 250-cps frequency was selected for the vibration dwell in horizontal plane No. 1 because of the broad output response characteristic in that particular frequency range. The vibration dwell caused an increase in generator output, continuing for six hours after the dwell was completed. Table 4 summarizes the generator vibration data.

2. Battery and Converter Vibration

The battery and converter were attached to a flat fixture plate and tested simultaneously. Figure 41 illustrates the battery and converter positions for vertical and horizontal excitation. Figures 32 and 33 are pictures of the test apparatus. The converter and battery behavior were monitored throughout the test with the circuitry illustrated in Fig. 42.

Individual cell voltage checks and checks of converter output with simulated generator input prior to and after all vibration tests indicated satisfactory performance (see Table 5).

---

*Circuitry for performance measurements was connected as shown in Fig. 40.
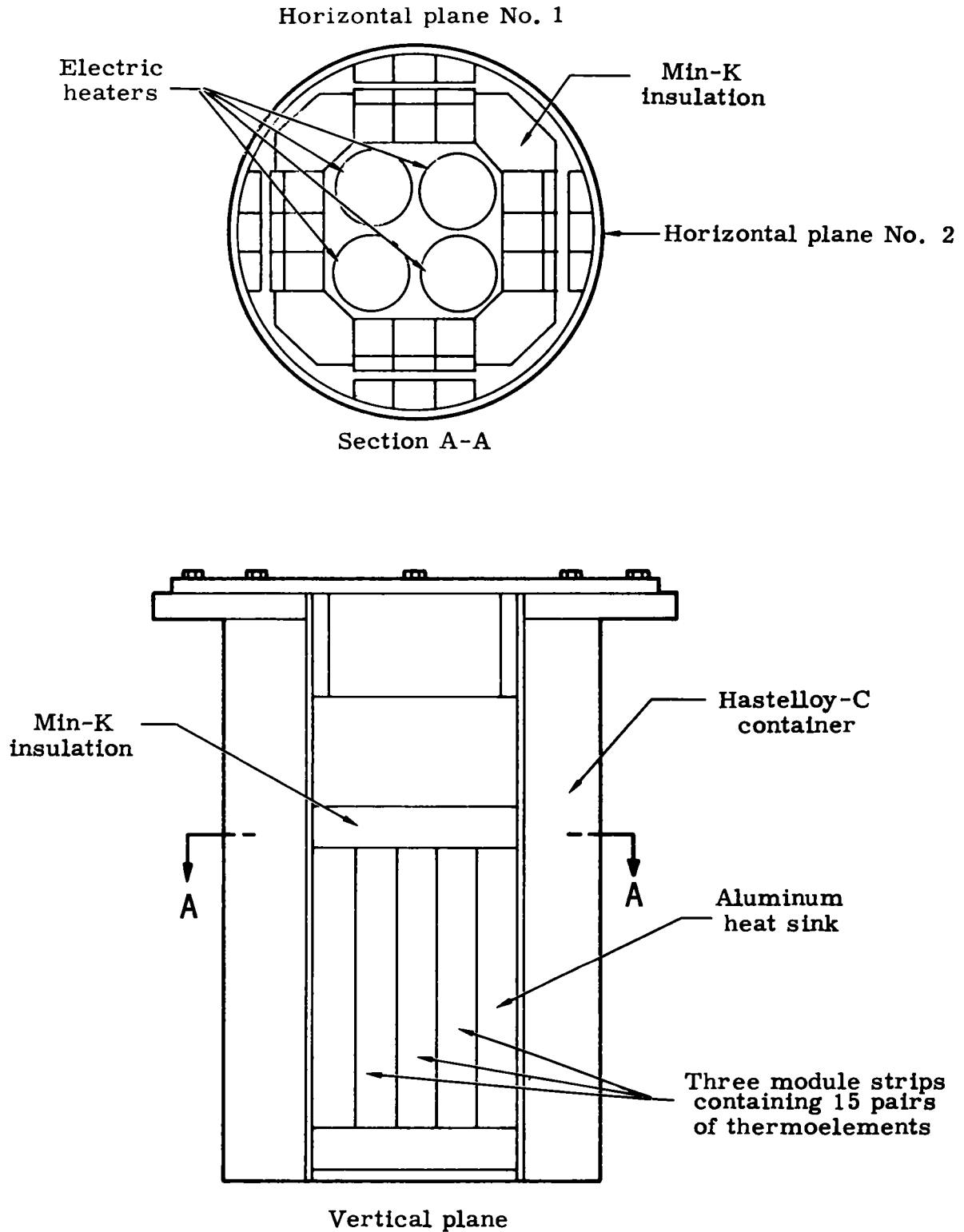
Fig. 34. Reference Axis for Vibration and Shock Testing

Aluminum jacket is water cooled
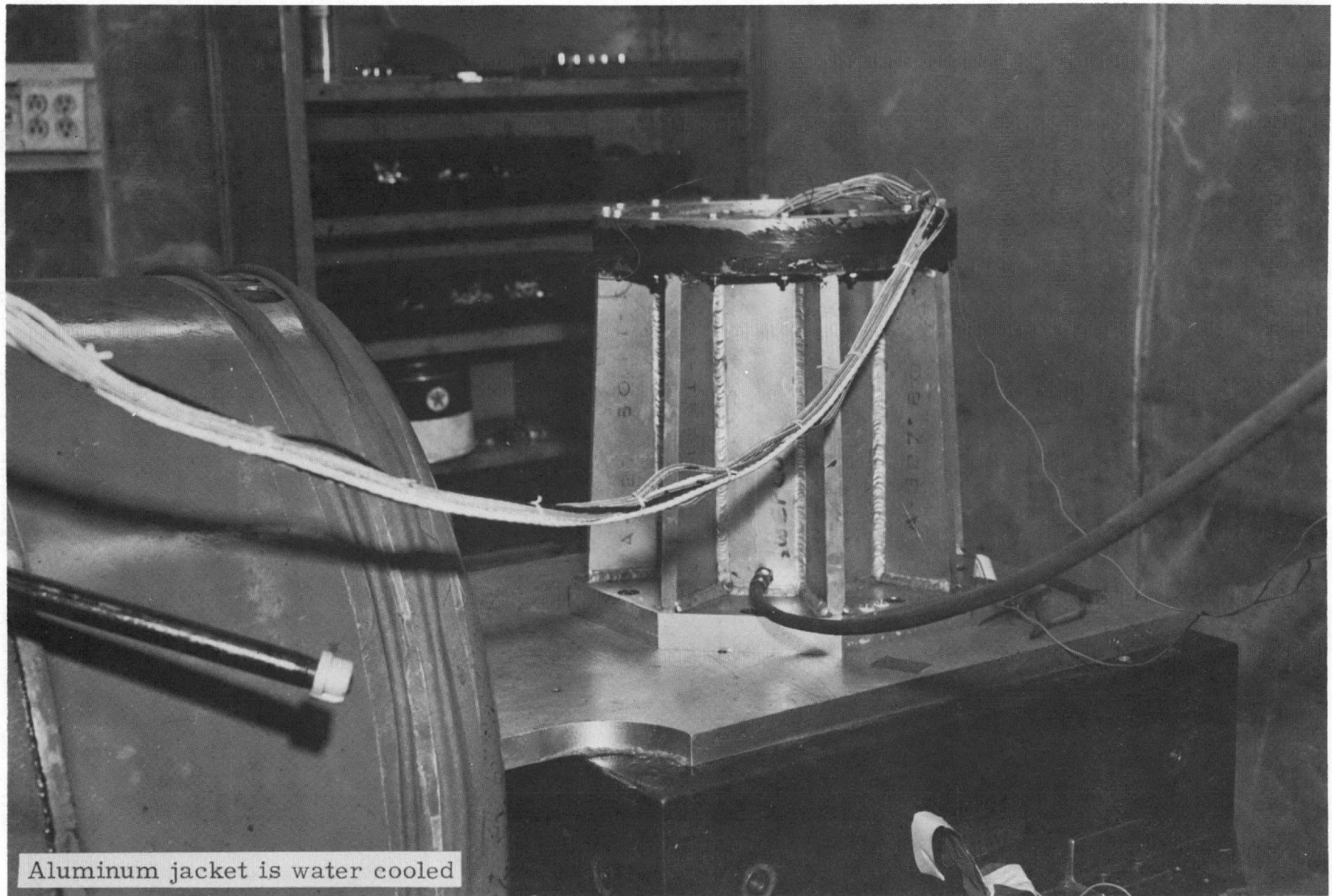
Fig. 35. SNAP 7A-7C Thermoelectric Generator and Test Fixture Positioned on Vibration Slide Table for Horizontal Excitation
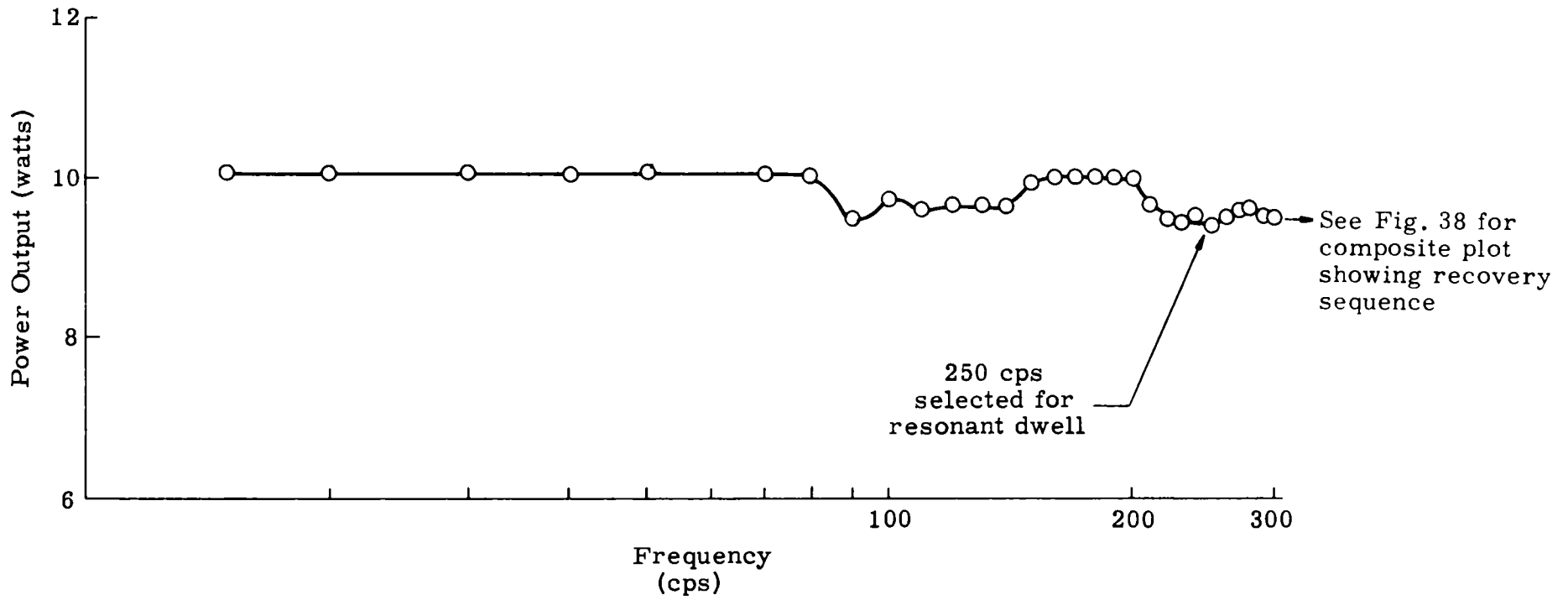
Fig. 36. Power Output Versus Frequency in Horizontal Plane No. 1

Decreasing

Output voltage

Output current

80 cps   90 cps   100 cps

Fig. 37. Oscillograph Reproduction of Generator Output Response at 90 cps

Decreasing

Output voltage

Output current
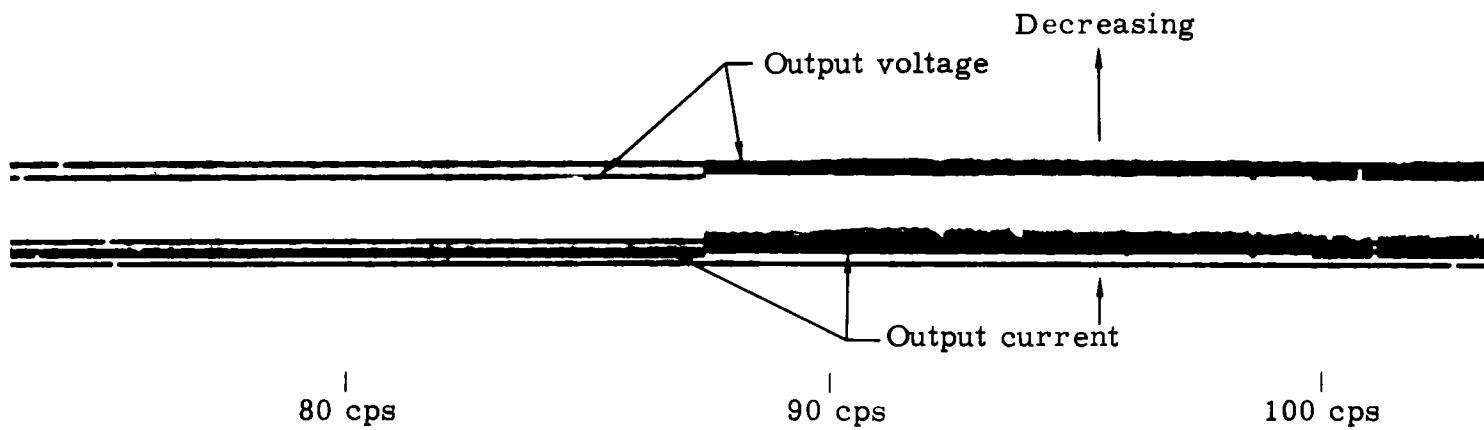
200 cps   300 cps
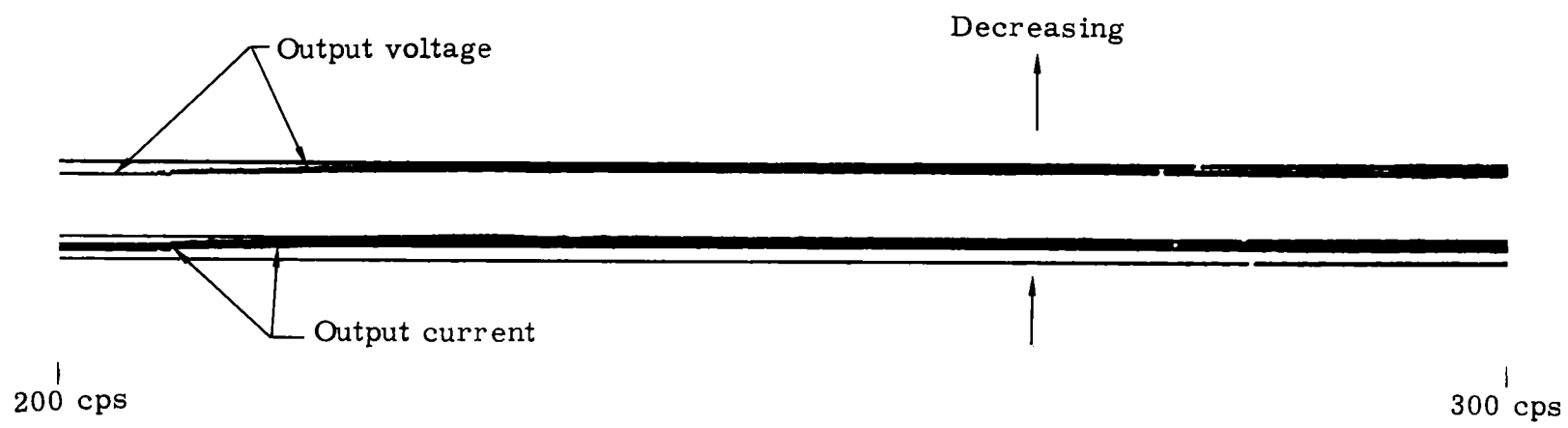
Fig. 38. Oscillograph Reproduction for Generator Output Response at 250 cps
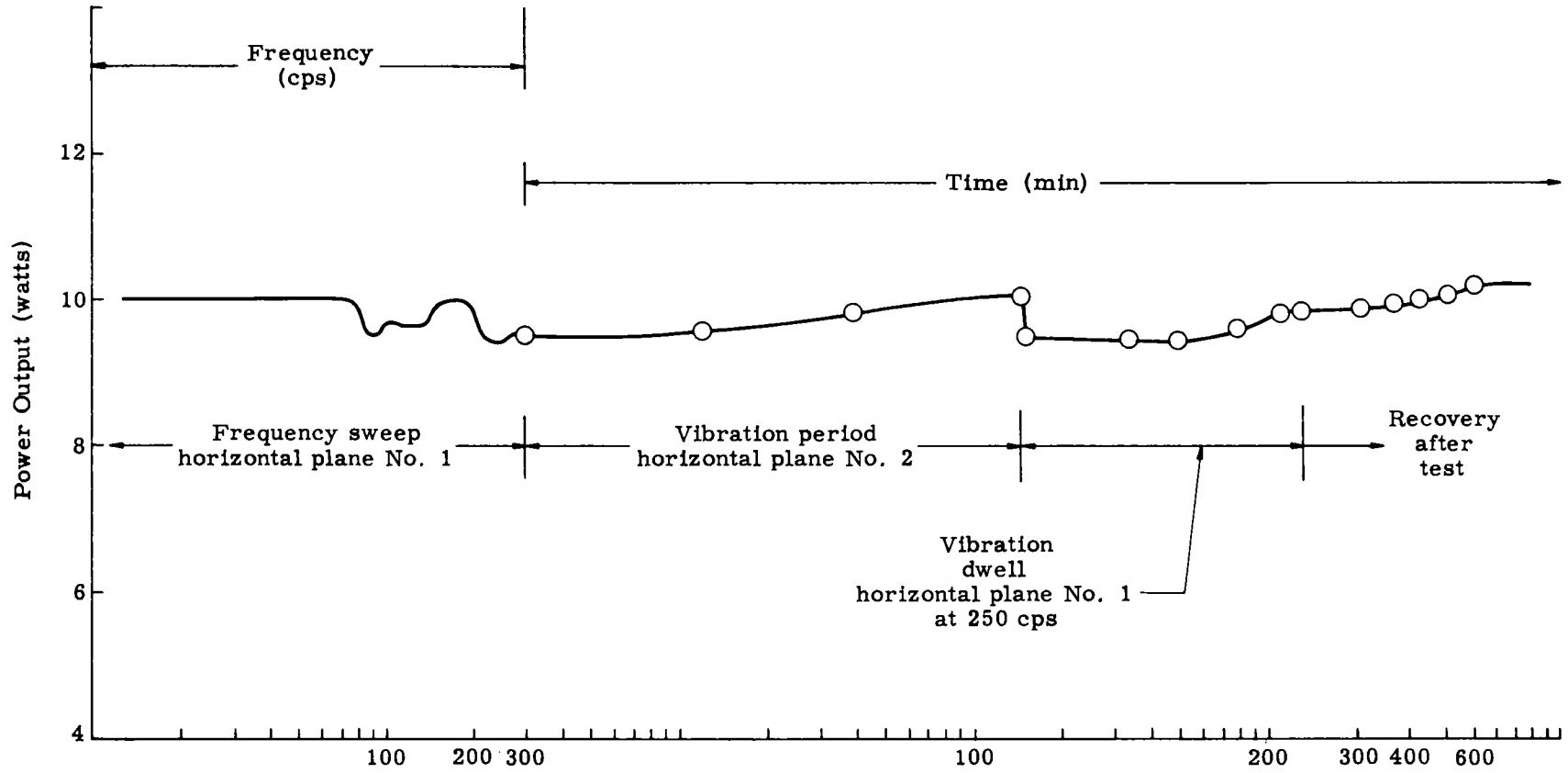
Fig. 39. Time History of Generator Output During and After Horizontal Vibration
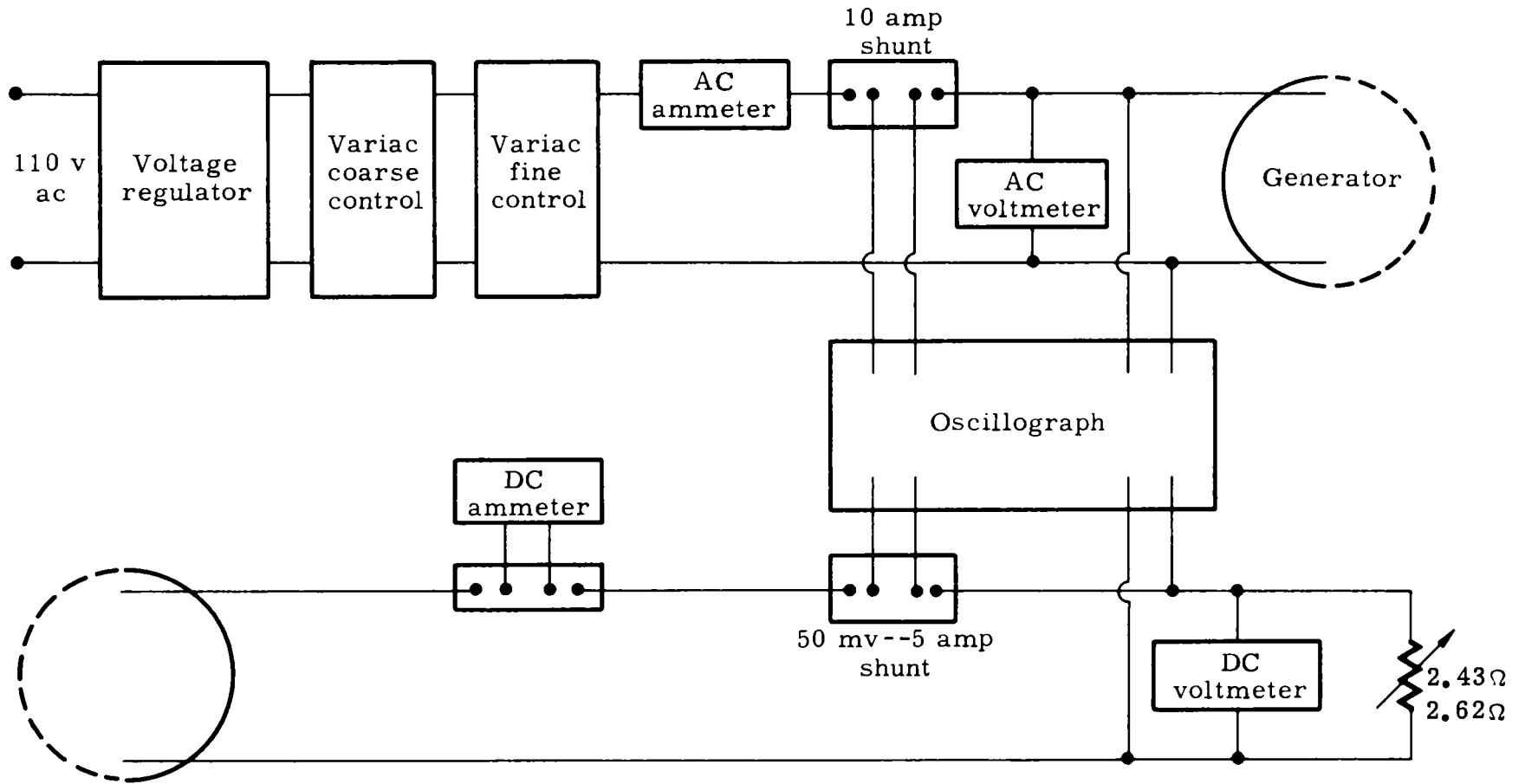
Fig. 40. Instrumentation Circuitry for Generator Test
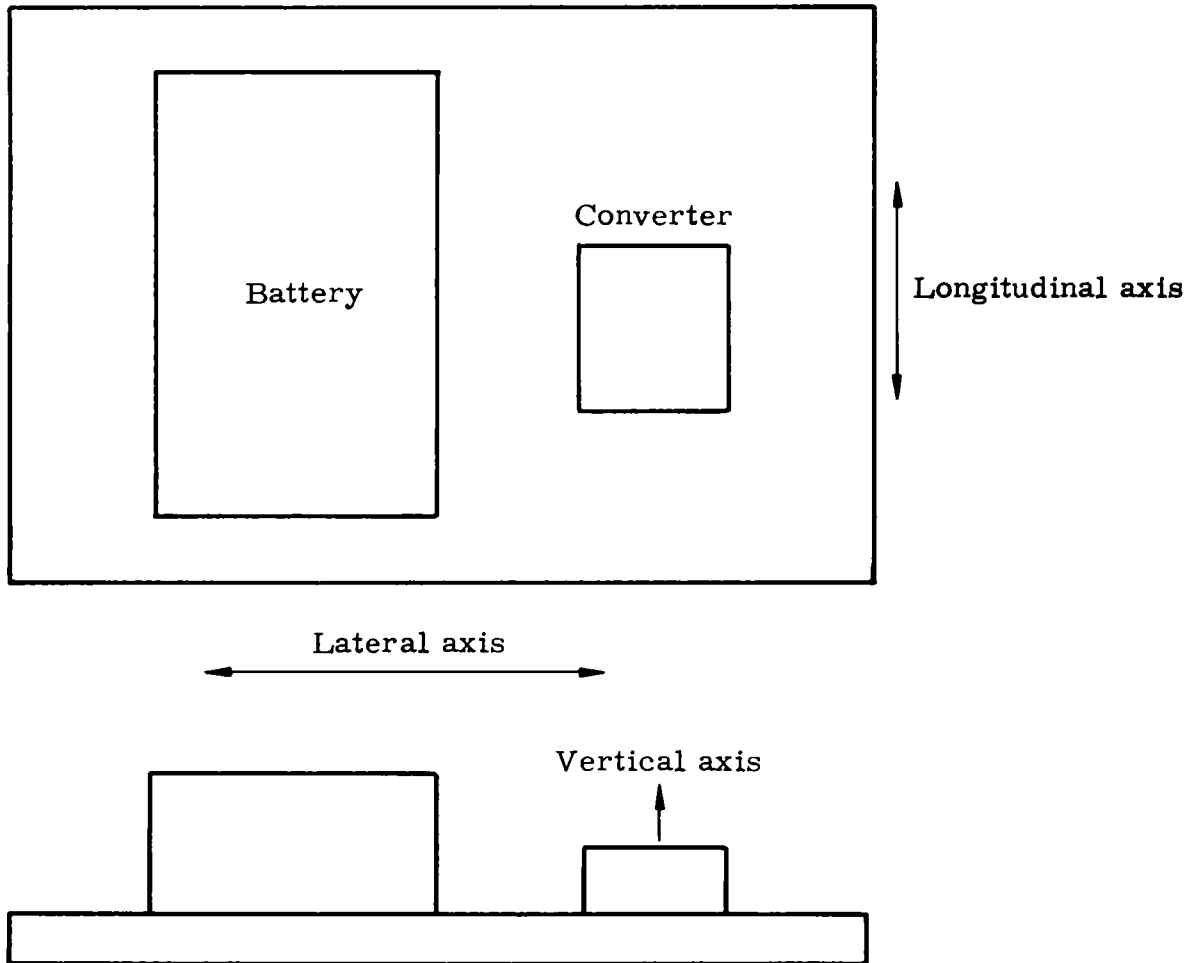
Fig. 41. Reference Axes for Vibration and Shock Testing of SNAP 7A Battery and Converter
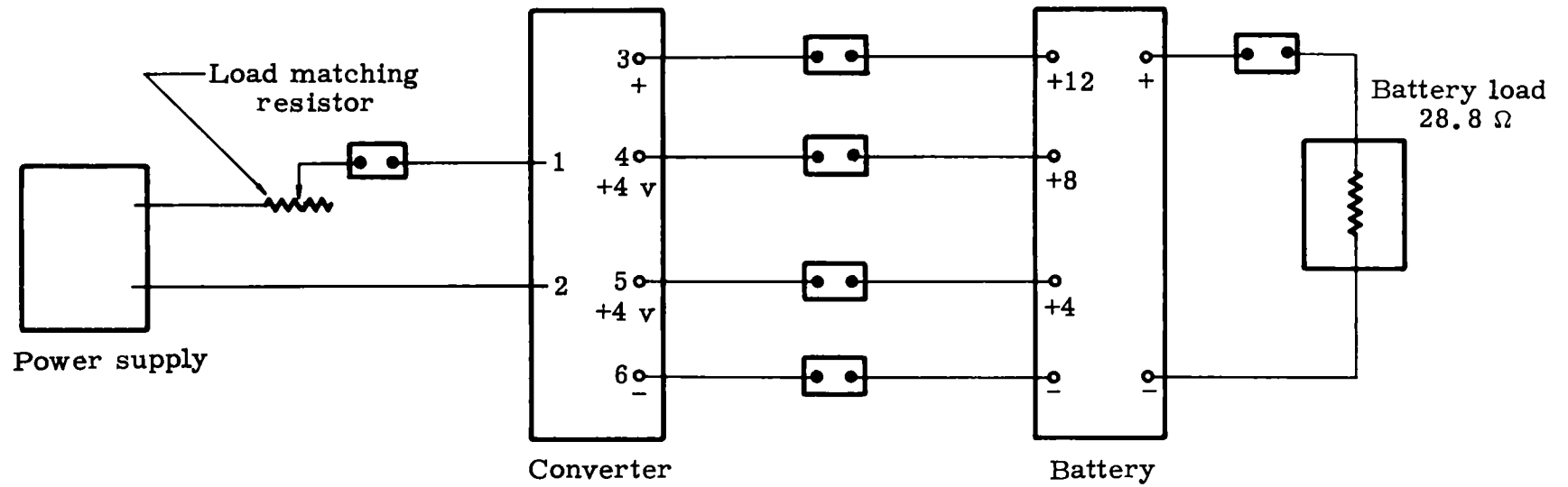
Fig. 42. SNAP 7A Battery and Converter Test Instrumentation Circuitry

Aluminum jacket is water cooled

Fig. 43. SNAP 7A-7C Thermoelectric Generator Positioned on Barry Medium Impact Shock Machine for Vertical Shock Tests

Aluminum jacket is water cooled
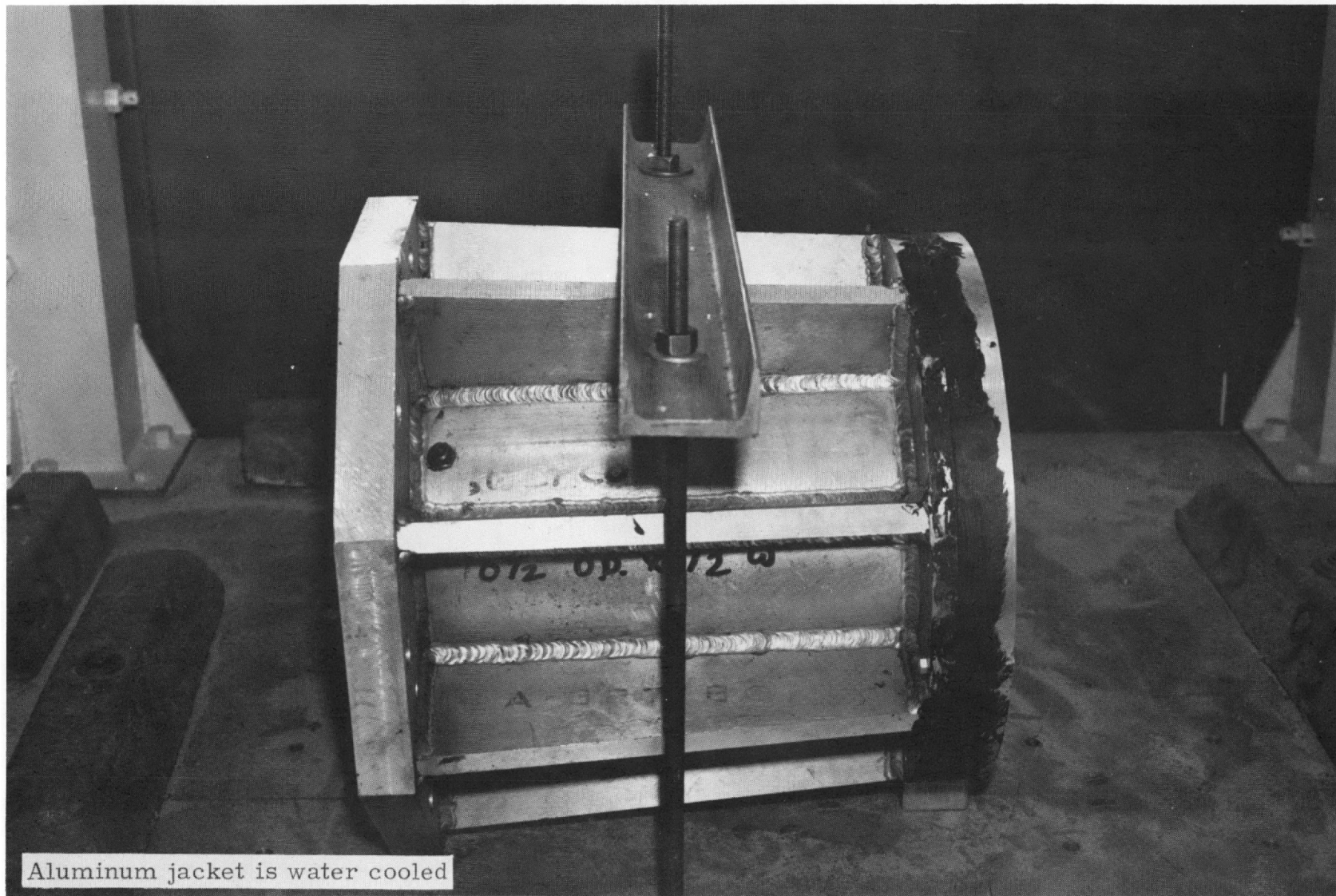
Fig. 44. SNAP 7A-7C Thermoelectric Generator and Test Fixture Positioned on Barry Medium Impact Shock Machine for Horizontal Shock Tests
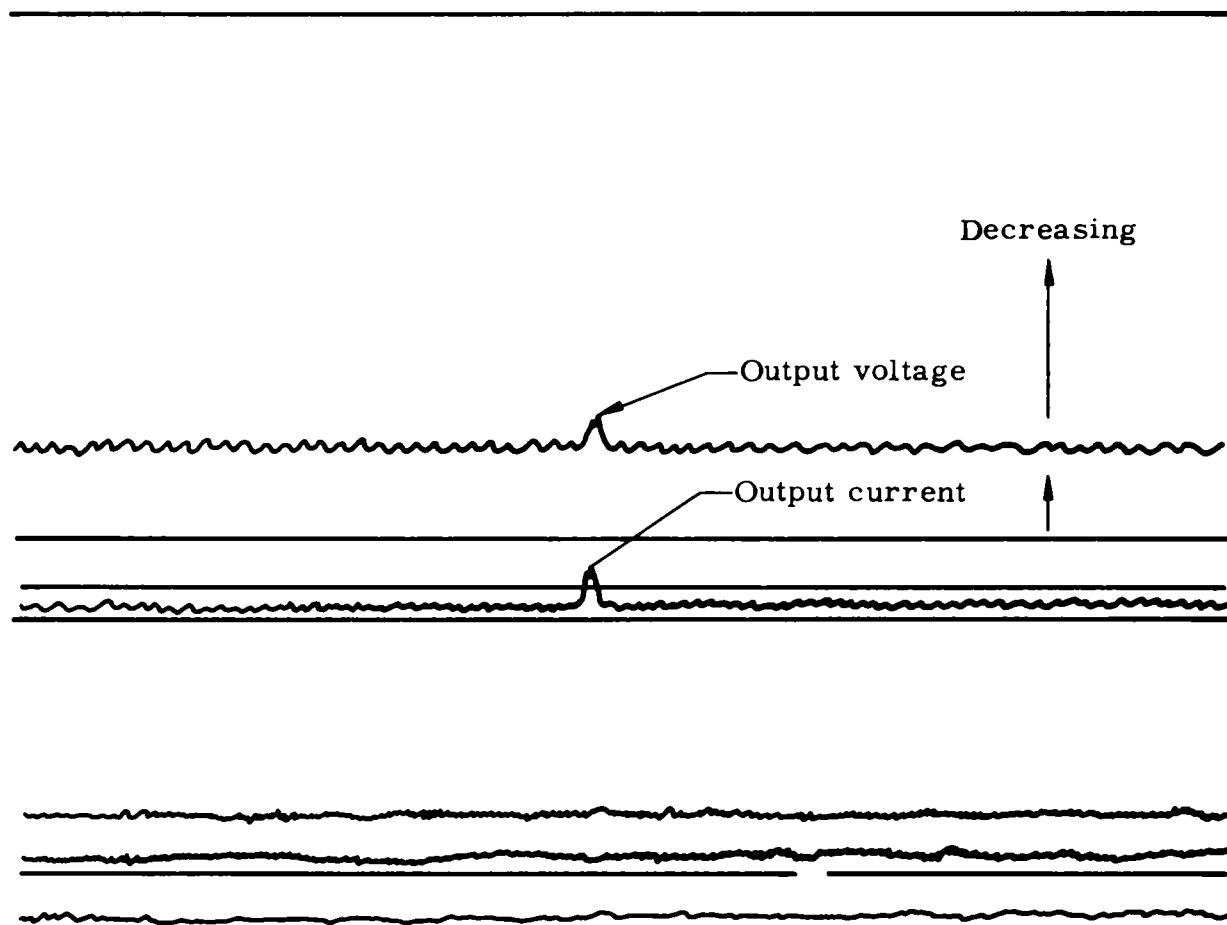
Fig. 45. Oscillograph Reproduction of Generator Output Effect of Horizontal Shock
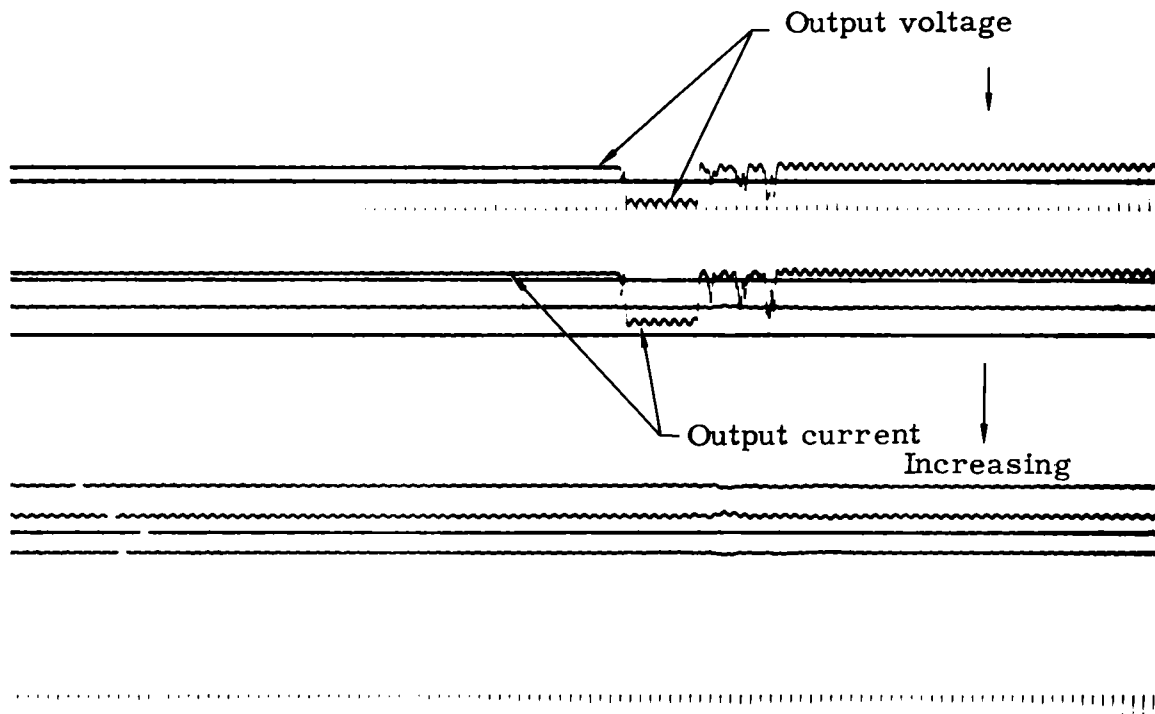
Fig. 46. Oscillograph Reproduction of Effect on Output from Horizontal Shock After Discrepancy in Output
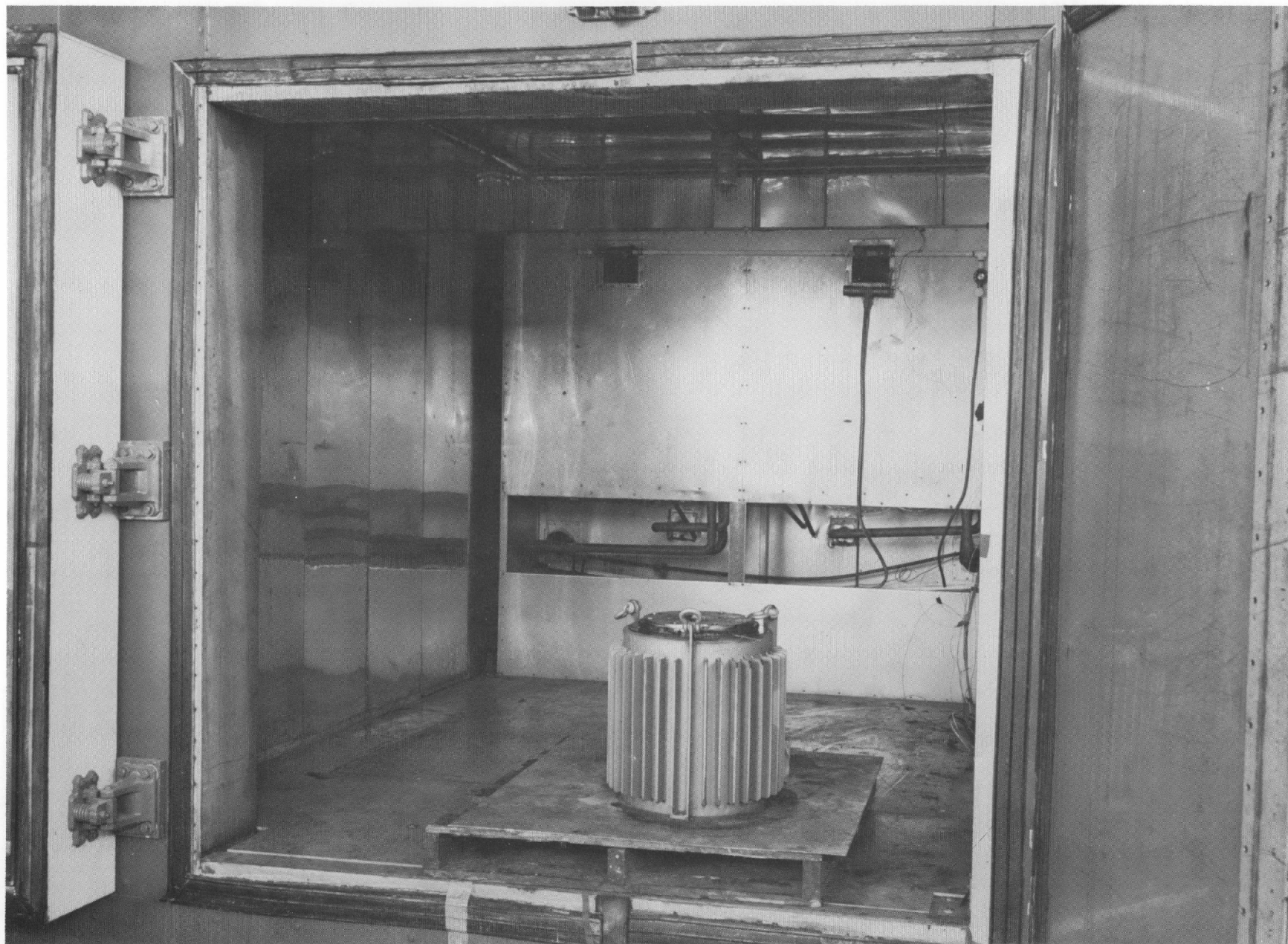
Fig. 47. SNAP 7A-7C Thermoelectric Generator with Biological Shield Positioned in Temperature Chamber for Temperature Output Tests

TABLE 4

SNAP 7A, 7C Thermoelectric Generator--Vibration Test Data

Ref Plane	Environment	Exposure Time (min)	Power Input Before (watts)	Power Input After (watts)	Power Output Before (watts)	Power Output After (watts)	Remarks
Vert	5-300 cps at 0.06DA and 1/2 g	7-1/2	240	240	10.05	10.05	Investigation for major resonant conditions--none noted
Vert	5-33 cps at 0.06DA and 3 g	87	240	240	10.05	10.05	Satisfactory
Vert	5-300-5 cps at 0.06DA and 3 g	15	240	240	10.05	10.05	Satisfactory
Horiz 1	5-300 cps at 0.06DA and 1/2 g	7-1/2	238	239	10.02	10.02	No resonances noted
Horiz 1	5-33 cps at 0.06DA and 3 g	87	238	238	10.02	10.02	Satisfactory
Horiz 1	5-300-5 cps at 0.06DA and 3 g	15	238	238	10.05	9.51	Discontinuity on output and ripple at 90 cps and decrease at 250 cps with ripple
Horiz 2	5-300 cps at 0.06DA and 1/2 g	7-1/2	238	238	9.51	9.82	No resonances noted
Horiz 2	5-33 cps at 0.06DA and 3 g	87	238	238	9.89	9.94	Satisfactory
Horiz 2	5-300-5 cps at 0.06DA and 3 g	15	238	238	9.94	10.05	Satisfactory
Horiz 1	250 cps at 3-g dwell	120	238	238	10.05	9.8	At start of vibration, output decreased to 9.43 watts. Ripple on output ceased after 90 minutes and output increased to 10.2 watts 6 hours after vibration was complete.

TABLE 5

SNAP 7A Battery and Converter--Vibration Test Data

Item	Before Vertical Vibration	After Vertical Vibration	Before Longi-tudinal Vibration	After Longi-tudinal Vibration	Before Lateral Vibration	After Lateral Vibration	Before 33 cps Vibration Dwell	After 33 cps Vibration Dwell
Battery cell								
Voltage	1.32 v	1.32 v	1.32 v	1.32 v	1.32 v	1.32 v	1.32 v	1.32 v
Converter input								
Voltage	6.05 v	6.32 v	6.28 v	6.40 v	6.20 v	6.30 v	6.27 v	6.35 v
Current	1.96 a	2.02 a	2.02 a	2.03 a	2.02 a	2.03 a	2.02 a	2.02 a
Converter output Section No. 1								
Voltage	12.23 v	12.21 v	12.24 v	12.22 v	12.25 v	12.23 v	12.16 v	12.16 v
Current	366 ma	370 ma	373 ma	373 ma	372 ma	372 ma	405 ma	405 ma
Section No. 2								
Voltage	8.16 v	8.14 v	8.16 v	8.15 v	8.16 v	8.15 v	8.11 v	8.10 v
Current	24 ma	14 ma	10 ma	12 ma	6 ma	9 ma	14 ma	15 ma
Section No. 3								
Voltage	4.09 v	4.06 v	4.08 v	4.07 v	4.08 v	4.07 v	4.05 v	4.04 v
Current	-18 ma	-9 ma	-8 ma	-9 ma	-4 ma	-9 ma	-11 ma	-10 ma
Battery output								
Voltage	11.99 v	11.97 v	12.0 v	11.99 v	12.0 v	11.99 v	11.90 v	11.89 v
Current							405 ma	400 ma

No vibration resonance was detected over the range of frequencies examined. To fulfill test conditions a two-hour dwell was conducted at 33 cps with excitation in the vertical plane. No significant effect on battery and converter performance was noted.

3. Generator Shock

The generator and fixture were mounted on the table of the Barry Medium Impact Shock Machine (Fig. 43) for the 6 g, 6-millisecond impacts in the vertical plane. Generator functions were monitored in the same fashion as during vibration testing.

The generator was then repositioned for shock impacts in the two horizontal planes (see Fig. 44).

The generator functioned properly throughout two drops in the vertical and horizontal axes. A typical effect on output is shown in Fig. 45, and a summary of the test results is given in Table 6.

About five minutes after the second shock in horizontal plane No. 1, the output suddenly dropped approximately 15%. Testing was continued in horizontal plane No. 2. The output during both shock pulses momentarily returned to the maximum output as recorded in Fig. 46. After testing was complete, another slight shock in the vertical plane restored continuous, near maximum output. It was then noted that handling of the input-output plug on the generator produced the same 15% decrease in output (deficiency corrected). The decrease can be attributed to this plug and not the basic thermoelectric generator.

After the shock tests were completed, discrepancies in the shock machine were noted and a check made of the actual shock loads. It was found that the generator had been subjected to 18 g, 6-millisecond, half sine shock pulses. This represented a shock value three times greater than required by the statement of work.

4. Battery and Converter Shock

The battery and converter were secured to the table of the Barry Medium Impact Shock Machine for the 6 g, 6-millisecond impacts in the vertical plane. Battery and converter performance were monitored throughout the test.

The units were then positioned for shock impulses in the two remaining principal orthogonal axes. The battery and converter functional checks made before and after each plane of shock showed no structural damage or effects on the operation of the battery and converter. The data obtained from the shock tests are listed in Table 7.

TABLE 6

SNAP 7A, 7C Thermoelectric Generator--Shock Test Data*

Ref Plane***	Orientation	Required Environment**	Power Input Before (watts)	Power Input After (watts)	Power Output Before (watts)	Power Output After (watts)	Results
Vert No. 1	Bottom impact	6 g, 6 ms Half sine	238	238	9.92	9.92	Satisfactory
Vert No. 2	Top impact	6 g, 6 ms Half sine	238	238	9.92	9.92	Satisfactory
Horiz No. 1	Side impact	6 g, 6 ms Half sine	238	238	9.92	9.92	Satisfactory
Horiz No. 1	180° opposite	6 g, 6 ms Half sine	238	238	9.92	9.92	Approximately 5 minutes after drop, output noted to have decreased to 8.3 watts
Horiz No. 2	Side impact	6 g, 6 ms Half sine	238	238	8.3	8.3	Impulse caused momentary increase to normal output
Horiz No. 2	180° opposite	6 g, 6 ms Half sine	238	238	8.3	8.3	Impulse caused momentary increase to normal output

*After the last shock test, the generator was placed in the vertical position. A slight shock impulse in this plane instantly restored output power to 9.875 watts. Further handling of the generator in the vicinity of the input-output plug produced a similar decrease in power output as experienced during the shock test.

**Actual shock environment was approximately 18 g, 6 ms half sine.

***Refer to Fig. 34 for ref plane.

TABLE 7

SNAP 7A Battery and Converter--Shock Test Data

Item	Before Vertical Shock	After Vertical Shock	Before Lateral Shock	After Lateral Shock	Before Longitudinal Shock	After Longitudinal Shock
Battery cell						
Voltage	1.32 v	1.32 v	1.32 v	1.32 v	1.32 v	1.32 v
Converter input						
Voltage	5.88 v	5.92 v	5.92 v	5.93 v	5.93 v	5.93 v
Current	1.90 a	1.92 a	1.92 a	1.92 a	1.92 a	1.92 a
Converter output Section No. 1						
Voltage	12.11 v	12.11 v	12.11 v	12.10 v	12.10 v	12.10 v
Current	411 ma	413 ma	413 ma	411 ma	411 ma	410 ma
Section No. 2						
Voltage	8.07 v	8.07 v	8.07 v	8.07 v	8.07 v	8.09 v
Current	15 ma	15 ma	15 ma	15 ma	15 ma	15 ma
Section No. 3						
Voltage	4.02 v	4.02 v	4.02 v	4.03 v	4.03 v	4.02 v
Current	-14 ma	-13 ma	-13 ma	-11 ma	-11 ma	-11 ma
Battery output						
Voltage	11.84 v	11.84 v	11.84 v	11.83 v	11.83 v	11.82 v
Current	408 ma	405 ma	405 ma	408 ma	408 ma	403 ma

5. Temperature Tests

The generator assembly was placed in the finned biological shield using a glycol-water solution to conduct heat from the generator to the shield, and the complete unit was positioned in the Bowser temperature chamber shown in Fig. 47. Generator functions and temperatures were monitored throughout the temperature cycles and for a stabilization period at each temperature step. Figure 31 and Figs. 48 through 50 present the effect of ambient temperatures on the generator output. Tables 8 and 9 contain all data taken during the temperature-output tests.

The battery and converter were operated in an environmental test chamber at the three required temperatures and also at 80° F. The data obtained are presented in Table 10.

LEGEND:

O Hot junction, TC No. 27   △ Fin temperature (avg)

□ Cold cap, TC No. 28   ● Power output
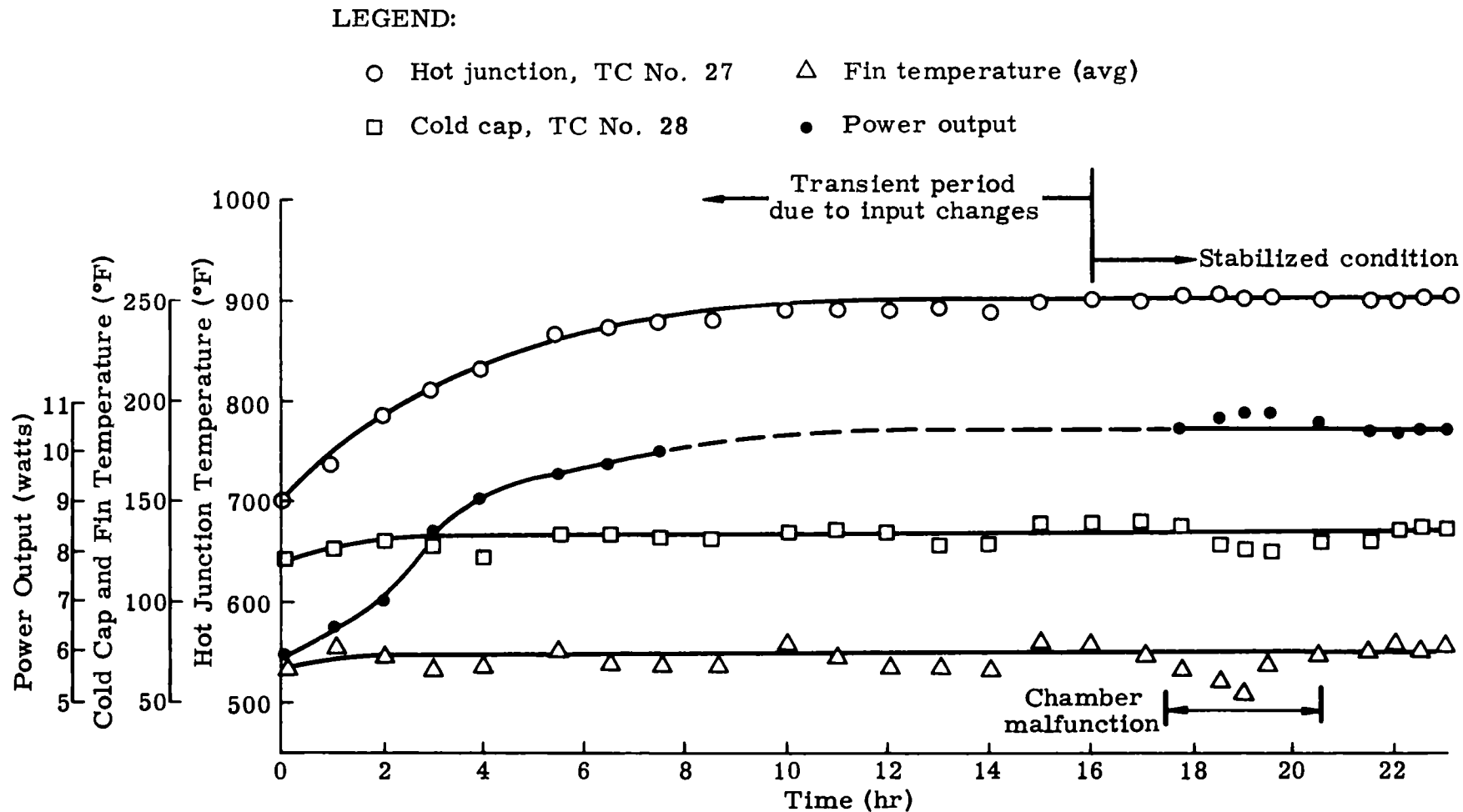
Fig. 48. Results of SNAP 7A and SNAP 7C Generator Temperature Chamber
Tests, Where Nominal Power Input Was 257 Watts, Ambient Air
Temperature Was 70° F, and Generator Atmosphere Was 50%
Argon and 50% Hydrogen
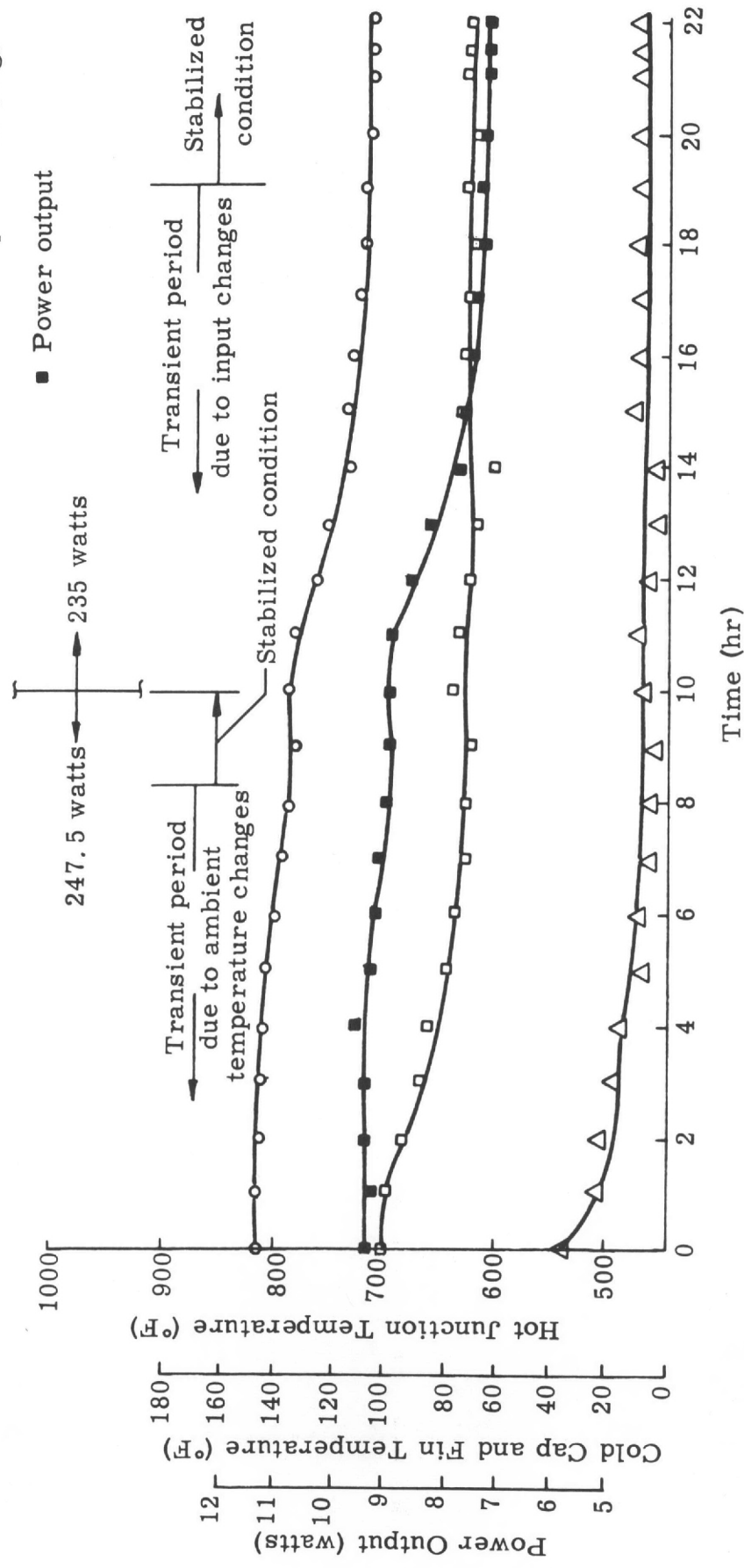
Fig. 49. Results of SNAP 7A and SNAP 7C Generator Temperature Chamber Tests, Where Nominal Power Input Was 247.5 and 235 Watts, Ambient Air Temperature Was 0° F, and Generator Atmosphere Was 50% Argon and 50% Hydrogen
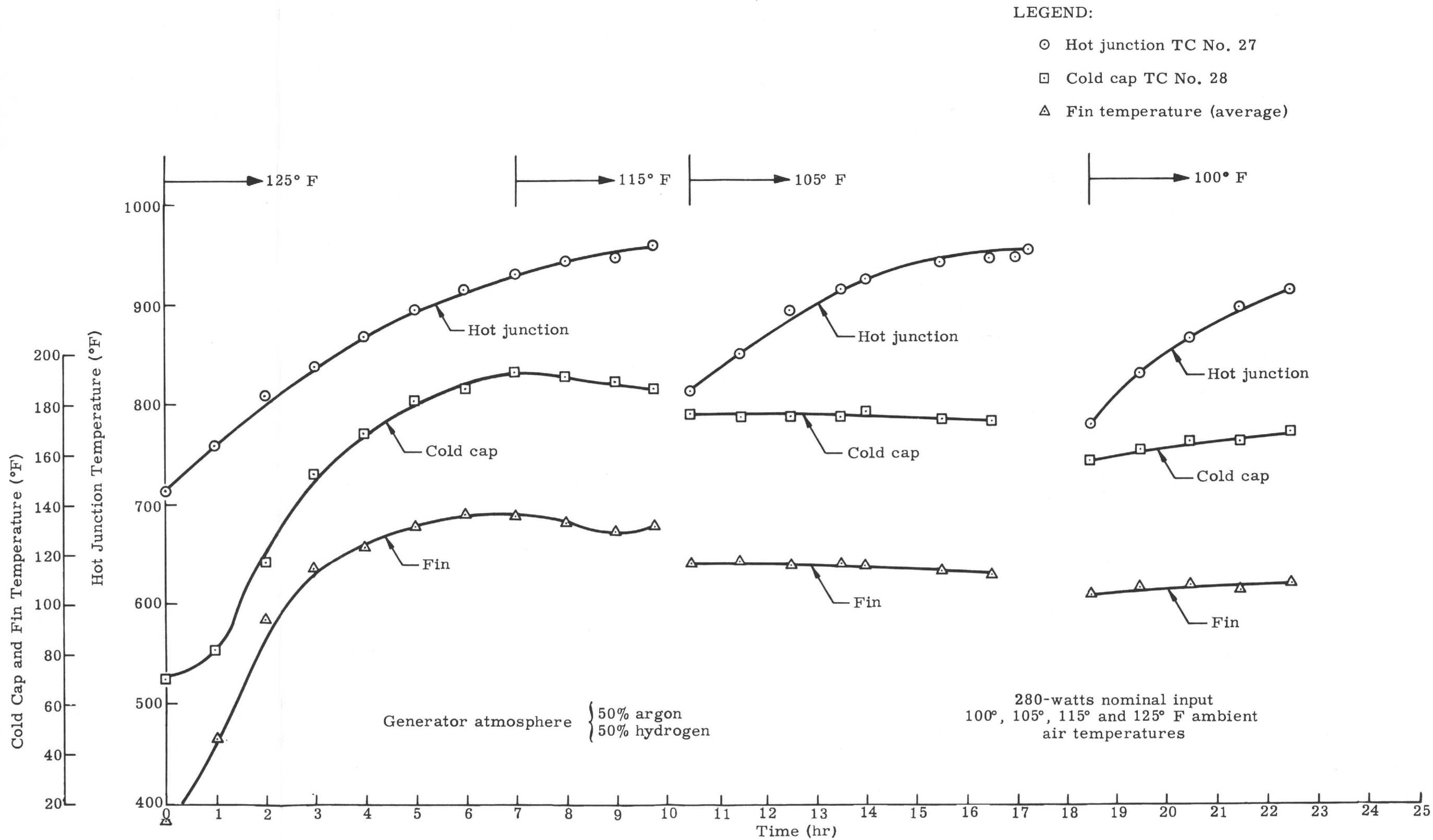
Fig. 50. SNAP 7A-7C Thermoelectric Generator Output Short-Circuit Shipping Condition

TABLE 8

SNAP 7A, 7C Generator--Thermocouple Locations

Thermocouple No.	Location
25	Fuel block No. 3 couple, No. 5 module, No. 2 section fuel block
26	Hot shoe, center No. 1 couple, No. 5 module
27	Hot shoe, center No. 5 couple, No. 5 module
28	Cold cap, No. 1 couple, "P" element, No. 5 module
29	Cold cap, No. 5 couple, "N" element, No. 5 module
30	Heat sink bar "L", No. 3 couple, No. 5 module
31	Heat sink top, between heat sink bars A&M Fin No. 1 Fin No. 2

TABLE 9

SNAP 7A, 7C Thermoelectric Generator--Temperature Test Data

	Time	Power In (watts)	Power Out (watts)	Thermocouple No. 25 (°F)	No. 26 (°F)	No. 27 (°F)	No. 28 (°F)	No. 29 (°F)	No. 30 (°F)	No. 31 (°F)	Fin	Fin
8/24	4:00 pm	240	5.91	726	649	702	121	118	108	101	--	72
	5:00 pm	255	6.52	765	683	739	126	124	112	107	--	77
	6:00 pm	255	7.07	813	730	785	130	124	113	105	--	72
	7:00 pm	257	8.46	841	762	812	127	122	111	103	--	67
	8:00 pm	257	9.12	859	786	831	123	119	108	101	--	67
	9:30 pm	257	9.56	894	814	864	133	127	115	109	--	75
	10:30 pm	257	9.75	899	822	871	134	126	115	106	--	70
	11:30 pm	257	10.04	907	830	879	132	126	113	106	--	69
8/25	12:30 am	257	--	907	836	878	130	124	112	102	--	71
	2:00 am	257	--	919	842	890	136	132	119	112	--	76
	3:00 am	257	--	920	842	891	135	130	119	110	--	74
	4:00 am	257	--	920	844	891	135	126	119	106	--	69
	5:00 am	257	--	921	845	892	130	125	114	106	--	70
	6:00 am	256	--	917	845	888	130	124	112	104	--	67
	7:00 am	257	--	926	853	899	139	132	112	113	--	81
	8:00 am	258	--	926	852	900	138	133	119	114	--	80
	9:00 am	257	--	928	851	899	138	131	119	112	--	75
	9:45 am	257	10.45	932	852	901	136	130	118	111	--	67
	10:30 am	257	10.65	934	855	906	128	122	111	103	--	61
	11:00 am	257	10.75	929	851	900	124	120	106	99	--	57
	11:30 am	257	10.75	935	853	902	125	120	108	99	--	70
	12:30 pm	257	10.55	929	850	899	131	125	111	103	--	74
	1:00 pm	void										
	1:30 pm	258	10.40	931	853	899	132	128	114	107	--	76
	2:00 pm	258	10.40	929	854	899	136	130	117	110	79	79
	2:30 pm	258	10.40	929	851	900	136	130	117	110	75	77
	3:00 pm	257	10.45	929	851	901	137	131	118	111	77	79

TABLE 9 (continued)

Thermocouple

	Time	Power In (watts)	Power Out (watts)	No. 25 (°F)	No. 26 (°F)	No. 27 (°F)	No. 28 (°F)	No. 29 (°F)	No. 30 (°F)	No. 31 (°F)	Fin	Fin
8/25	3:30 pm	247.5	10.50	924	848	895	132	128	114	108	59	64
	4:00 pm	247.5	10.40	918	842	889	125	120	107	100	50	56
	4:30 pm	247.5	10.60	909	836	881	117	102	99	93	45	49
	5:00 pm	248	10.45	904	830	875	112	107	94	86	40	45
	6:00 pm	247.5	10.45	898	827	870	111	106	93	86	42	45
	7:00 pm	246	10.15	890	820	861	110	104	89	81	40	43
	8:00	248	10.09	881	811	851	104	101	87	80	40	42
	8:30	247.5	9.875	873	803	845	102	99	84	76	37	40
	9:30	247.5	9.875	868	799	839	100	95	80	73	35	37
	10:30	248.5	9.80	860	793	831	96	91	77	70	32	34
	11:30	247.5	9.50	860	787	830	101	96	81	74	36	36
8/26	1:00 am	246	9.55	856	786	826	97	91	80	72	34	34
	2:00	245	9.55	853	782	823	97	93	80	72	32	35
	3:00	245	9.46	850	781	821	96	92	79	71	34	35
	4:00	245	9.36	848	778	818	96	91	77	71	32	35
	5:00	245	9.36	846	778	818	97	91	77	69	34	35
	6:00	245	9.36	846	773	815	95	91	78	71	33	34
	7:00	245	9.36	844	772	815	95	91	77	72	33	33
	8:00	--	--	842	775	811	95	91	78	71	33	33
	9:00	248	9.26	842	773	813	94	89	76	69	32	32
	10:00	248	9.24	844	775	814	96	91	79	72	34	34
	11:00	248	9.24	845	776	816	99	93	80	73	36	36
	12:00	248	9.24	845	776	816	99	93	80	73	36	36
8/26	1:00 pm	248	9.24	844	776	816	99	95	81	74	26	20
	2:00	248	9.30	843	774	814	93	88	75	67	21	25
	3:00	248	9.36	842	773	813	87	82	69	60	15	19
	4:00	248	9.40	841	772	812	84	79	65	58	14	17
	5:00	247.5	9.24	834	768	804	78	74	53	51	8	9

TABLE 9 (continued)

	Time	Power In (watts)	Power Out (watts)	No. 25 (°F)	No. 26 (°F)	No. 27 (°F)	No. 28 (°F)	No. 29 (°F)	No. 30 (°F)	No. 31 (°F)	Fin	Fin
	6:00 pm	248	9.12	828	766	798	75	72	57	50	8	10
	7:00	247.5	9.08	823	758	794	72	67	54	45	5	8
	8:00	247	8.93	816	754	787	71	68	54	45	5	7
	9:00	248	8.88	811	751	780	68	65	50	42	3	5
	10:00	248	8.88	817	761	787	76	72	57	50	6	11
	11:00 pm	235	8.83	812	748	782	74	70	55	47	8	11
	12:00	234	8.46	792	733	763	70	67	53	44	4	8
8/27	1:00 am	235	8.10	770	720	747	67	62	49	40	3	4
	2:00	235	7.70	761	710	734	61	57	47	38	3	3
	3:00	235	7.66	763	700	735	73	68	55	48	12	12
	4:00	234	7.45	757	690	729	71	67	55	46	9	9
	5:00	235	7.35	754	687	723	70	66	51	44	9	9
	6:00	235	7.35	749	684	720	70	66	54	47	10	10
	7:00	235	7.28	749	682	718	70	66	53	47	8	8
	8:00	235	7.20	744	680	715	67	63	51	45	9	9
	9:00	235	7.16	743	675	714	71	67	54	46	8	10
	9:30	235	7.16	743	676	714	71	67	54	45	10	11
	10:00 am	235	7.16	743	675	714	70	66	53	45	9	11
	11:00	278	7.84	790	718	758	81	78	64	57	49	43
	11:30	278	8.23	817	748	786	98	95	82	74	77	69
	12:00	278	8.48	839	768	808	117	114	101	93	98	90
	12:30	280	--	853	782	823	138	134	120	111	112	102
	12:45	280	--	862	791	833	147	143	127	120	117	108
	1:00 pm	280	--	870	798	839	152	147	134	126	119	110
	1:30	280	--	883	813	854	161	156	143	136	124	117
	2:00	280	8.80	897	828	869	168	163	149	142	125	122
	2:30	280	9.09	914	844	885	176	171	158	152	133	129
	3:00	280	9.12	925	854	895	181	175	162	156	132	131
	3:30	280	9.35	934	864	906	183	178	165	159	134	133
	4:00	280	9.56	944	874	915	186	181	168	162	136	136
	4:30	279	--	954	884	923	192	185	172	165	138	138
	5:00	280	--	960	892	931	193	188	174	167	134	136
	5:30	280	--	968	898	938	192	186	173	166	131	134
	6:00	280	--	970	901	943	191	184	173	165	131	134

Thermocouple

TABLE 9 (continued)

	Time	Power In (watts)	Power Out (watts)	No. 25 (°F)	No. 26 (°F)	No. 27 (°F)	No. 28 (°F)	No. 29 (°F)	No. 30 (°F)	No. 31 (°F)	Fin	Fin
										Thermocouple		
	6:30 pm	279	--	973	908	947	189	182	169	162	130	130
	7:00	279	--	978	913	949	189	182	168	162	129	129
	7:30	279	--	979	918	950	186	179	165	158	127	127
	7:45	279	--	984	918	954	193	186	173	166	131	131
	8:30	279	--	839	781	814	176	170	157	150	116	116
	9:30	280	--	891	824	850	175	169	157	149	117	117
	10:30	280	--	922	849	895	174	167	153	146	115	115
	11:30 pm	280	--	945	878	915	175	169	154	148	116	116
8/28	12:00	280	--	956	890	926	177	170	156	148	115	115
	12:40 am	280	--	963	899	935	175	168	154	147	112	114
	1:30	280	--	973	908	943	174	168	154	147	111	114
	2:30 am	280	--	976	913	946	173	166	153	145	110	112
	3:00	280	--	--	--	947	--	--	--	--	--	--
	3:15	280	--	--	--	952	--	--	--	--	--	--
	4:30	280	--	808	744	780	157	152	141	135	103	104
	5:30	280	--	861	795	830	161	156	143	136	107	107
	6:30	280	--	896	832	867	165	159	145	138	106	108
	7:30	280	--	925	862	896	165	159	145	138	104	107
8/28	8:30 am	240	--	944	878	914	169	162	150	142	107	110
	9:00	240	10.20	934	869	906	165	161	148	141	108	110
	9:30	240	10.00	922	858	896	161	157	144	138	102	106
	1:00 pm	240	8.79	880	813	856	160	155	144	136	109	109

TABLE 10

SNAP 7A Battery and Converter--Temperature Test

	Ambient Temperature	+60° F	+90° F	+0° F	+80° F
Converter input					
Voltage	5.87 v	5.93 v	6.03 v	5.73 v	5.86 v
Current	1.86 a	1.91 a	1.92 a	1.96 a	1.90 a
Converter output					
Section No. 1					
Voltage	12.12 v	12.17 v	12.09 v	12.08 v	12.13 v
Current	413 ma	417 ma	414 ma	411 ma	412 ma
Section No. 2					
Voltage	8.08 v	8.12 v	8.06 v	8.06 v	8.10 v
Current	34 ma	11 ma	17 ma	4 ma	9 ma
Section No. 3					
Voltage	4.03 v	4.05 v	4.02 v	4.01 v	4.04 v
Current	-28 ma	-9 ma	-13 ma	-2 ma	-6 ma
Battery output					
Voltage	11.82 v	11.87 v	11.79 v	11.78 v	11.82 v
Current	408 ma	408 ma	403 ma	402 ma	406 ma

REFERENCES

1. "Instruction Manual -- SNAP 7A Electric Generation System," MND-P-2661, The Martin Company, October 1, 1961, changed October 25, 1961.

2. Schneider, P. J., "Conduction Heat Transfer," Addison-Wesley, Reading, Massachusetts, 1955.

3. Perry, J. H., "Chemical Engineers' Handbook," McGraw-Hill Book Company, Inc.,New York, 1950.

4. "Statement of Work for SNAP 7 Generators," Revision C, MN-SW-1013, The Martin Company, September 27, 1961.

5. "Final Safety Analysis, SNAP 7A Generator," MND-P-2614, The Martin Company, 1961.

6. Evans, R. D., "The Atomic Nucleus," McGraw-Hill Book Company, Inc., New York, 1955.

7. Marshall, J. H., "How to Figure Shapes of Beta Ray Spectra," Nucleonics, Vol. 13, No. 8, p. 34, August, 1955.

8. Marinelli, L. O., Quimby, E. H., and Hine, G. J., "Dosage Determination with Radioactive Isotopes," Nucleonics, Vol. 2, No. 4, p. 60, April 1948.

9. Haybittle, Phys in Med Biol 1, 3:270, 1956.

10. ORNL-CF-61-1-25 (to be published).

11. McAdams, W., "Heat Transmission," 3rd Edition, McGraw-Hill Book Company, Inc., New York, 1950.

APPENDIX A

SHIELDING KILOCURIE AMOUNTS OF STRONTIUM-90

I. INTRODUCTION

Strontium-90 is one of the radioactive isotopes used to generate heat for small auxiliary power systems. Kilocurie amounts of this isotope are required to produce several watts of heat. Since the decay sequence of Strontium-90 contains no nuclear gamma radiation, it would be easy to believe that no shielding is required. However, bremsstrahlung X-ray radiation is present, and shielding must be provided for it. Most of the bremsstrahlung is generated when the beta particles are slowed down in the compound or mixture of which the fuel pellet is made. A smaller amount of bremsstrahlung is generated by the betas which escape the pellet and slow down in the cladding material.

Bremsstrahlung from Strontium-Yttrium-90 is usually measured by using small sources in the microcurie and millicurie range. These results invariably stress the large quantity of low energy gamma rays produced, but do not give adequate distributions for the high energy end of the spectrum. These results are wholly inadequate for use in designing shields for high kilocurie amounts of Strontium-90. Calculated bremsstrahlung distributions indicate that heavier shielding is required than is indicated by experimental results obtained in measuring microcurie and millicurie amounts of Strontium-90.

To obtain a confirmation of the amount of shielding required for large Strontium-90 sources, Oak Ridge National Laboratory was requested to measure the attenuation by lead absorbers of the radiation from a 1000-curie source of strontium titanate. The purpose of this report is to compare the experimental results with calculated values.

II. BREMSSTRAHLUNG

The total intensity (number of photons times the photon energy) of bremsstrahlung from monoenergetic beta rays in thick targets is given by

$$I = kZE^2$$

where

I = bremsstrahlung intensity

k   = constant

Z   = atomic number of absorber

E   = beta energy (mev).

The spectral distribution of photons is a straight line function with the maximum photon energy equal to the beta ray energy (Ref. 6). The number of photons at the maximum energy is, however, zero. By equating the total intensity to the area of the triangle formed by the distribution curve and the coordinate axes, the number of photons at zero energy is easily found to be equivalent to $2EkZ$. If the photon distribution is divided into energy groups, the average number of photons in each group is equal to the area under the distribution curve bounded by the energy limits of the range, divided by the energy increment.

Beta rays from isotope decay are not emitted monoenergetically but in spectral distributions which vary greatly for different isotopes (Ref. 7).

If the distribution of betas is known for a particular isotope, it may be broken into energy groups and the photon production for each group found.

By means of data from the curves in Ref. 7 the beta distribution of the nominal 2.2-Mev beta from the disintegration of Yttrium-90 was found. The results were normalized to have the area under the curve represent the distribution from one Yttrium-90 disintegration. The average energy of the betas calculated from this curve was found to be 0.876 Mev, which compares favorably with the value 0.90 Mev given in Ref. 8.

The beta distribution was divided into 10 equal energy groups; the number of betas in each group per Yttrium-90 disintegration is given in Table A-1. This grouping of betas was then used to calculate bremsstrahlung distribution. The energy grouping for the bremsstrahlung was chosen to be the same as that for the betas. The number of gammas for each group and the number of gammas divided by kZ are listed in Table A-1.

$$Z_{eff} = \frac{N_1 Z_1^2 + N_2 Z_2^2 + N_3 Z_3^2 + \ldots}{N_1 Z_1 + N_2 Z_2 + N_3 Z_3 + \ldots}$$

TABLE A-1

Grouped Spectral Distribution of Betas and
Bremsstrahlung from Yttrium-90

Energy Group	Number of Betas per Yttrium-90 Disintegration	Number of Gammas, $\div kZ$	Number of Gammas per Yttrium-90 Disintegration	
			As Used, $k = 0.0007$ $Z = 26$	Adjusted, $k = 0.000175$ $Z = 26$
2.2-1.98	0.0068	0.000157	2.97×10^{-6}	7.42×10^{-7}
1.98-1.76	0.0349	0.00143	2.70×10^{-5}	6.75×10^{-6}
1.76-1.54	0.0696	0.00611	1.155×10^{-4}	2.89×10^{-5}
1.54-1.32	0.1013	0.0180	3.404×10^{-4}	8.51×10^{-5}
1.32-1.10	0.1231	0.0425	8.035×10^{-4}	2.09×10^{-4}
1.10-0.88	0.1389	0.0924	1.747×10^{-3}	4.37×10^{-4}
0.88-0.66	0.1482	0.188	3.550×10^{-3}	8.87×10^{-4}
0.66-0.44	0.1469	0.385	7.286×10^{-3}	1.82×10^{-3}
0.44-0.22	0.1308	0.887	1.677×10^{-2}	4.19×10^{-3}
0.22-0	0.0993	3.50	6.612×10^{-2}	1.65×10^{-2}

Published values for the constant k vary widely from 0.4×10^{-3} to 1.1×10^{-3} (Ref. 6). One theoretical determination gives values one order of magnitude lower. The value 0.7×10^{-3} was used in the calculations presented here.

An effective value of Z = 26 was obtained for strontium titanate by using the following relation, found in Ref. 6.

where N_1, N_2, N_3, . . . are the atoms per cm^3 of the mixture having atomic numbers Z_1, Z_2, Z_3, . . .

The total intensity of bremsstrahlung from a distribution of beta energies is expressed by

$$I = kZ(E_{rms})^2 = \sum_{\substack{all \\ groups}} N_i \overline{E}_i$$

or

$$(E_{rms})^2 = \sum_{\substack{all \\ groups}} \frac{N_i}{kZ} \overline{E}_i$$

E_{rms} is the root mean square energy of the beta distribution; $\overline{E}_i$ is the average group energy of the bremsstrahlung, and N_i is the number of bremsstrahlung in the group. The root mean square energy of the betas was calculated and found to be 1.015 Mev. The sum of the number of gammas, divided by kZ, multiplied by the average energy, was calculated and found to have a value of 1.217 Mev. This is about 18% higher than the calculated $(E_{rms})^2$.

Reference 9 states that the dose rate from one curie of Strontium-90 is about the same as that from 12 milligrams of radium, and the average energy of the bremsstrahlung is about 300 kev. The dose rate at one meter from 12 milligrams of radium is 12 mr/hr. Using the distribution of bremsstrahlung given in Table A-1, the bare (without self-absorption and shielding) dose rate at one meter from one curie of Strontium-Yttrium-90 was found to be 12.53 mr/hr, and the average energy of the bremsstrahlung was calculated to be 236 kev.

The bremsstrahlung from the 0.5-Mev beta of Strontium-90 were not included, since these beta particles will be in the low kilovolt range and will be attenuated rapidly in the first few mils of shielding.

III. SHIELDING PROGRAM

Dose rates were calculated by means of a generalized shielding program coded for the IBM 709. The source is divided into a number

of point sources, and the program calculates the dose rate from each of these points. The program was coded to accommodate up to 400 source points and a maximum of 10 initial source energies. Path lengths through the various materials, along a line joining a point source and the dose point, are found and used to calculate relaxation lengths and buildup for each of the materials between these two points. The individual relaxation lengths are added to obtain the total relaxation length. Buildup along the individual path segments is defined as the infinite medium buildup factor minus one. The total buildup factor along the path from the source to the dose point is assumed to be one plus the sum of the individual buildups. Infinite media buildup factors are approximated by the sum of two exponentials.

The direct energy flux at the dose point is evaluated for each source energy and source position and converted to dose rates by the appropriate flux-to-dose conversion factor. The total dose rate is, of course, equal to the sum of the dose rates from each individual source point.

IV. DESCRIPTION OF EXPERIMENTS*

Dose rates from a 1000-curie source of Strontium-Yttrium-90 were measured by ORNL personnel. The kilocurie of Strontium-90 was contained in 65 grams of titanate powder which had been compacted and sintered to a density of 4.5 grams per cubic centimeter. The only radioactive contamination in the pellet was 305 millicuries of Cerium-144 at the time the measurements were made.

Measurements were made with a Cutie Pie Model 740 (Victoreen Instrument Company) and a survey meter No. 2610A (Nuclear Instrument and Chemical Company) which had been calibrated by the ORNL Health Physics Department, using standard radium gamma sources.

The physical arrangement used when the measurements were made is shown in Fig. A-1. Two sets of measurements were made. Case I was made with the detector located 16-3/8 inches above the pellet when the pellet was shielded with a 1/8-inch Hastelloy-C plate and with lead plates which varied in increments of 1/2 inch up to 6-1/2 inches. The measurements for Case II were made with the detector 19-1/4 inches above the pellet when it was shielded with 1/2 inch of Hastelloy-C and various thicknesses of lead. The results of these experiments are plotted in Figs. A-5 and A-6.

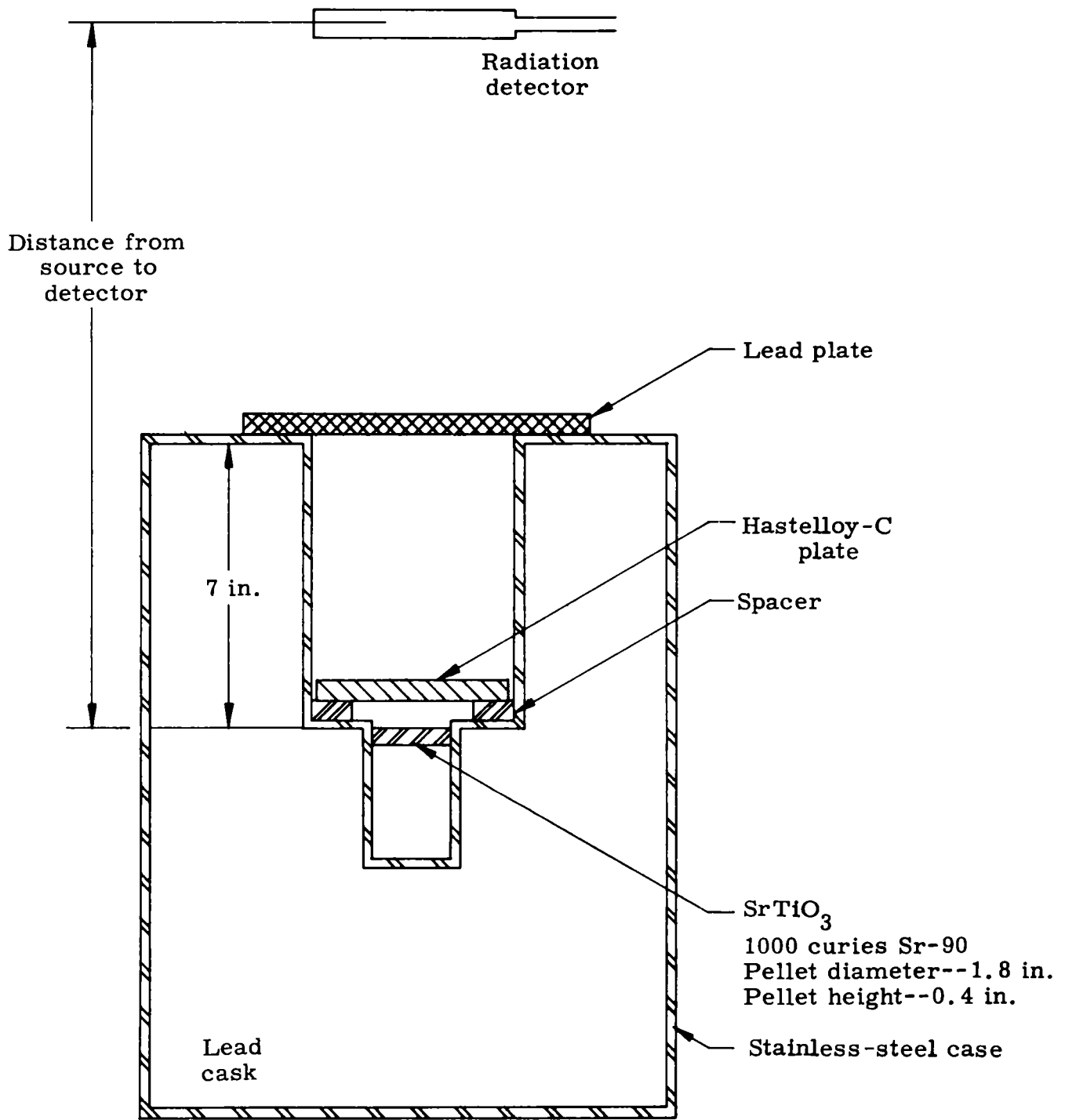*This information was drawn freely from an advance copy of Ref. 10.

Fig. A-1. Physical Arrangement Used in Measuring Dose Rates

V. RESULTS OF CALCULATIONS

The accuracy of point-by-point approximations to integrals depends upon the number of points used. To determine the number of points to use to obtain reasonably accurate results, several problems are run with different numbers of points. Experience has shown that comparatively few points are required to have the third and fourth significant figures in agreement with the results from a greater number of points. To determine the number of source points to use for the present problem, the source was divided into 5, 10, 20 and 40 points. The circular cross section of the fuel pellet was divided into 5 and 10 approximately equal areas, as shown in Figs. A-2 and A-3, and the height was divided into 1, 2 and 4 equal divisions. Calculated results are given in Table A-2. After examining these results, it was decided to run the remainder of the problems with 20 source points. Dose rates versus thickness of lead shielding are tabulated in Table A-3 and are plotted in Figs. A-5 and A-6. Table A-3 also contains the contribution to total dose rate from the 305 millicuries of Cerium-144 present in the strontium pellet. As with Strontium-90, most of the gamma radiation associated with Cerium-144 is bremsstrahlung radiation. The bremsstrahlung radiation from Cerium-144 results from the 2.97-Mev beta of Praseodymium-144. The higher energy beta of Praseodymium-144 causes the bremsstrahlung to be more penetrating than the bremsstrahlung of Yttrium-90. If the contribution from Cerium-144 to Strontium-90 dose rates were limited to a percentage of the Strontium-90 dose rate, the allowable amount of cerium would vary with the shield thickness. To illustrate this point, it was assumed that a 10% increase in dose rate would be acceptable. The curies of Cerium-144 per curie of Strontium-90 were calculated for various thicknesses of lead shielding, and are plotted in Fig. A-4.

VI. COMPARISON OF RESULTS AND CONCLUSIONS

Examination of Figs. A-5 and A-6 shows that the calculated results are higher than the experimental results by an almost constant amount. Analysis of the data shows the calculated results are higher than the experimental results by a factor of about 4.

This could be caused by either of two items used in the calculations. One of these could be the curie strength, and the second, the product, kZ, which enters into the bremsstrahlung calculation. The curie strength used should be close to the stated amount, since care was exercised to determine the amount of Strontium-90 present in the pellet. When the spread of values given for k is considered (Ref. 6), it would be safe to assume that the factor, kZ, used in the calculations is incorrect. The factor, kZ, will be corrected to obtain agreement between calculated and experimental results.
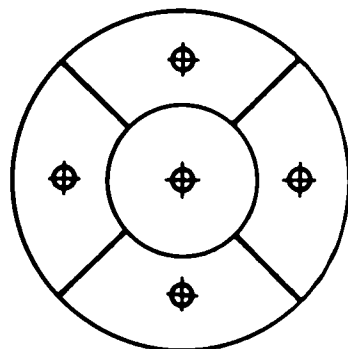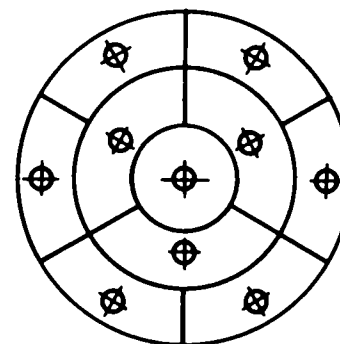
Fig. A-2
Source Point Configuration--
Five Divisions

Fig. A-3
Source Point Configuration--
10 Divisions

TABLE A-2

Comparison of Dose Rates for Various Numbers of Source Points

			Dose Rate*		
Number of Divisions in Circular Area	Number of Divisions in Height	Total Number of Source Points	No Lead (mr/hr)	1/2-in. Lead (mr/hr x 10⁴)	5-in. Lead (mr/hr)
5	1	5	38.181	1.0144	6.6837
	2	10	38.318	1.0146	6.6937
	4	20	38.354	1.0146	6.6963
10	1	10	38.175	1.0142	6.6787
	2	20	38.311	1.0143	6.6890
	4	40	38.347	1.0144	6.6914

*Detector--16-3/8 in. from pellet;
Self absorption in pellet and 1/8-in. Hastelloy-C.

TABLE A-3

Calculated Dose Rates Versus Thickness of Lead
for Comparison with ORNL Data--

Self Absorption + Hastelloy-C + Lead

Thickness of Lead (in.)	Sr-Y-90* 1000 Curies	Dose Rates (mr/hr) Ce-144* 305 Millicuries	Sr-Y-90** 1000 Curies
1/2	1.015×10^4	23.6	5.61×10^3
1	3.828×10^3	12.0	2.08×10^3
1-1/2	1.575×10^3	6.4	8.47×10^2
2	6.81×10^2	3.5	3.62×10^2
2-1/2	3.03×10^2	1.9	1.60×10^2
3	1.38×10^2	1.045	7.26×10
3-1/2	6.38×10	0.575	3.34×10
4	2.98×10	0.316	1.55×10
5	6.70	0.0952	3.47
6	1.54	0.0285	8.00×10^{-1}
7	3.64×10^{-1}	0.00851	1.87×10^{-1}

*Distance, source to detector = 16-3/8 in.
 Hastelloy-C thickness = 1/8 in.

**Distance, source to detector = 19-1/4 in.
 Hastelloy-C thickness = 1/2 in.

NOTE:

The 0.305 curie of Ce-144 in pellet
amounts to 0.0003 curie of Ce-144
per curie of Sr-90
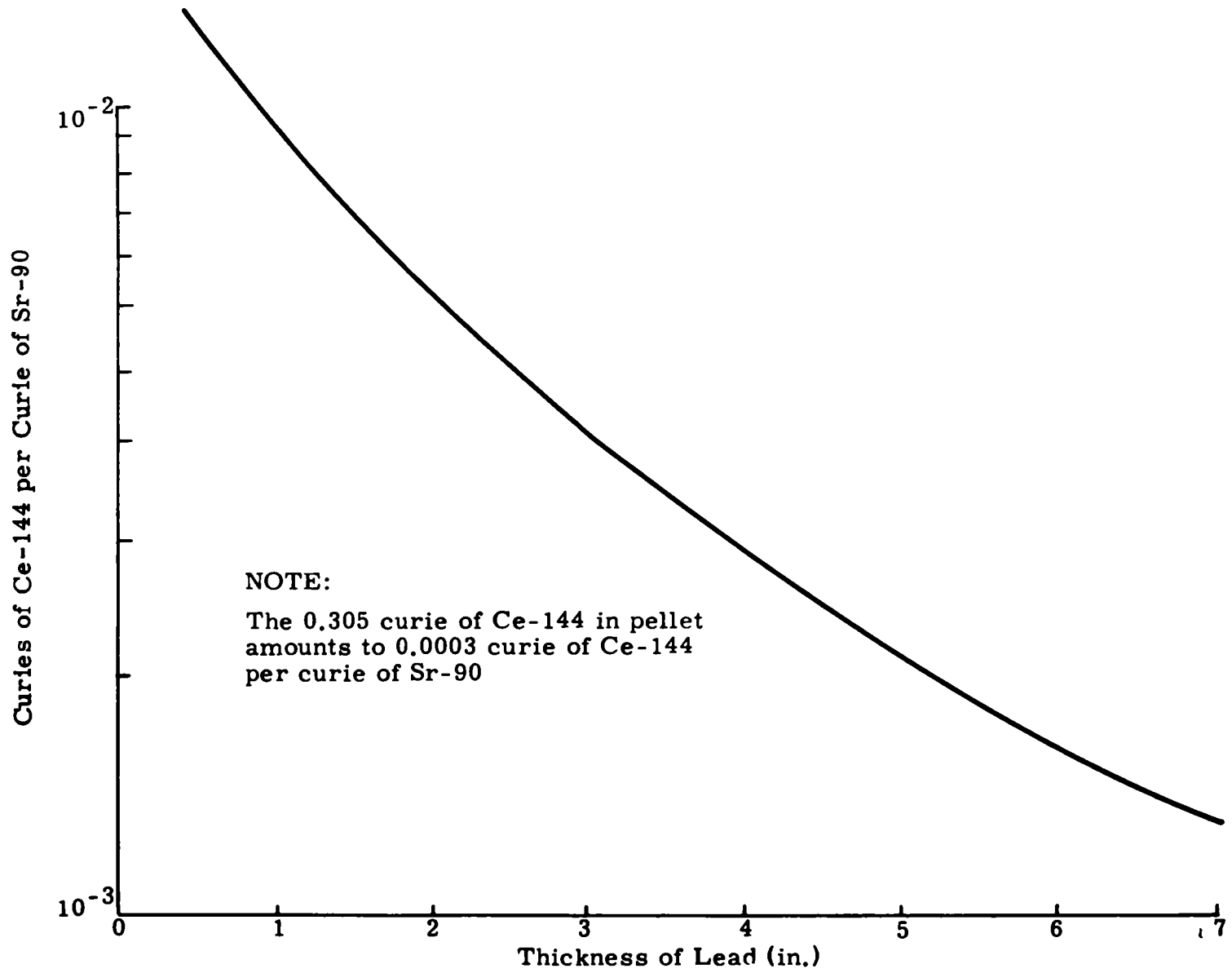
Fig. A-4. Curies of Ce-144 per Curie of Sr-90 Required to Increase Strontium-90
Dose Rate by 10%

The originally calculated values were divided by 4 and plotted as the dashed curves in Figs. A-5 and A-6. These curves are in close agreement with the experimental points.

The value of kZ used to make the original calculations is 0.0007 x 26 = 0.0182, and the value which gave the dashed curve is 0.00455. If it is assumed that the calculated effective Z of 26 is correct, the value of k would become 1.75×10^{-4}. The number of gammas per disintegration of Yttrium-90, using the adjusted value of kZ, are tabulated in Table A-1.

The Cerium-144 present in the pellet while the experiments were being performed did not contribute appreciably to the Strontium-90 dose rates. Depending upon the shield thickness, the amount of cerium present in the pellet could be increased by factors between 4 and 40 to have a 10% increase in dose rate.
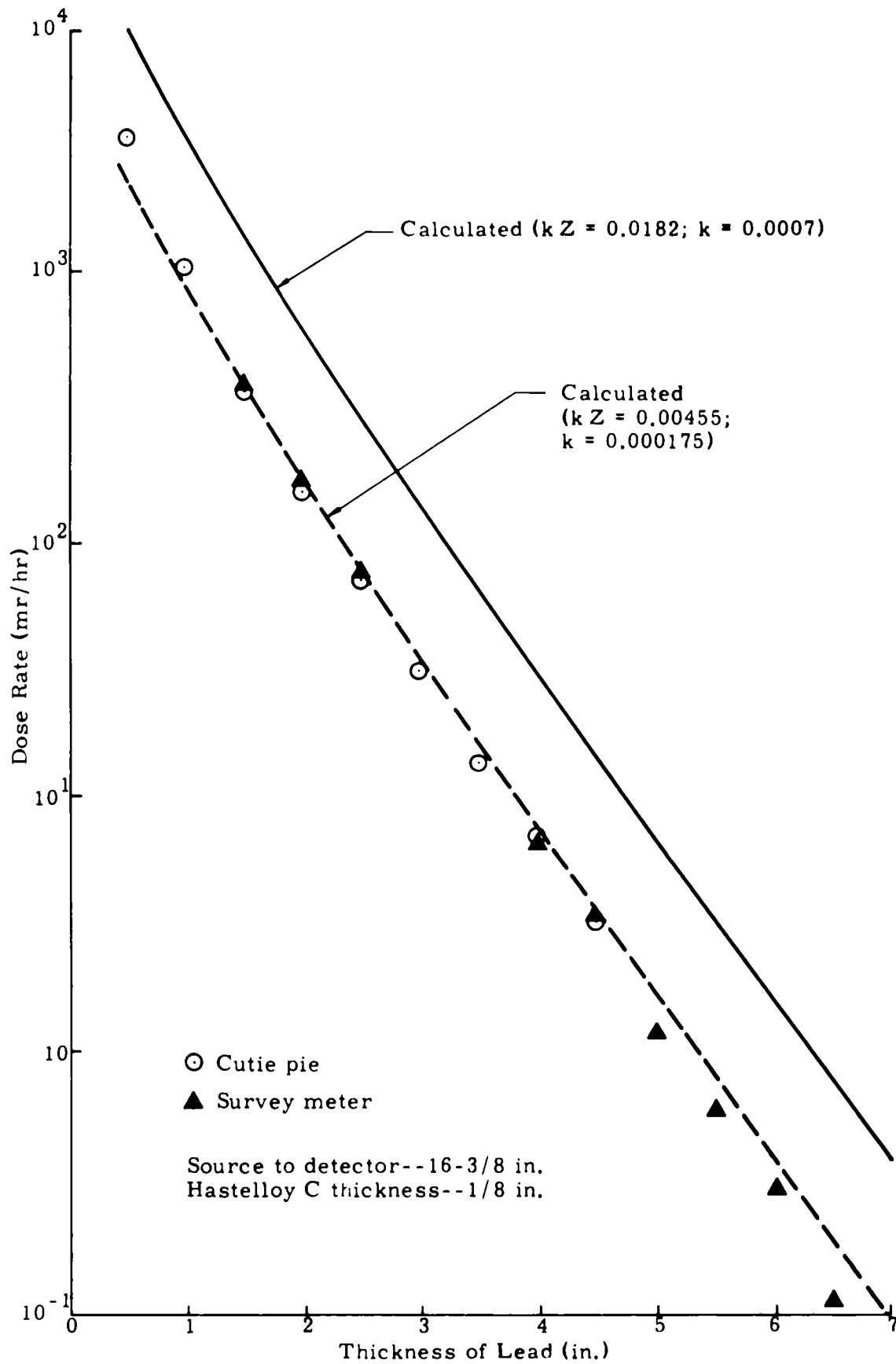
Fig. A-5. Measured and Calculated Dose Rates for Case 1

MND-P-2720
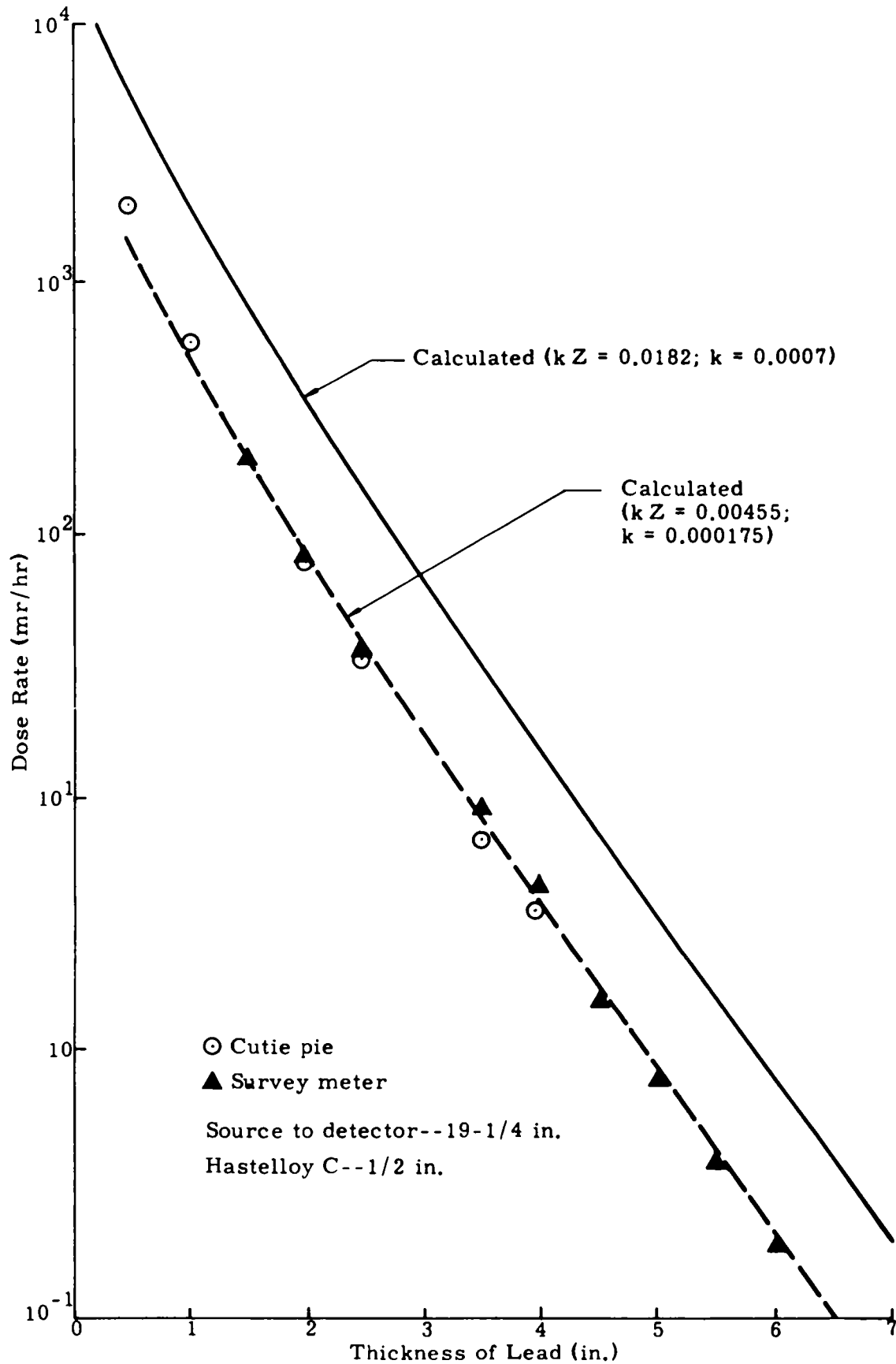
Fig. A-6. Measured and Calculated Dose Rates for Case 2

APPENDIX B

PHOTOGRAPHS OF SNAP 7A FUEL LOADING AND GENERATOR INSTALLATION PROCEDURES

Fig. B-1. The Cover of the Shipping Cask (converted biological shield)
Is Removed to Unload Sr-90 Capsules
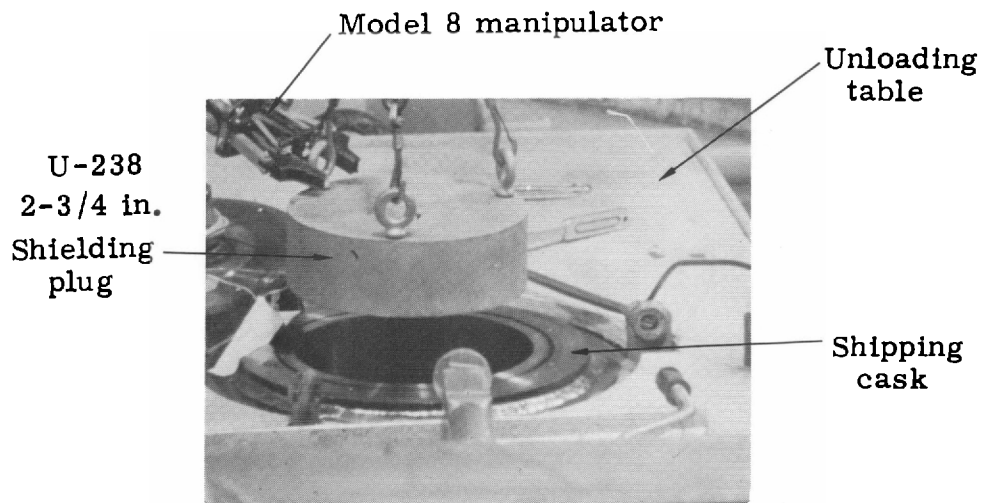
Fig. B-2. The Depleted-Uranium Shielding Plug Is
Removed from the Shipping Cask

Note: Photos B-1 through B-8 were prepared from color motion picture film
taken through the leaded glass window of a hot cell at Quehanna,
Pennsylvania.
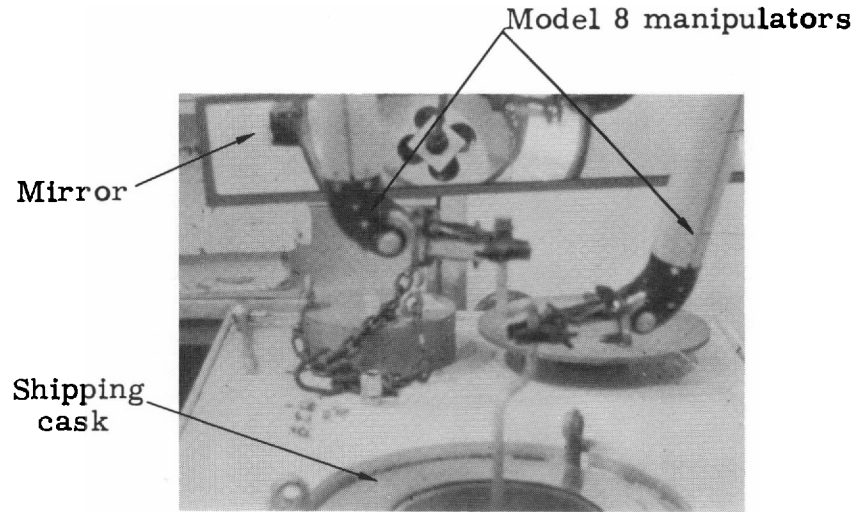
Fig. B-3. The Hold-Down Plug Is Removed from Shipping Cask by Means of Wrench and Manipulators
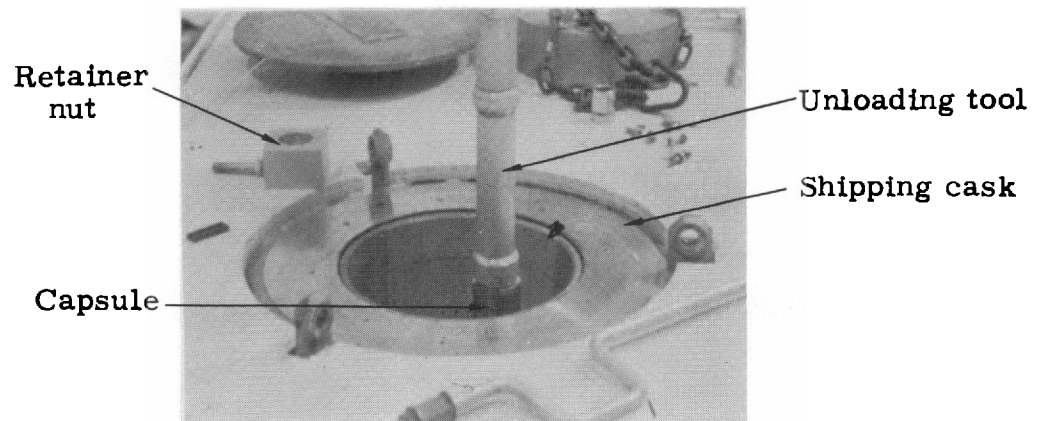
Fig. B-4. The First Sr-90 Capsule Is Removed from Shipping Cask
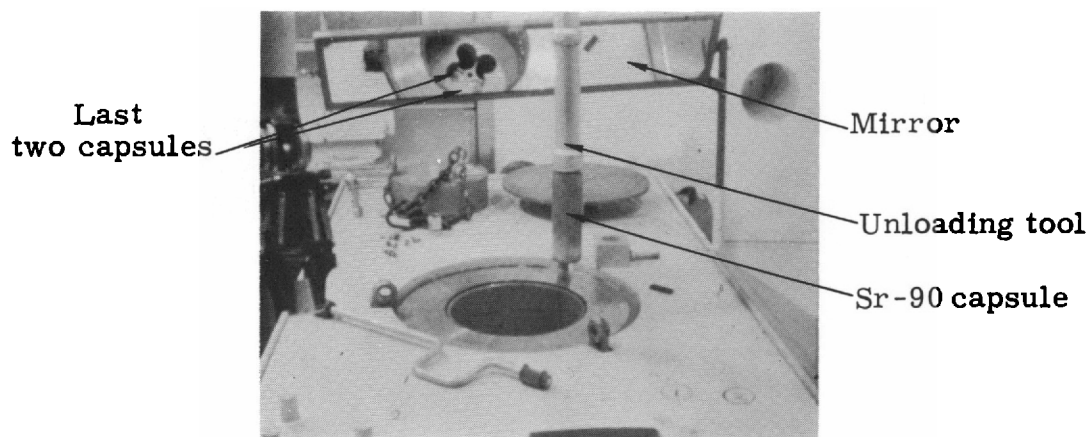
Fig. B-5.   The Second Sr-90 Capsule (10,000 curies)
Is Removed from Shipping Cask
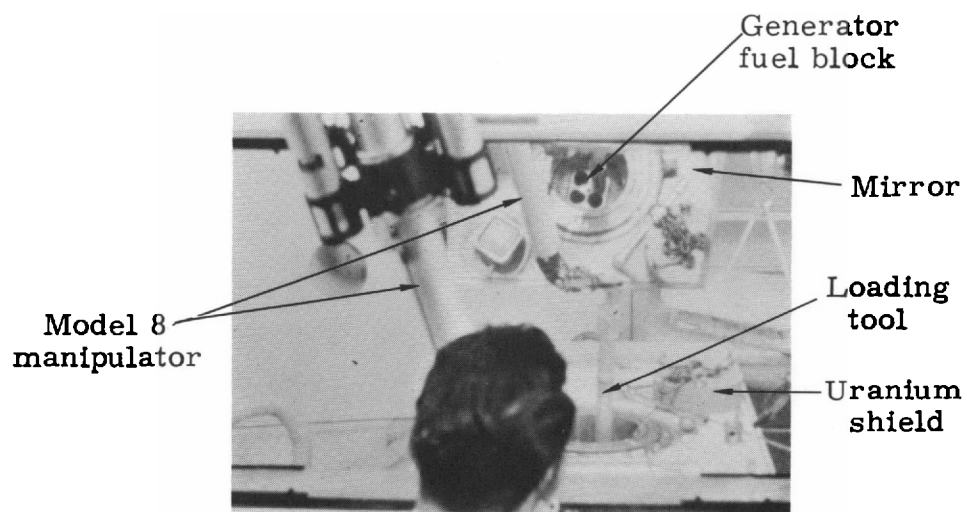
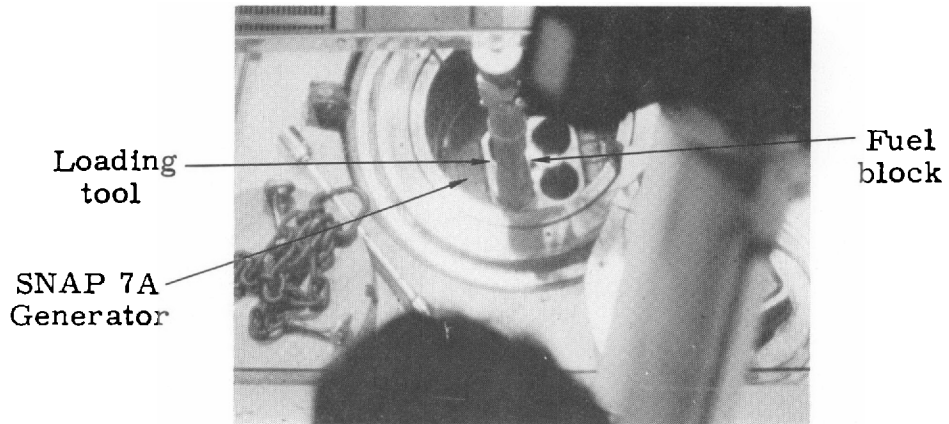Fig. B-6.   The First Sr-90 Capsule is Loaded
into SNAP 7A Generator

Fig. B-7. The Second Sr-90 Capsule Is Inserted into
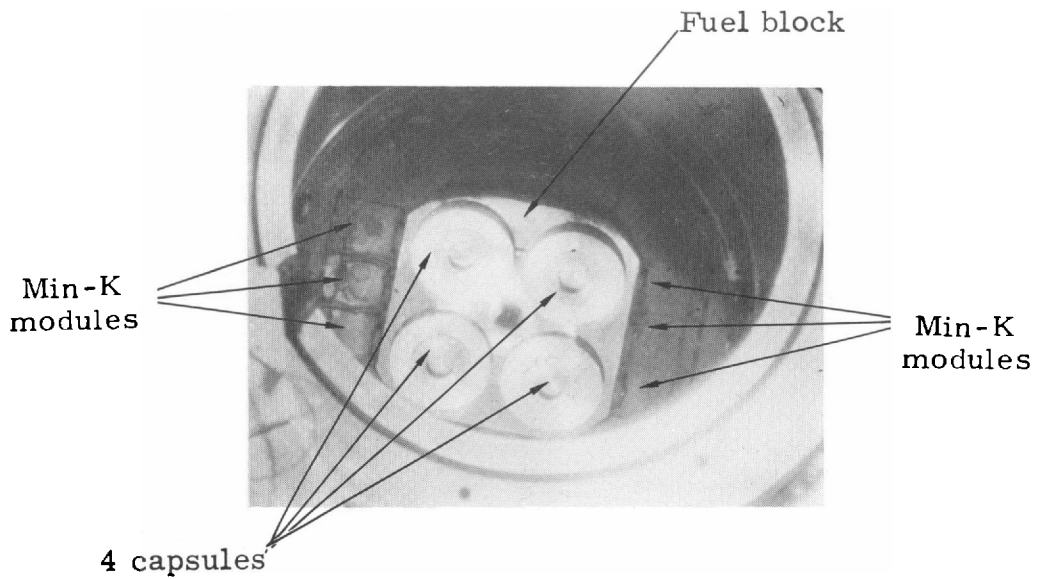Generator Fuel Block (closeup view)

Fig. B-8. Four Sr-90 Capsules (40,800 curies)
Are in Position in SNAP 7A Generator
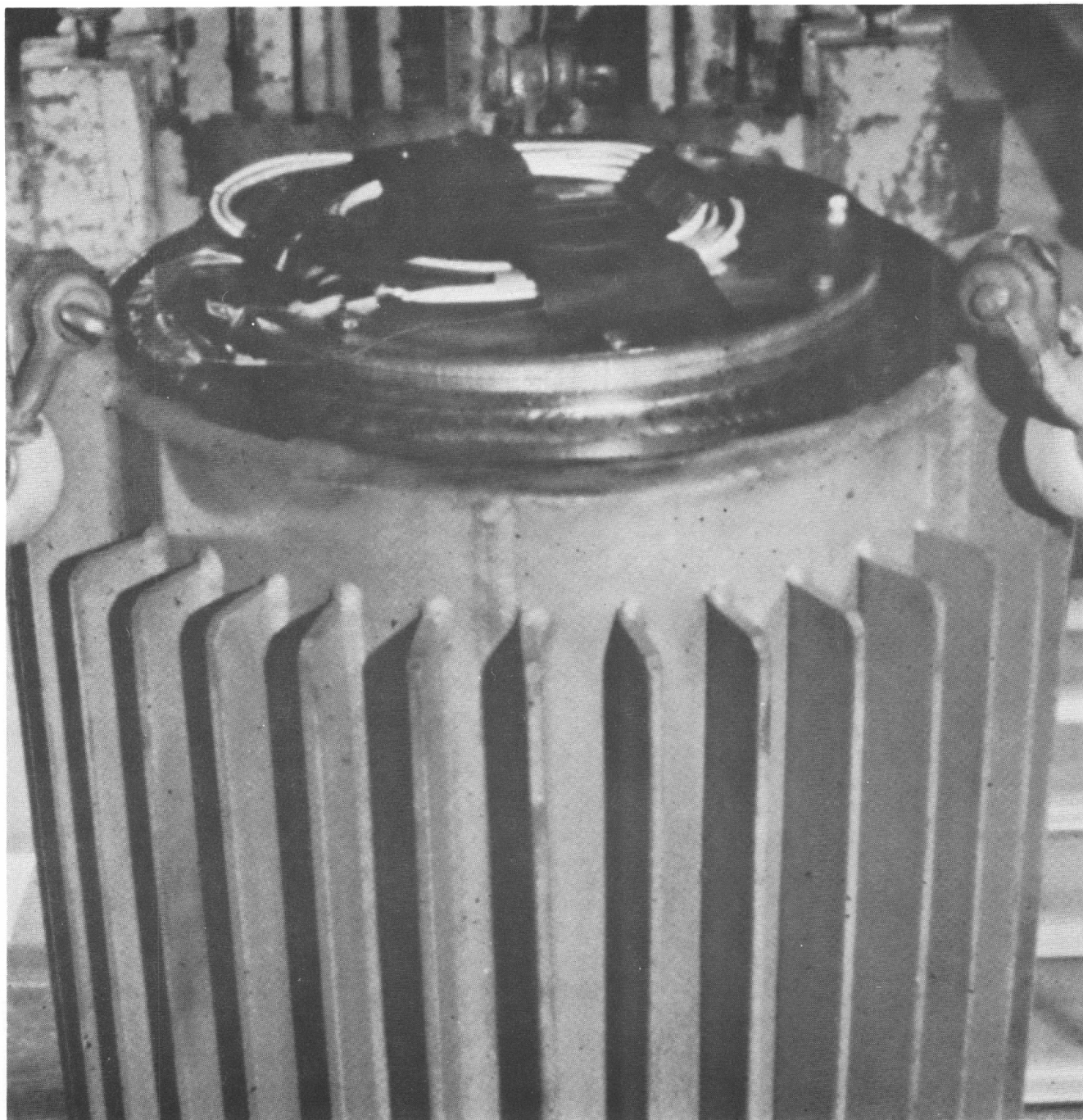Fuel Block (closeup view through mirror)

Fig. B-9. Assembled SNAP 7A Generator Is Removed from Hot Cell and Prepared for Shipping to Martin Marietta, Baltimore, Maryland
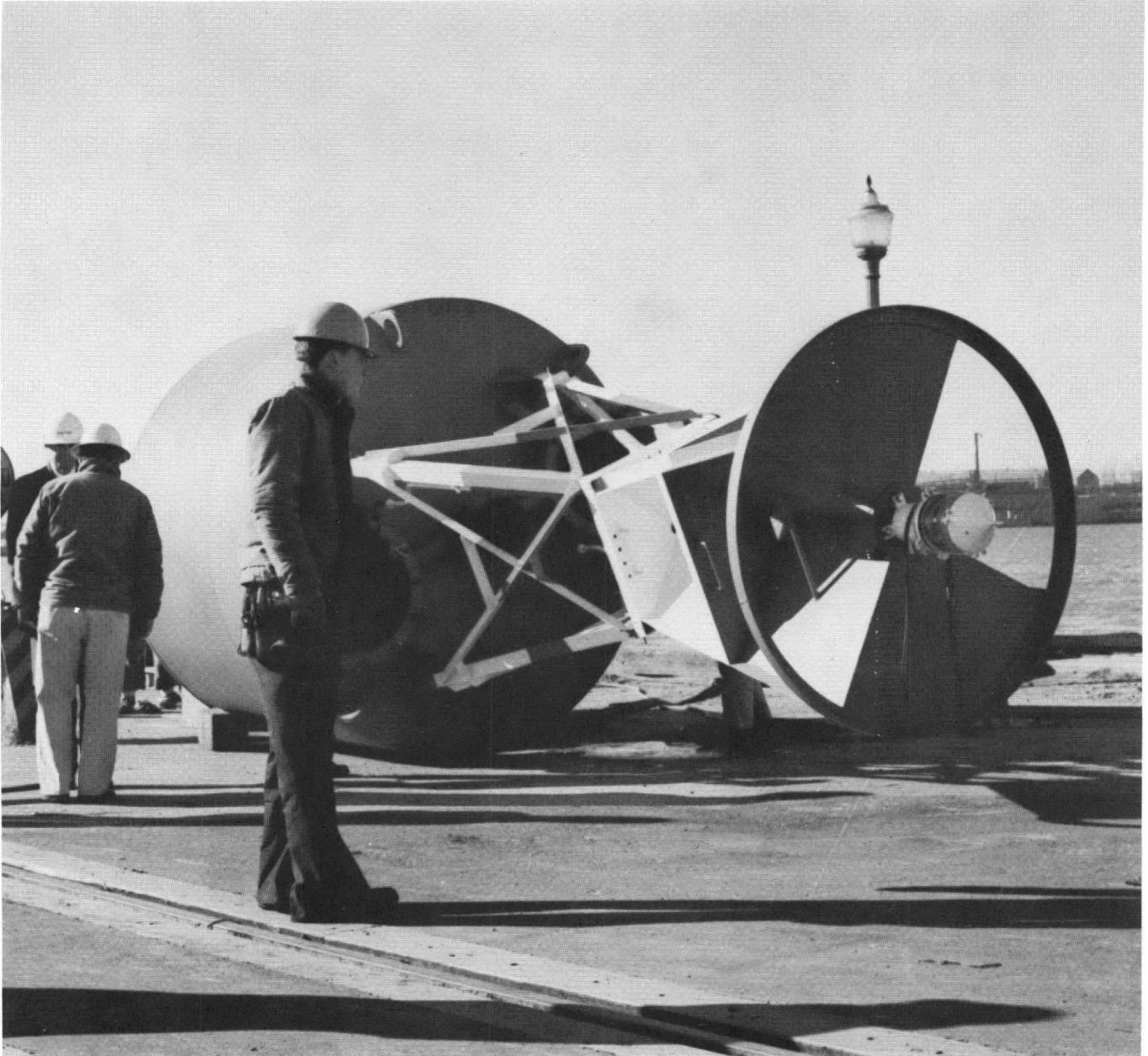
Fig. B-10. U. S. Coast Guard 8x26E Light Buoy at Curtis Bay Coast Guard Station, Baltimore, Maryland

Fig. B-11. SNAP 7A Generator Is Transported from Moving
Van to Coast Guard Buoy

Fig. B-12. Generator Is Released from Shipping Pallet
Restraining Cables

Fig. B-13. Health Physicists from Coast Guard and Martin Marietta Corporation Examine SNAP 7A Generator

Fig. B-14. Generator Is Removed from Shipping Pallet
(note gantry crane cables attached)

Fig. B-15. Generator Is Lowered onto Steel Flange
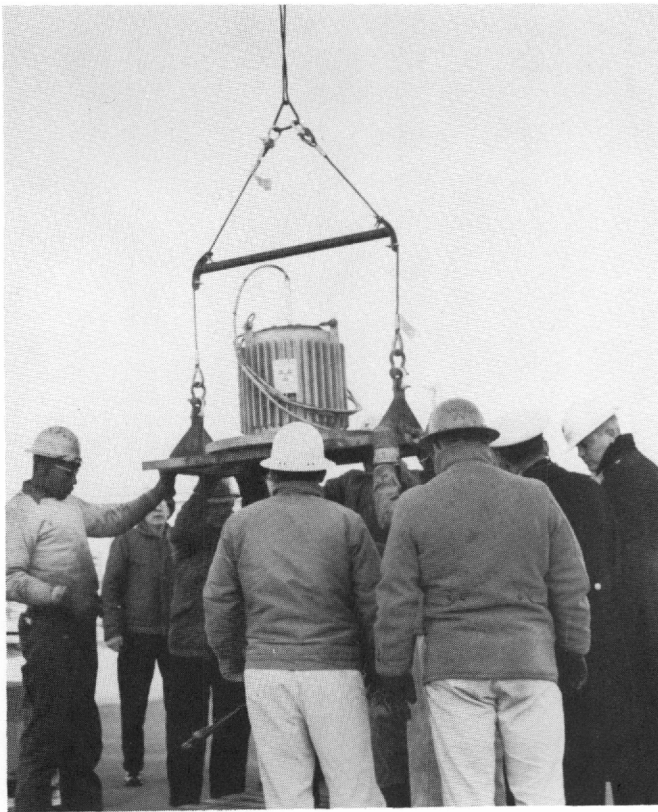and Loading Fixture

Fig. B-16. Generator Is Raised
to Install Tilting Rod

Fig. B-17. Generator Is Tilted
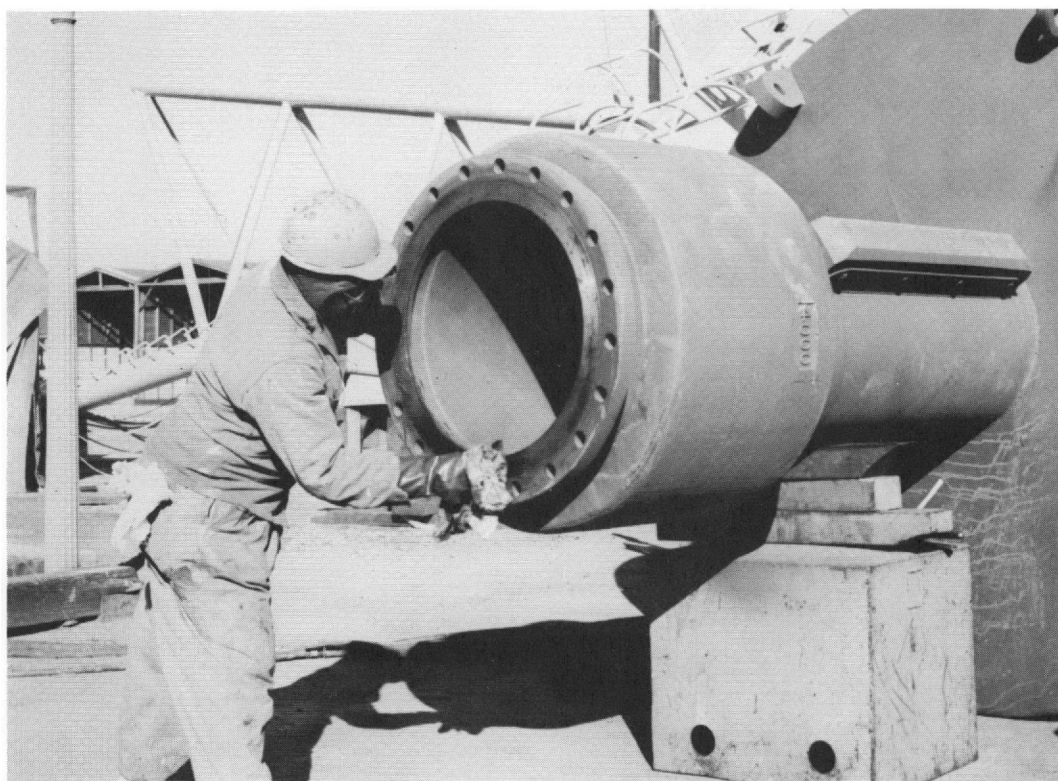to the Horizontal Position
by Loading Fixture

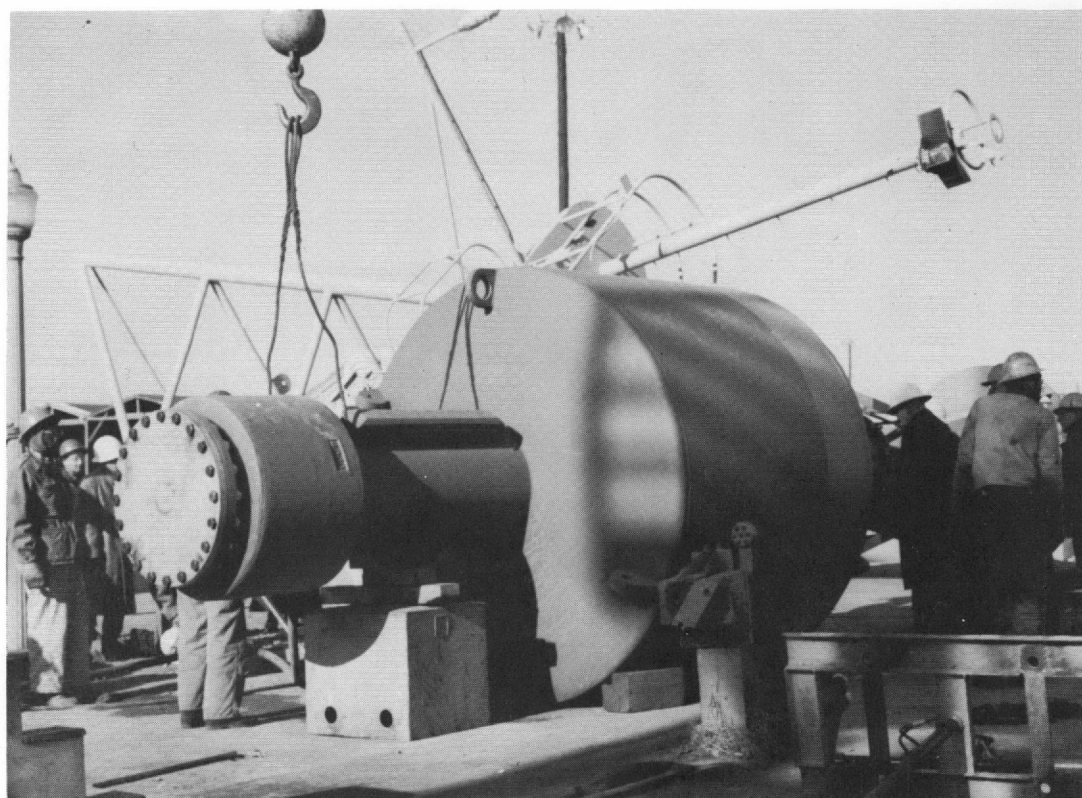Fig. B-18. Flange Face of Light Buoy Counterweight Tube Is Cleaned for Application of Sealing Compound

Fig. B-19. Generator Is Installed and Bolted into Position at the Base of the Counterweight Tube

Fig. B-20. Light Buoy with SNAP 7A Generator Is Launched at Coast Guard Pier

Fig. B-21. Battery and Converter Compartment Is Lowered into Light Buoy After Launching

Fig. B-22. Light Buoy with SNAP 7A Installed Is Towed to Mooring Test Site

APPENDIX C

SNAP 7A ENGINEERING DRAWINGS, WEIGHTS AND DIMENSIONS

1. SNAP 7A--Five-Watt Electric Generation System Drawings

Title	Number
Installation--USCG Electric Lighted Buoy	398A1080000
Modifications--USCG Electric Lighted Buoy	398A1080050
Details--Buoy Modification	398A1080051
Battery--Converter Enclosure	398A1080052
Thermoelectric Generator Assembly	398A1080053
Schematic Diagram	398A1080054
Cable Clamp Assembly	398A1080055
Schematic Converter SI611118 (Single Section)	398A1080056
Schematic Converter SI611119 (Three Section)	398A1080057
Generator--Biological Shield Assembly	398-3021000
Cylinder	398-3021001
End Plate	398-3021002
Fuel Capsule Assembly	398-3021003
Fuel Block	398-3021004
Details--Fuel Block	398-3021005
Shield	398-3021006

Title	Number
Shield Block	398-3021007
Insulation Strip	398-3021008
Insulation Block	398-3021009
Thermoelectric Elements	398-3021010
Shoe--Hot Junction	398-3021011
Details--Cold Junction	398-3021012
Piston	398-3021013
Washer	398-3021014
Frame--Heat Sink	398-3021015
Bars--Heat Sink	398-3021016
Insulation--Corner Strip	398-3021017
Insulation--Spacer	398-3021018
Insulation--Plate	398-3021019
Wire Guide	398-3021020
Plug	398-3021021
Electrical Connector	398-3021022
Connector Mount	398-3021023
Connecting Bar	398-3021025
Shipping Pallet	398-3021026
Nameplate	398-3021027
Cover, Generator Test	398-3021028
Cap Screw	398-3021029
Fuel Capsule Shipping Cask	398-3021040

Title	Number
Biological Shield Container	398-3021041
Generator Assembly	398-3021042
Generator Cover Assembly	398-3021043
Details and Assembly--Fuel Shipping Cask	398-3021044
Hot Shoe--Element Assembly	398-3021045
Cold Cap Assembly	398-3021046
Thermoelectric Module Assembly	398-3021047
Heat Sink Assembly	398-3021048
Generator Shell Assembly	398-3021049
Generator--Pallet, Shipping Assembly	398-3021050

2. SNAP 7A Weights and Dimensions

	Length (in.)	Width (in.)	Height (in.)	Weight (lb)
Thermoelectric Generator and Biological Shield		19 (dia)	21	1870
Shipping Pallet	60	48	6	360
Battery and Converter Compartment		20 (dia)	12-1/4	25
Hastelloy Pipe		3/4 (dia)	153	--
Hastelloy Coupling		3/4 (dia)	1-1/2	--
Sling 200L46-IT				
Clamp Assembly		1-1/4 (dia)	1	--

	Length (in.)	Width (in.)	Height (in.)	Weight (lb)
Electrical Cables				
a.) 398A1080054-9	180	--	--	--
b.) 398A1080054-19	180	--	--	--
Electrical Shunt (50 millivolt, 5 ampere)	--	--	--	--

Note: The Shipping Pallet and Sling 200L46-IT are to be returned to the Martin Marietta Corporation. All dimensions and weights are approximate.